The fractionally damped Van der Pol oscillator

Hilfer-derivative existence and uniqueness, structure, chaos and a Bernstein-splines approach

Niels Goedegebure

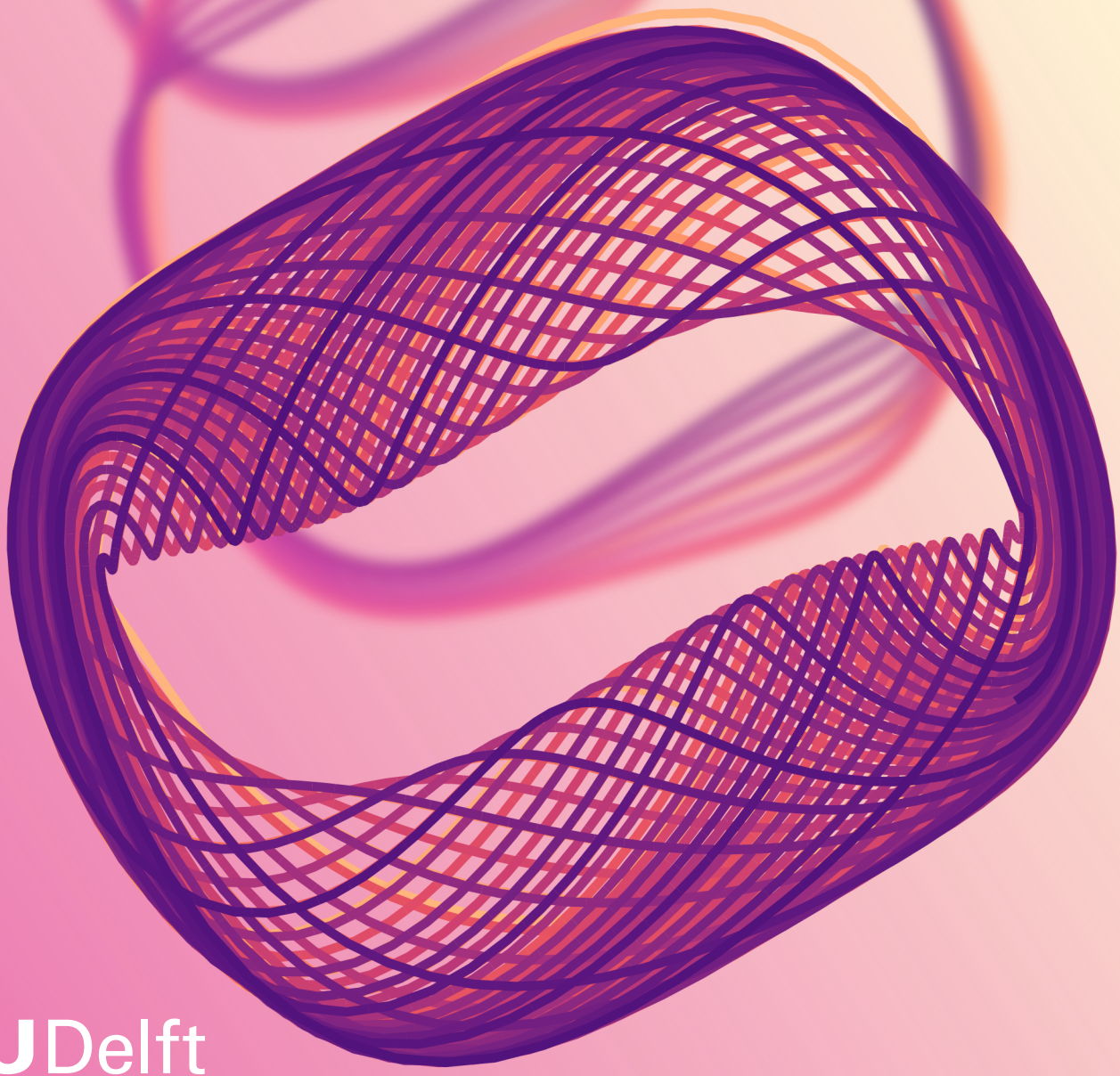

Delft University of Technology

TU Delft

The fractionally damped Van der Pol oscillator

Hilfer-derivative existence and uniqueness, structure, chaos and a Bernstein-splines approach

by

Niels Goedegebure

to obtain the degree of Master of Science

at the Delft University of Technology,

to be defended publicly on Friday January 24, 2025 at 15:00.

Student number:	4912594	
Project duration:	May 1, 2024 – January 24, 2025	
Thesis committee:	Dr. K. Marynets,	TU Delft, daily supervisor
	Dr. ir. W. van Horssen,	TU Delft, responsible supervisor
	Dr. D. Toshniwal,	TU Delft

Cover: Phase portrait of the forced fractionally damped Van der Pol oscillator for $\alpha = 0.8$, $\mu = 1$, $A = 3$, $\omega = 3.3$ for $0 \leq t \leq 100\pi$ with Bernstein splines using $h = 0.05$ and $q = 1$. Approximate unforced limit cycles for increasing μ and various values of α in the background.

TU Delft

Abstract

In this thesis, we study fractional differential equations with Hilfer derivative operators. Solutions are approximated using a newly developed Bernstein-splines approach and subsequently applied to the Van der Pol oscillator with fractional damping. Fractional derivatives generalize differentiation to the order $\alpha \in \mathbb{R}^+$ resulting in differential operators $\frac{\mathrm{d}^\alpha}{\mathrm{d}t^\alpha}$. The Hilfer-derivative of order $\alpha \in (0,1)$ and type $\beta \in [0,1]$ is one of such operators and combines two of the most commonly used operators through parametrization: the Riemmann-Liouville-derivative ($\beta = 0$) and Caputo-derivative ($\beta = 1$). The choice of β results in different kernel behavior of the operator, commonly yielding singular behavior of solutions of initial value problems (IVP's) and boundary value problems (BVP's) for $\beta \in [0,1)$. Based on existing results for IVP's, we develop a new proof for existence and uniqueness of solutions to BVP's for Hilfer-fractional derivatives. To obtain solution approximations numerically for IVP's and BVP's, a Bernstein splines solution approach is developed and implemented[1], providing accurate convergence results for nonlinear IVP's and BVP's in an efficient vectorized approach. Implementation difficulties for the singular behavior of solutions for $\beta \in [0,1)$ are successfully resolved through time-domain transformation approximation techniques. Finally, the methods are applied to numerically study the behavior of the fractionally damped Van der Pol oscillator, a nonlinear equation of interest in electrical engineering and control theory. We study the approximate limit cycle, of which behavior corresponds with existing analytical results for the Caputo-derivative ($\beta = 1$). Convergence of solutions can also be obtained for Hilfer type values of $\beta \in [0,1)$, appearing to be of little influence on the long-term limit cycle. Furthermore, when forcing is applied, we observe periodic, quasiperiodic and chaotic behavior.

[1] Source code available at `https://github.com/ngoedegebure/fracnum`.

Acknowledgements

One of the most well-known explanations of chaos theory is without doubt the *butterfly effect*: the idea of a butterfly waving its wings and causing a tornado in a place far away. Regardless of the specific example, it is clear chaos is not merely an effect on paper and in theses: real life tends to be just as chaotic and *nonlinear*. For example, until only a few years ago, I would not have believed anyone who told me I would be doing a master's degree in Applied Mathematics right now. Yet, here I am. The road to mathematics has often been rocky, intense and demanding. But all the hard work and hardships pale in comparison to the feeling of gratefulness and the love for mathematics I have discovered, even if it took some time. Especially working on this thesis has been the most rewarding and motivating project I have thus far undertaken.

Luckily, motivation and enthusiasm does not appear spontaneously but is highly contagious. For this, I would like to thank a few people. First of all, I would like to thank Dr. Kateryna Marynets for her thorough and incredibly motivated supervision. Not only did you help improve and develop the plans we made, you also gave me the trust and freedom to make me tackle problems in my own way. Moreover, you always cared about my work load and mental health, which is worth incredibly much. Hence, all the work I did in weekends and evenings can solely be attributed to my own questionable choices. I would like to thank Dr. ir. Wim van Horssen for his insights on oscillating systems and his teachings in differential equations, sparking my love for the field. Dr. Deepesh Toshniwal showed me how fun numerical methods could be, and gave me tremendous insights on function space approximations with polynomial bases used throughout this thesis. Some DIAM Mathematical Physics researchers I would like to thank specifically are Prof. dr. Henk Schuttelaars, giving me very helpful input regarding physics and dimensional analysis, Dr. Yoeri Dijkstra on ideas for numerical simulation and Dona Pantova, who gave me a lot of valuable early-stage ideas. Furthermore, I am thankful for the enthusiasm and hard work of Prof. dr. Jan van Neerven, who taught me a tremendous amount of useful knowledge in the course functional analysis. Finally, I sincerely thank Prof. dr. ir. Martin van Gijzen, without whom I would not be writing this thesis.

Apart from research, I want to thank some fellow students I met along this mathematical journey. Firstly my gratitude to all the amazing people I met in my year of bridging courses, who gave me the warmest welcome I could have wished for. With partial overlap, all the inspiring and colorful people of the students I met in the MSc. programme, many of whom have become very close friends. My roommates Lourens Touwen, Karim Guettache and Pietro Pezzoli, who turned the house into a home and cold into warmth. Finally, a very special and warm word of thanks for Mauditra Matin. A large part of this document was typed during our joined thesis sessions, and I am sure our respective mathematical problems were better off shared. In general, I can only agree with what a wise person told me: "everyone should have a Ditra in their lives".

And finally, a heartfelt thanks to my parents. To my mother, who taught me the language of learning and vice versa, and my father, teaching me the patience to challenge everything.

Niels Goedegebure
Den Haag, January 2025

Contents

Frequently used notation

Below, a list is provided of some frequently used notations used throughout the text, corresponding to a definition or first in-text usage.

Operators

${}_a\mathrm{I}_b^\alpha$	α-fractional Riemann-Liouville integral on interval $[a,b]$	Definition 2.2.1
${}_a\mathrm{D}_t^\alpha$	α-fractional Riemann-Liouville derivative from a evaluated at $t>a$	Definition 2.3.1
${}_a^{\mathrm{C}}\mathrm{D}_t^\alpha$	α-fractional Caputo-derivative from a evaluated at $t>a$	Definition 2.3.2
${}_a\mathrm{D}_t^{\alpha,\beta}$	α-fractional Hilfer derivative of type β from a evaluated at $t>a$	Definition 2.3.3
B^n	Bernstein polynomial operator	Definition 4.1.2
$S_{\mathcal{A}}^q$	Bernstein spline operator on knot selection $\mathcal{A}$	Definition 4.2.1
${}_a^q\Phi_b^\alpha$	α-fractional splines integral on interval $[a,b]$	Definition 4.3.1

Norms

For norms, the convention of $a=0$ and $b=T$ is used in text unless stated otherwise.

$\|\|f\|\|_\infty$	$=\sup_{t\in[a,b]}\|f(t)\|$	Proposition 2.2.4
$\|\|g\|\|_{1-\gamma}$	$=\sup_{t\in[a,b]}\left\|(t-a)^{1-\gamma}g(t)\right\|$	Section 3.1

Function spaces

$C[a,b]$	$=\left\{f:[a,b]\to\mathbb{R}^d,\quad f \text{ continuous}\right\}$	Proposition 2.2.4
$C_{1-\gamma}[a,b]$	$=\left\{f:[a,b]\to\mathbb{R}^d,\quad (t-a)^{1-\gamma}f\in C[a,b]\right\}$	Section 3.1
$C_{1-\gamma}^\zeta$	$=\left\{f:[a,b]\to\mathbb{R}^d,\quad f\in C_{1-\gamma}[a,b],\quad {}_a\mathrm{D}_t^\zeta f(t)\in C_{1-\gamma}[a,b]\right\}$	Theorem 3.1.1

Various

$\mathcal{A}$	$=\{[t_0,t_1),...,[t_{k-1},t_k),[t_k,T]\}$, $\cup_{A_i\in\mathcal{A}}A_i=[0,T]$ (knot collection)	Definition 4.2.1
$\|A\|$	$=\sup_{a,b\in A}\|b-a\|$, for $A\subset\mathbb{R}$ (knot size)	Theorem 4.2.1
$\omega\left(f;\delta\right)$	$=\sup_{\|t-s\|\leq\delta}\|f(t)-f(s)\|$ (modulus of continuity)	Definition 4.1.3
$[x]$	Physical unit of measurement of x	Section 7.1.1

Notation shorthands

${}_0\mathrm{I}_t^\alpha f(0)$	$=\lim_{t\downarrow 0}{}_0\mathrm{I}_t^\alpha f(t)$	Equation 3.1

1 Introduction

Fractional calculus is the field of mathematics concerned with derivation and integration of the α'th order, where $\alpha \in \mathbb{R}^+$ is not necessarily integer. The concept dates back to the 17th century, with a question of l'Hôpital to Leibniz, asking what the interpretation of the derivative $\frac{\mathrm{d}^n}{\mathrm{d}y^n}x$ would be if $n = \frac{1}{2}$ were to be the order of derivation [16]. The answer of Leibniz in 1695 has become a famous citation in the field of fractional calculus:

> "This is an apparent paradox for which, one day, useful consequences will be drawn." [17]

In the centuries that followed, mathematicians such as Euler, Lagrange, Laplace, Fourier, Riemann and Liouville have contributed to the field, developing the early stages of fractional calculus. More recently, applications of fractional calculus to differential equations have been developed, creating the field of *fractional differential equations* (fDE's). Fractional differential equations take on the general form of

$$\frac{\mathrm{d}^\alpha}{\mathrm{d}t^\alpha}x(t) = f(t, x(t)), \quad \alpha \in (0, \infty), \tag{$\sim$}$$

subject to prescribed initial or boundary conditions. Some recent fundamental results and works in this field include the publications of Samko, Kilbas, and Marichev [29], Podlubny [27], Hilfer [15] and the book of Kilbas, Srivastava, and Trujillo [16]

A notable difficulty in fractional differential equations is the *nonlocality* of the fractional derivative. On the contrary to integer-order differentiation, the fractional derivative $\frac{\mathrm{d}^\alpha}{\mathrm{d}t^\alpha}x(t)$ is not merely dependent on information of $x(t)$, but depends on all $x(s)$ for an interval $s \in (a, t]$. This poses both an analytical and a computation problem:

- For most functions f, it is not possible to yield a closed-form nontrivial solution to differential equations of the formulation ($\sim$).
- Approximating a solution to ($\sim$) requires computationally expensive methods because of the nonlocality of the fractional derivative.

A number of numerical algorithms have been employed to overcome these challenges. Roughly, the numerical methods can be divided into three groups:

- *Finite difference methods*, using quadrature integration rules and / or finite differences to obtain an approximate solution. A seminal and frequently cited method is provided by the predictor-corrector approach of Diethelm, Ford, and Freed [6]. Furthermore, the Grünwald–Letnikov scheme as proposed by Samko, Kilbas, and Marichev [29] also provide another simple and efficient technique.
- *Frequency-domain methods*, such as the popular singularity function method proposed by Charef et al. [4] which can be used for Laplace-decomposition approaches.
- *Numerical-analytic methods*, using analytical fractional integration and differentiation of basis functions constructing an approximating solution space. Examples include series methods such as

provided in Podlubny [27] and polynomial approaches such as the Lagrange-polynomial approach taken by Fečkan and Marynets [10] or Bernstein-polynomial approach of Satmari [30].

A major advantage of using numerical-analytic approaches is the analytical expression obtained for the solution and its fractional integral. Furthermore, most numerical-analytic methods allow for an inherently more explicit error calculation as error bounds are obtained in the proofs of convergence. However, drawbacks to these methods for solving fractional differential equations are their longer computational times, approximation function complexity choices and stricter convergence requirements. Furthermore, as of current most methods only consider the Caputo fractional derivative, not taking other fractional derivative definitions into account.

This thesis consists of three parts to challenge and test these problems. First, after an introduction to fractional calculus in Chapter 2, nonlinear IVP's and BVP's are analyzed analytically for the generalized Hilfer derivative in Chapter 3, providing a very general setup incorporating the commonly used Riemann-Liouville and Caputo derivative in a parametrized way for existence and uniqueness proofs.

Secondly, this thesis introduces a new numerical-analytic approach using Bernstein-basis splines. The method has minimal convergence requirements, is able to solve a wide class of Hilfer derivative ODE's accurately and is efficiently implemented using full vectorization. Theory on splines is established in Chapter 4, which is used to approximate solutions to the fractional order IVP's and BVP's in Chapter 5 and 6 respectively. The approach takes away many of the disadvantages while still providing the advantages of numerical-analytic methods for a general Hilfer derivative setting.

Finally in Chapter 7, as an example case with applications to physics, numerical results are obtained for the Van der Pol oscillator with a Caputo fractional derivative in its damping, of which the fractional differential equation is provided as:

$$\frac{\mathrm{d}^2}{\mathrm{d}t^2}x(t) - \mu(1 - x(t)^2)\frac{\mathrm{d}^\alpha}{\mathrm{d}t^\alpha}x(t) + x(t) = 0, \quad \mu > 0, \quad \alpha \in (0, 1).$$

This fractional differential equation is an adaption of the classical differential equation as proposed by Van der Pol [37]. The fractional system can be seen as an adaptation with a memory-effect in the capacitator or damping [1]. The system shows both oscillatory and non-oscillatory behavior, dependent on the parameter and differential order values [35]. For oscillatory systems, a limit cycle exists as proven by Liu, Liu, and Chen [20]. Furthermore, chaotic behavior is found when forcing frequences are applied [5, 12]. We analyze the dynamics of the fractional Van der Pol oscillator using the developed Bernstein-splines approach, with special attention to the physical interpretation of the fractional damping and the effect of the fractional order α and damping parameter μ on the the limit cycle. The equation is also studied using sinusoidal forcing, showing multiperiodic, quasiperiodic and chaotic behavior. Furthermore, solutions are obtained for the non-Caputo type Hilfer derivative of type $\beta \in [0, 1)$, showing a successful nonlinear example of the Bernstein-splines approach for Hilfer derivative fractional differential equations.

2

Fractional calculus: an introduction and selected results

This chapter will present an introduction to fractional calculus, providing some results which will serve as the basis for further chapters and can function as a standalone work of reference. Motivation for fractional calculus is given in Section 2.1, after which the fractional integral and its properties are introduced in Section 2.2, used to establish fractional differentiation in Section 2.3.

2.1. Motivation

The well-known derivative is one of the core concepts in calculus of functions. Seen as an operator acting on a function $f : \mathbb{R} \to \mathbb{R}$, the derivative at point t can be interpreted as the slope of f at point t. This is defined by taking the limit of the tangent. Hence, we can write

$$\frac{\mathrm{d}}{\mathrm{d}t} f(t) = \lim_{h \to 0} \frac{f(t+h) - f(t)}{h}.$$

Now, one can wonder what the expression of the "slope of the slope" of a function looks like. This definition immediately presents a method to provide higher order differentiation by repeating the operator $\frac{\mathrm{d}}{\mathrm{d}t}$: for $n \in \mathbb{N}$, one can write the n'th derivative as

$$\frac{\mathrm{d}^n}{\mathrm{d}t^n} f(t) = \underbrace{\frac{\mathrm{d}}{\mathrm{d}t} ... \frac{\mathrm{d}}{\mathrm{d}t}}_{n \text{ times}} f(t), \tag{2.1}$$

provided this expression exists. Beautiful, we now know how to differentiate 1, 2, ..., n times for any arbitrary n. However, what if one, like l'Hôpital would want to know the value of the "half" derivative? How does one define the above for $n = \frac{1}{2}$? Or for that matter, for any $n \in (\mathbb{R}_{\geq 0} \setminus \mathbb{N})$? Let us take $\alpha \in (0, \infty)$. The question is how to find

$$\frac{\mathrm{d}^\alpha}{\mathrm{d}t^\alpha} f(t).$$

Taking again $\alpha = \frac{1}{2}$, the operator $\frac{\mathrm{d}^{1/2}}{\mathrm{d}t^{1/2}}$ would intuitively yield results "in between the function and its derivative". But how do we make this more precise? And what is the interpretation of this value? These questions will be answered and formalized in the following subsections.

2.2. Fractional integration

2.2.1. The Riemann-Liouville Fractional Integral

Before diving into the fractional derivatives, it is crucial to establish a definition of fractional *integration*. For $f : [a, \infty) \to \mathbb{R}$ and $a \leq t$, let us take the standard integral operator ${}_a\mathrm{I}_t$, frequently reffered to as

antiderivative, as

$$ {}_a\mathrm{I}_t f(t) = \int_a^t f(s)\,\mathrm{d}s. $$

For $f : [a, \infty) \to [0, \infty)$, the function ${}_a\mathrm{I}_t f(t)$ can be interpreted as the "area below" $f(s)$ from a until t, The integral can be thought of the limit of simple functions in the Lebesque sense, a result which will be omitted in this text but can be found in more detail in for instance [24], Appendix F. Now, similarly to (2.1), one can extend the integral operator ${}_a\mathrm{I}_t$ to a repeated integral ${}_a\mathrm{I}_t^n$ by writing

$$ {}_a\mathrm{I}_t^n f(t) = \underbrace{{}_a\mathrm{I}_t \dots {}_a\mathrm{I}_t}_{n \text{ times}} f(t) = \int_a^t \int_a^{s_{n-1}} \dots \int_a^{s_2} f(s_1)\,\mathrm{d}s_1 \dots \mathrm{d}s_{n-2}\ \mathrm{d}s_{n-1}. $$

By Cauchy's formula for repeated integration (see e.g. [27], Section 2.3.1), this expression is given explicitly by

$$ {}_a\mathrm{I}_t^n f(t) = \frac{1}{(n-1)!} \int_a^t (t-s)^{n-1} f(s)\,\mathrm{d}s. \tag{2.2} $$

Now, to generalize expression (2.2) to $n \notin \mathbb{N}$, we are in luck. Compared to derivatives, the definition of a repeated integral can easily be generalized to orders of $\alpha \in \mathbb{R}_{\geq 0}$ by the observation that the special Gamma function $\Gamma(x) = \int_0^\infty t^{x-1} e^{-t}\,\mathrm{d}t$ generalizes the factorial function such that $\Gamma(n) = (n-1)!$ for $n \in \mathbb{N}$. Using this gives:

Definition 2.2.1 (Left-sided Riemann-Liouville fractional integral)**.** For $a \leq x$ and $\alpha \in [0, \infty)$, define the left-sided Riemann-Liouville fractional integral as:

$$ {}_a\mathrm{I}_t^\alpha f(t) = \frac{1}{\Gamma(\alpha)} \int_a^t (t-s)^{\alpha-1} f(s)\,\mathrm{d}s. $$

A visual illustration of values "in between" the function and the regular integral operator is provided in Figure 2.1.

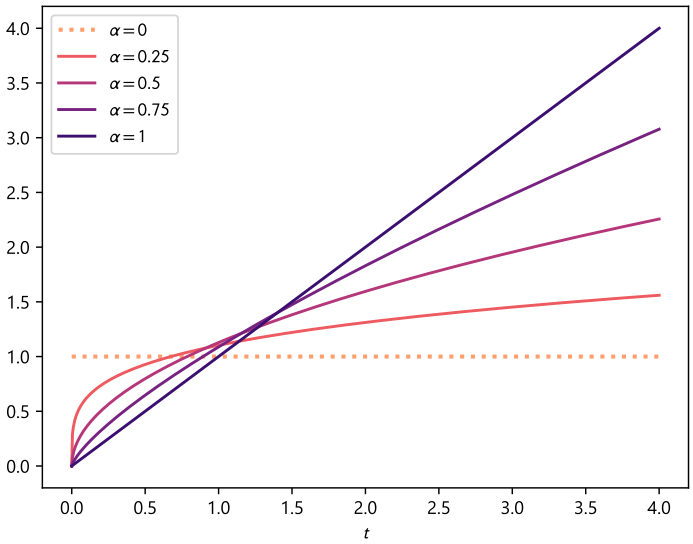

Figure 2.1: Results of the Riemann-Liouville integral for selected values of $\alpha \in (0, 1]$ of the constant function $f(t) = 1$, as shown for $\alpha = 0$. Note that $\alpha = 1$ gives the classical integral operator.

Now that we have an expression in place, let us look at the properties of this operator.

2.2.2. Properties of the Riemann-Liouville Fractional Integral

In this section, a number of useful properties of fractional integration will be presented, which will be used in later sections.

Proposition 2.2.1 (Linearity)**.** *The Riemman-Liouville integral is a linear operator. Hence, taking $a < t \leq b$, for all α-fractionally integrable $f, g : [a, b] \to \mathbb{R}$, $\eta \in \mathbb{R}$,*

- ${}_a\mathrm{I}_t^\alpha\{\eta f(t)\} = \eta\, {}_a\mathrm{I}_t^\alpha f(t)$,
- ${}_a\mathrm{I}_t^\alpha\{f(t) + g(t)\} = {}_a\mathrm{I}_t^\alpha f(t) + {}_a\mathrm{I}_t^\alpha g(t)$.

Proof. The proof of both items follows quickly from Definition 2.2.1 and linearity of the standard integral operator. □

Proposition 2.2.2 (Semigroup property of fractional integration)**.** *For $\alpha, \beta > 0$, if $f \in L^p[a, b]$, $1 \leq p \leq \infty$ we have:*

$$({}_a\mathrm{I}_t^\alpha\, {}_a\mathrm{I}_t^\beta) f(t) = {}_a\mathrm{I}_t^{\alpha+\beta} f(t), \tag{2.3}$$

almost everywhere for $t \in [a, b]$. Furthermore, if $\alpha + \beta > 1$, the equality (2.3) *holds pointwise.*

Proof. See Samko, Kilbas, and Marichev [29], Chapter 1, (2.21). □

Proposition 2.2.3 (Boundedness in L^p)**.** *The Riemann-Liouville integral is bounded in $L^p[a, b]$ for $p \in [1, \infty]$, satisfying:*

$$||{}_a\mathrm{I}_t^\alpha f||_{L^p[a,b]} \leq \frac{(b-a)^\alpha}{\Gamma(\alpha+1)} ||f||_{L^p[a,b]}.$$

Proof. Writing the fractional integral as a convolution yields

$${}_a\mathrm{I}_t^\alpha f = \frac{1}{\Gamma(\alpha)} f * g, \quad \text{where} \quad g(s) = (t-s)^{\alpha-1} \mathbb{1}_{[a,t]}(s).$$

Now, using Young's Inequality for convolutions (see e.g. [24], Proposition 2.33) gives for $a < t \leq b$:

$$\begin{aligned} ||{}_a\mathrm{I}_t^\alpha f||_{L^p[a,b]} &\leq \frac{1}{\Gamma(\alpha)} ||f||_{L^p[a,b]} ||g||_{L^1(a,b)}, \\ &= \frac{1}{\Gamma(\alpha)} ||f||_{L^p[a,b]} \int_a^t (t-s)^{\alpha-1}\, \mathrm{d}s, \\ &= \frac{(t-a)^\alpha}{\Gamma(\alpha+1)} ||f||_{L^p[a,b]}, \\ &\leq \frac{(b-a)^\alpha}{\Gamma(\alpha+1)} ||f||_{L^p[a,b]}. \end{aligned}$$

□

Remark 2.2.1 (Continuity in f)*.* Since the Riemann-Liouville integral is both bounded and linear, it also acts continuously on f. Indeed, for some $f_1, f_2 : [a, b] \to \mathbb{R}$, $a < t \leq b$, we have

$$||{}_a\mathrm{I}_t^\alpha f_1 - {}_a\mathrm{I}_t^\alpha f_2||_{L^p[a,b]} = ||{}_a\mathrm{I}_t^\alpha\{f_1 - f_2\}||_{L^p[a,b]} \leq \frac{(b-a)^\alpha}{\Gamma(\alpha+1)} ||f_1 - f_2||_{L^p[a,b]},$$

proving continuity with respect to f.

Furthermore, the operator is continuous in t for continuous functions $f \in C[a, b]$:

Proposition 2.2.4 (Uniform continuity in t)**.** *Let $f : [a, b] \to \mathbb{R}$, $f \in C[a, b]$ and $\alpha \in (0, 1)$. Then, the Riemann-Liouville integral ${}_a\mathrm{I}_t^\alpha$ is uniformly continuous in t.*

Proof. Let $\varepsilon > 0$ arbitrary. Take $a < t < t' \leq b$ and $t' - t \leq \delta$. Then,

$$\begin{aligned}
|{}_a\mathrm{I}^\alpha_{t'} f - {}_a\mathrm{I}^\alpha_t f| &= \frac{1}{\Gamma(\alpha)}\left| \int_a^{t'} f(s)(t'-s)^{\alpha-1}\,\mathrm{d}s - \int_a^t f(s)(t-s)^{\alpha-1}\,\mathrm{d}s \right|, \\
&= \frac{1}{\Gamma(\alpha)}\left| \int_a^t f(s)\left[(t'-s)^{\alpha-1} - (t-s)^{\alpha-1}\right]\,\mathrm{d}s + \int_t^{t'} f(s)(t'-s)^{\alpha-1}\,\mathrm{d}s \right|, \\
&\leq \frac{1}{\Gamma(\alpha)} \int_a^t \left| f(s)\left[(t'-s)^{\alpha-1} - (t-s)^{\alpha-1}\right] \right| \mathrm{d}s + \frac{1}{\Gamma(\alpha)} \int_t^{t'} \left| f(s)(t'-s)^{\alpha-1} \right| \mathrm{d}s.
\end{aligned}$$

Now, since $a - 1 \in (-1, 0)$ and $(t' - s) > (t - s)$, we have $(t' - s)^{\alpha-1} - (t - s)^{\alpha-1} \geq 0$ for $a \leq s \leq t$. Furthermore, $(t' - s)^{\alpha-1} \geq 0$. Hence, we can apply Hölder's inequality twice, yielding:

$$\begin{aligned}
|{}_a\mathrm{I}^\alpha_{t'} f - {}_a\mathrm{I}^\alpha_t f| &\leq \frac{1}{\Gamma(\alpha)} \int_a^t \left((t'-s)^{\alpha-1} - (t-s)^{\alpha-1}\right)\,\mathrm{d}s\, ||f||_\infty + \frac{1}{\Gamma(\alpha)} \int_t^{t'} (t'-s)^{\alpha-1}\,\mathrm{d}s\, ||f||_\infty, \\
&= \frac{(t-a)^\alpha - (t'-a)^\alpha + 2(t'-t)^\alpha}{\Gamma(\alpha+1)} ||f||_\infty, \\
&= \frac{-\left((t'-a)^\alpha - (t-a)^\alpha\right) + 2(t'-t)^\alpha}{\Gamma(\alpha+1)} ||f||_\infty, \\
&\leq \frac{2(t'-t)^\alpha}{\Gamma(\alpha+1)} ||f||_\infty,
\end{aligned}$$

Here, the final inequality follows since $t' > t$ gives $(t'-a)^\alpha - (t-a)^\alpha > 0$. Now, taking $\delta = \left(\frac{\Gamma(\alpha+1)\varepsilon}{2\,||f||_\infty}\right)^{1/\alpha}$ and taking the supremum over t with $t' \in [a, T]$ gives $||{}_a\mathrm{I}^\alpha_{t'} f - {}_a\mathrm{I}^\alpha_t f||_\infty \leq \varepsilon$, proving uniform continuity. Here, $||f||_\infty := \sup_{s\in[a,b]} |f(s)|$. □

And finally, under conditions of integrability of f, the Riemann-Liouville derivative depends continuously on the fractional derivative order α:

Proposition 2.2.5 (Continuity in α)**.** *For $f \in L^p[a, b]$, the Riemann-Liouville fractional integral ${}_a\mathrm{I}^\alpha_t f(t)$, $a < t \leq b$, is continuous with respect to α in $L^p[a, b]$. Hence,*

$$\lim_{\alpha\to\alpha'} ||{}_a\mathrm{I}^\alpha_t f - {}_a\mathrm{I}^{\alpha'}_t f||_{L^p[a,b]} = 0.$$

Proof. See the proof of Theorem 2.6 of [29]. □

2.2.3. Results for polynomial functions

In this section, the results of a few fundamental integrated polynomial functions will be presented. These results will be used throughout the rest of the thesis. First, we define a special function which of much use in the field of fractional differential equations: the beta function.

Definition 2.2.2 (Beta function ([27], (1.20)))**.** For $x, y > 0$, denote the beta function as

$$\mathrm{B}(x, y) = \int_0^1 \vartheta^{x-1}(1-\vartheta)^{y-1}\,\mathrm{d}\vartheta.$$

A frequently used characterization, obtained by for instance the Laplace transform (see for instance [27], (1.24)), is given as follows:

Remark 2.2.2 (Relationship beta and gamma function)*.*

$$\mathrm{B}(x, y) = \frac{\Gamma(x)\Gamma(y)}{\Gamma(x+y)}.$$

Here, as before, $\Gamma(x) = \int_0^\infty t^{x-1}e^{-t}\,\mathrm{d}t$ generalizes the factorial function such that $\Gamma(n) = (n-1)!$ for $n \in \mathbb{N}$. In this expression, it can easily be seen that the beta function is symmetric, as $\mathrm{B}(x, y) = \mathrm{B}(y, x)$. Armed with this equipment, let us assess the fractional integral of a polynomial function.

Proposition 2.2.6 (Fractional integral of a polynomial)**.** *For $\alpha \in (0, \infty), k > -1$, the fractional integral order α of a monomial of degree k gives:*

$$ {}_0\mathrm{I}_t^\alpha t^k = \frac{\Gamma(k+1)}{\Gamma(\alpha+k+1)} t^{\alpha+k}. $$

Proof. Writing out the fractional integral and using a substitution $z := \frac{s}{t}$, corresponding to $\mathrm{d}s = t\,\mathrm{d}z$, gives:

$$ \begin{aligned} {}_0\mathrm{I}_t^\alpha t^k &= \frac{1}{\Gamma(\alpha)} \int_0^t (t-s)^{\alpha-1} s^k \,\mathrm{d}s, \\ &= \frac{t}{\Gamma(\alpha)} \int_0^1 (t-tz)^{\alpha-1} (tz)^k \,\mathrm{d}z, \\ &= \frac{t^{\alpha+k}}{\Gamma(\alpha)} \int_0^1 (1-z)^{\alpha-1} z^k \,\mathrm{d}z, \\ &= \frac{t^{\alpha+k}}{\Gamma(\alpha)} \mathrm{B}(k+1, \alpha), \\ &= \frac{\Gamma(k+1)}{\Gamma(\alpha+k+1)} t^{\alpha+k}. \end{aligned} $$

□

Another useful result is the fractional integral of an incomplete part of the domain of the function. First, define the incomplete beta function as:

Definition 2.2.3 (Incomplete beta function [25])**.** For $x, y, t > 0$, denote the incomplete beta function as

$$ \mathrm{B}_t(x, y) = \int_0^t \vartheta^{x-1} (1-\vartheta)^{y-1} \,\mathrm{d}\vartheta. $$

Taking $0 < b \leq t$, this now gives us a description of the fractional integral of a polynomial with support $[0, b]$ at evaluation point t:

Proposition 2.2.7 (Incomplete endpoint fractional integral of a polynomial)**.** *For $\alpha \in (0, \infty)$, $k > -1$, $0 < b \leq t$, the fractional integral order $\alpha \in [0, \infty)$ of a monomial $\mathbb{1}_{[0,b]} s^k : [0, b] \to \mathbb{R}$ gives:*

$$ {}_0\mathrm{I}_t^\alpha \{\mathbb{1}_{[0,b]} s^k\}(t) = \frac{1}{\Gamma(\alpha)} \int_0^b (t-s)^{\alpha-1} s^k \,\mathrm{d}s = \frac{t^{\alpha+k}}{\Gamma(\alpha)} \mathrm{B}_{b/t}(k+1, \alpha) $$

.

Proof. Similar to the proof of Proposition 2.2.6, using the substitution $z := \frac{s}{T}$ gives

$$ \begin{aligned} \frac{1}{\Gamma(\alpha)} \int_0^b (t-s)^{\alpha-1} s^k \,\mathrm{d}s &= \frac{t^{\alpha+k}}{\Gamma(\alpha)} \int_0^{b/t} (1-z)^{\alpha-1} z^k \,\mathrm{d}z, \\ &= \frac{t^{\alpha+k}}{\Gamma(\alpha)} \mathrm{B}_{b/t}(k+1, \alpha). \end{aligned} $$

□

Remark 2.2.3 (Fractional on functions of limited support are non-constant). Combining the results of Proposition 2.2.6 and 2.2.7, we can now formulate the fractional integral of a polynomial with limited support. Write $\mathbb{1}_{[0,b]} s^k : [0, b] \to \mathbb{R}$ for $k > -1$. Then using the results written out as Beta functions, one has:

$$ {}_0\mathrm{I}_t^\alpha \mathbb{1}_{[0,b]} s^k = \begin{cases} \frac{t^{\alpha+k}}{\Gamma(\alpha)} \mathrm{B}(k+1, \alpha) & \text{if} \quad t \leq b \\ \frac{t^{\alpha+k}}{\Gamma(\alpha)} \mathrm{B}_{b/t}(k+1, \alpha) & \text{if} \quad t > b \end{cases} = \frac{t^{\alpha+k}}{\Gamma(\alpha)} \mathrm{B}_{\min(1, b/t)}(k+1, \alpha). $$

One very important result of this observation is the fact that fractional integrals of functions of limited support remain non-constant after the function's support. This contrasts the regular integral operator $\alpha = 1$, where one always has ${}_0\mathrm{I}_t \mathbb{1}_{[0,b]} f(s) = c \in \mathbb{R}$ for all $t > b$. An illustration of this phenomenon is provided in Figure 2.2. In practice, this is in an illustration of the "unlimited memory" required for the Riemann-Liouville fractional integral, since the operator at t will always be influenced by every value of the function at $s \leq t$.

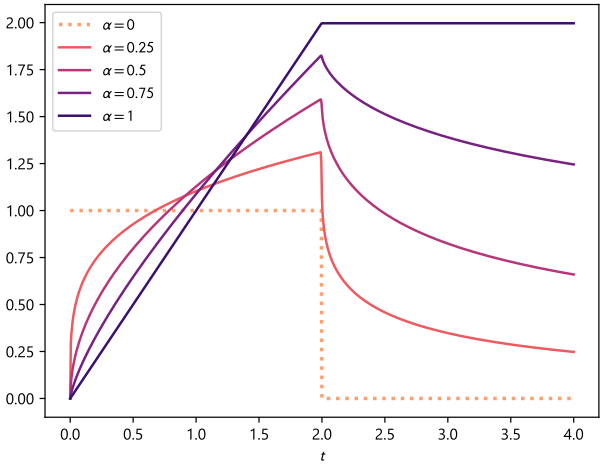

Figure 2.2: The fractional integral of order α of the function $f(t) = \mathbb{1}_{[0,2]}(t)$, showing nonconstant values after its support for fractional values of α. Note that the result for $\alpha = 0$ yields f itself.

Finally, for the incomplete starting point, integrating on $[t, T]$ with its evaluation point at T gives:
Proposition 2.2.8 (Incomplete starting point fractional integral of a polynomial)**.** *For $\alpha \in (0, \infty)$, $k > -1$, $0 \leq t \leq T$, the fractional integral order α of a monomial of degree k gives:*

$$ {}_t\mathrm{I}^{\alpha}_T t^k = \frac{1}{\Gamma(\alpha)} \int_t^T (T-s)^{\alpha-1} s^k \,\mathrm{d}s = \frac{T^{\alpha+k}}{\Gamma(\alpha)} \mathrm{B}_{1-t/T}(\alpha, k+1). $$

.

Note the change in arguments of the (non-symmetric!) incomplete beta function as compared to the result of Proposition 2.2.7.

Proof. First, using the substitution $\varphi := T - s$ gives $\mathrm{d}s = -\mathrm{d}\varphi$ and thus:

$$ \frac{1}{\Gamma(\alpha)} \int_t^T (T-s)^{\alpha-1} s^k \,\mathrm{d}s = \frac{1}{\Gamma(\alpha)} \int_0^{T-t} \varphi^{\alpha-1} (T-\varphi)^k \,\mathrm{d}\varphi. $$

Now, as in Proposition 2.2.7, use the substitution $z := \frac{\varphi}{T}$, providing

$$ \begin{aligned} \frac{1}{\Gamma(\alpha)} \int_0^{T-t} \varphi^{\alpha-1} (T-\varphi)^k \,\mathrm{d}s &= \frac{T^{\alpha+k}}{\Gamma(\alpha)} \int_0^{1-t/T} z^{\alpha-1} (1-z)^k \,\mathrm{d}z, \\ &= \frac{T^{\alpha+k}}{\Gamma(\alpha)} \mathrm{B}_{1-t/T}(\alpha, k+1). \end{aligned} $$

□

2.3. Fractional derivation

Since we now have established a way to define fractional integration, one can establish fractional differentiation as a combination of integer-order differentiation and fractional integration. The most straightforward definition of a fractional derivative ${}_a\mathrm{D}^{\alpha}_x$ then becomes:

Definition 2.3.1 (Left-sided Riemann-Liouville fractional derivative [16, 15, 27])**.** For $a < t \leq b$, let $f \in L^1[a,b]$ and $n = \lceil \alpha \rceil$, hence, n is the smallest integer such that $n \geq \alpha$. The left-sided Riemann-Liouville fractional derivative is defined as

$$\begin{aligned} {}_a\mathrm{D}_t^\alpha f(t) &= \frac{\mathrm{d}^n}{\mathrm{d}t^n} {}_a\mathrm{I}_t^{n-\alpha} f(t), \\ &= \frac{1}{\Gamma(n-\alpha)} \frac{\mathrm{d}^n}{\mathrm{d}t^n} \int_a^t (t-s)^{n-\alpha-1} f(s)\,\mathrm{d}s, \end{aligned}$$

where ${}_a\mathrm{I}_t^{n-\alpha}$ represents the Riemann-Liouville fractional integral operator as defined in Definition 2.2.1.
Remark 2.3.1. Frequently, α is chosen to satisfy $\alpha \in (0,1]$, resulting in:

$${}_a\mathrm{D}_t^\alpha f(t) = \frac{1}{\Gamma(1-\alpha)} \frac{\mathrm{d}}{\mathrm{d}t} \int_a^t (t-s)^{-\alpha} f(s)\,\mathrm{d}s.$$

However, this derivative is not the only admissible definition. Another frequently used characterization of the fractional derivative is the derivative of Caputo-type, where the order of differentiation and integration is swapped:
Definition 2.3.2 (Left-sided Caputo fractional derivative [16, 15, 27])**.** For $a < t \leq b$, let $f \in C^n[a,b]$ for $n = \lceil \alpha \rceil$. The left-sided Caputo fractional derivative is defined as

$$\begin{aligned} {}_a^{\mathrm{C}}\mathrm{D}_t^\alpha f(t) &= {}_a\mathrm{I}_t^{n-\alpha} \frac{\mathrm{d}^n}{\mathrm{d}t^n} f(t), \\ &= \frac{1}{\Gamma(n-\alpha)} \int_a^t \left((t-s)^{n-\alpha-1} \frac{\mathrm{d}^n}{\mathrm{d}s^n} f(s) \right) \mathrm{d}s. \end{aligned}$$

Remark 2.3.2. As above, for $\alpha \in (0,1]$, this gives

$${}_a^{\mathrm{C}}\mathrm{D}_t^\alpha f(t) = \frac{1}{\Gamma(1-\alpha)} \int_a^t \left((t-s)^{-\alpha} \frac{\mathrm{d}}{\mathrm{d}t} f(s) \right) \mathrm{d}s.$$

The Caputo derivative has an interesting propery which gives it some advantages in application:
Remark 2.3.3 (Initial values and the Caputo derivative of constants). Note that since the derivative of a constant is 0, for any $f(t) = c \in \mathbb{R}$, one has ${}_a^{\mathrm{C}}\mathrm{D}_t^\alpha f(t) = 0$. Because of this property, the Caputo fractional derivative has the useful property that when used in fractional differential equations, it does not require initial values of fractional order but of integer order (see e.g. [27], Section 2.4.1). This makes the Caputo derivative more suitable for use in applications, as commonly, only integer-order initial conditions are known for physical problems. However, this poses another problem:
Remark 2.3.4 (Limit to 0'th order Caputo derivative). Take $\alpha \in (0,1]$. Then, by Remark 2.3.2 and Remark 2.2.5, one has:

$$\lim_{\alpha \downarrow 0} {}_a^{\mathrm{C}}\mathrm{D}_t^\alpha f(t) = f(t) - f(a),$$

which is not equal to the identity.

Now that the most frequently used fractional derivative operators have been established, let us look at a graphical outline of some calculation examples in Figure 2.3.

Finally, as a more general fractional derivative, we introduced a parametrization creating a continuous transition between the Caputo and Riemann-Liouville derivatives, often called the Hilfer derivative due to its first definition by Rudolf Hilfer in Chapter $\mathrm{II}.3$ of [15]:
Definition 2.3.3 (Hilfer derivative, [15])**.** For $\alpha \in (0,1]$, $\beta \in [0,1]$, define the Hilfer derivative as

$${}_a\mathrm{D}_t^{\alpha,\beta} = {}_a\mathrm{I}_t^{\beta(1-\alpha)} \frac{\mathrm{d}}{\mathrm{d}t} {}_a\mathrm{I}_t^{(1-\beta)(1-\alpha)},$$

where ${}_a\mathrm{I}_t$ denotes the left-sided Riemann-Liouville fractional integral as defined in Definition 2.2.1.

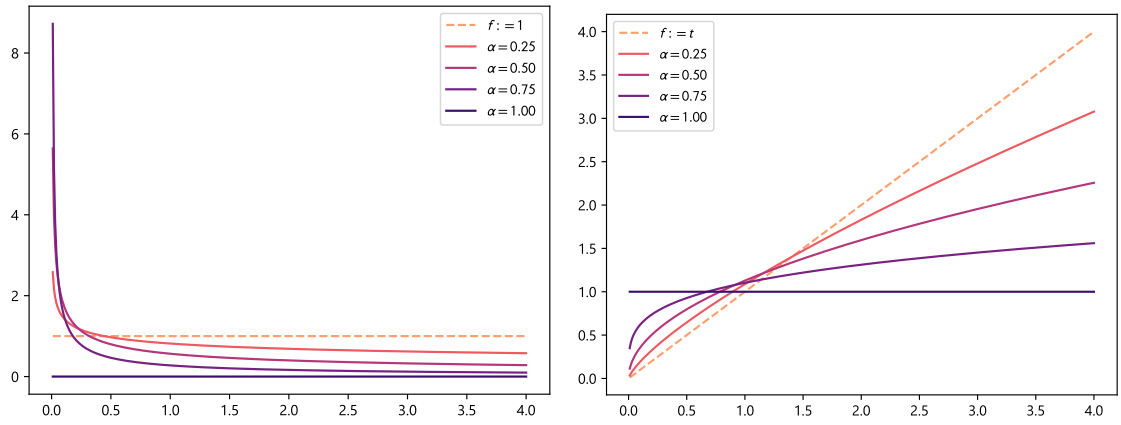

(a) Riemann-Liouville fractional derivative of $f(t) = 1$, with a cut-off of singular behavior near $t = 0$ in graphical presentation. Note that the Caputo derivative gives 0 for all $\alpha \in (0, 1]$ as f is constant.

(b) Fractional derivative of $f(t) = t$. In this case, both the Caputo and Riemann-Liouville derivative yield the same result.

Figure 2.3: Examples of explicit calculations of the fractional derivative.

Remark 2.3.5. In particular, the Hilfer derivative is equal to the Riemann-Liouville derivative ${}_a\mathrm{D}_t^{\alpha,\beta}$ and Caputo-derivative ${}_a^{\mathrm{C}}\mathrm{D}_t^{\alpha,\beta}$ for two respective choices of β:

$$\begin{cases} {}_a\mathrm{D}_t^{\alpha,\beta} = {}_a\mathrm{D}_t^{\alpha}, & \text{for } \beta = 0, \\ {}_a\mathrm{D}_t^{\alpha,\beta} = {}_a^{\mathrm{C}}\mathrm{D}_t^{\alpha}, & \text{for } \beta = 1. \end{cases}$$

Using a parametrization $\gamma := \alpha + \beta - \alpha\beta$, these cases are equal to $\gamma = \alpha$ and $\gamma = 1$ respectively. This gives a direct way of assessing the difference between solutions using the Riemann-Liouville and Caputo derivatives. Let us look at the main difference:

Remark 2.3.6. For most functions, Hilfer derivatives of different type β yield the same output. The main difference arises in the kernel behavior of ${}_a\mathrm{D}_t^{\alpha,\beta}$. As can be seen from Definition 2.3.3, we have that ${}_a\mathrm{D}_t^{\alpha,\beta} = 0$ if

$${}_a\mathrm{I}_t^{(1-\beta)(1-\alpha)} f = c,$$

where $c \in \mathbb{R}$ is a constant. With the notation $\gamma := \alpha + \beta - \alpha\beta$, this gives The Caputo derivative ($\beta = 1$) indeed gives 0 for $f = c$, whereas Riemann-Liouville ($\beta = 0$) maps to 0 for ${}_a\mathrm{I}_t^{1-\alpha} f = 0$. In particular, by Proposition 2.2.6 this yields that for a polynomial t^k with $k > -1$, ${}_a\mathrm{D}_t^{\alpha,\beta} t^k = 0$ for $k = \gamma - 1$.

To conclude, when applied to differential equations, the Caputo-derivative provides a more meaningful interpretation and a guarantee on regularity of solutions, as discussed above. However, this comes at a cost of more strict differentiability function requirements. To make the case for most general requirements and applications as possible, the Hilfer derivative will be used in this thesis for all theoretical proofs. In implementation of the numerical methods, the Caputo derivative will be used for the core of the methods where continuity of the solutions is required, with a note on the implementation and approximations using the general Hilfer derivative. Finally, for the applications to the fractionally damped Van der Pol oscillator, the Caputo derivative will be used for a more intuitive and clear physical interpretation.

3

Existence and uniqueness for Hilfer-derivative fractional differential equations

As discussed in the previous section, the fractional derivative of the Hilfer-type (Definition 2.3.3) generalizes the two most important fractional differential operators, the Riemann-Liouville and Caputo operator. Furthermore, it provides a direct intuition on the dependence of solutions on the type of operator by parametrizing this choice in the type parameter $\beta \in [0,1]$. The Hilfer derivative has already been applied to study initial value problems (IVP's) in the work of Furati, Kassim, and Tatar [11], of which a summary will be provided in Section 3.1. Furthermore, (semi-)periodic boundary-value problems (BVP's) have been studied using the Caputo derivative by for instance the work of Fečkan and Marynets [8]. To combine both strategies and provide the most general setting possible, this chapter presents the existence and uniqueness of solutions to BVP's using the Hilfer derivative in Section 3.2. These results will be used in later chapters on spline approximation techniques.

3.1. Initial value problems

Take the Hilfer-derivative Cauchy-type IVP:

$$\begin{cases} {}_0\mathrm{D}_t^{\alpha,\beta}\mathbf{x}(t) = \mathbf{f}(t,\mathbf{x}(t)), & 0 < t \leq T, \quad 0 < \alpha < 1, \quad 0 \leq \beta \leq 1, \\ {}_0\mathrm{I}_t^{1-\gamma}\mathbf{x}(0) = \tilde{\mathbf{x}}_0, & \gamma = \alpha + \beta - \alpha\beta. \end{cases} \tag{3.1}$$

Here, ${}_0\mathrm{D}_t^{\alpha,\beta}$ represents the Hilfer fractional derivative as defined in Definition 2.3.3 and ${}_0\mathrm{I}_t^{1-\gamma}$ the Riemann-Liouville derivative (Definition 2.2.1). Furthermore, we have $\mathbf{x} : [0,T] \mapsto D \subset \mathbb{R}^d$, $\mathbf{f} : [0,T] \times D \mapsto \mathbb{R}^d$ and $\mathbf{x}, \mathbf{f} \in C_{1-\gamma}[0,T] := \{g : [0,T] \to \mathbb{R}^d, t^{1-\gamma}g \in C[0,T]\}$, where domain D is closed and bounded in the norm $||g||_{1-\gamma} := \sup_{t\in[a,b]} \left|(t-a)^{1-\gamma}g(t)\right|$. The notational convention is taken of ${}_0\mathrm{I}_t^{\alpha} f(0) = \lim_{t\downarrow 0} {}_0\mathrm{I}_t^{\alpha} f(t)$. Note that as per Remark 2.3.5, the choice of $\beta = 0$ gives the Riemann-Liouville fractional derivative and $\beta = 1$ the Caputo fractional derivative. Furthermore, the problem reduces to a regular IVP for $\beta = 1$, yielding $\gamma = 1$.

Now, consider the space of ζ-Riemann-Liouville differentiable functions in the weighed norm space:

$$C_{1-\gamma}[a,b] := \left\{ f : [a,b] \to \mathbb{R}^d, \quad (t-a)^{1-\gamma} f \in C[a,b] \right\}.$$

This gives the necessary definitions to establish the equivalent integral equation to the IVP:

Theorem 3.1.1 (Hilfer-IVP equivalent integral equation ([11], Theorem 23))**.** *For* $\mathbf{x} \in C_{1-\gamma}^{\gamma}[0,T]$*,* $\mathbf{x}$ *satisfies IVP* (3.1) *if and only if* $\mathbf{x}$ *satisfies*

$$\mathbf{x}(t) = \frac{\tilde{\mathbf{x}}_0}{\Gamma(\gamma)} t^{\gamma-1} + {}_0\mathrm{I}_t^{\alpha}\mathbf{f}(t,\mathbf{x}(t)), \quad 0 < t \leq T. \tag{3.2}$$

Proof. See the proof of Theorem 23 of Furati, Kassim, and Tatar [11], extended componentwise to $\mathbb{R}^d$. □

Then, by using Banach's fixed point theorem and iterations over the interval $(0, T]$, existence and uniqueness of the IVP can be proven:

Theorem 3.1.2 (Hilfer IVP existence and uniqueness)**.** *Consider the Hilfer IVP* (3.1)*. Assume* $\mathbf{f} \in C_{1-\gamma}^{\beta(1-\alpha)}[0, T]$ *in* t*, and* $\mathbf{f}$ *satisfies the Lipschitz condition in* $\mathbf{x}$ *component wise, hence, there exists a nonnegative* $d \times d$ *matrix* $\mathbf{K}$ *such that:*

$$|\mathbf{f}(t, \mathbf{u}(t)) - \mathbf{f}(t, \mathbf{v}(t))| \leq \mathbf{K}|\mathbf{u}(t) - \mathbf{v}(t)|,$$

for all $t \in (0, T]$ *for* $\mathbf{u}(t), \mathbf{v}(t) \in D$*.*

Then, there exists a unique solution $\mathbf{x} \in C_{1-\gamma}^{\gamma}[0, T]$ *for initial value problem* (3.1)*.*

Proof. See the proof of Theorem 25 of Furati, Kassim, and Tatar [11], extended componentwise to $\mathbb{R}^d$. □

This provides the basis for the expansion to boundary value problems:

3.2. Boundary value problems

Consider the integral-BVP:

$$ {}_0\mathrm{D}_t^{\alpha,\beta}\mathbf{x}(t) = \mathbf{f}(t, \mathbf{x}(t)), \quad 0 < t < T, \quad 0 < \alpha < 1, \quad 0 \leq \beta \leq 1, \tag{3.3}$$

$$ {}_0\mathrm{I}_t^{1-\gamma}\mathbf{x}(0) = {}_0\mathrm{I}_t^{1-\gamma}\mathbf{x}(T), \quad \gamma = \alpha + \beta - \alpha\beta. \tag{3.4}$$

Here, ${}_0\mathrm{D}_t^{\alpha,\beta}$ represents the Hilfer fractional derivative as defined in Definition 2.3.3 and ${}_0\mathrm{I}_t^{1-\gamma}$ the Riemann-Liouville derivative (Definition 2.2.1). Furthermore, we have $\mathbf{x} : [0, T] \mapsto D \subset \mathbb{R}^d$, $\mathbf{f} : [0, T] \times D \mapsto \mathbb{R}^d$, where D is closed and bounded in the norm $||g||_{1-\gamma} := \sup_{t\in[a,b]} \left|(t-a)^{1-\gamma} g(t)\right|$. Finally, assume $\mathbf{f} \in C_{1-\gamma}^{\beta(1-\alpha)}[0, T]$. Note that as per Remark 2.3.5, the choice of $\beta = 0$ gives the Riemann-Liouville fractional derivative and $\beta = 1$ the Caputo fractional derivative. Furthermore, the problem reduces to a BVP with non-integral boundary condition $\mathbf{x}(0) = \mathbf{x}(T)$ for the Caputo case of $\beta = 1$, yielding $\gamma = 1$.

3.2.1. The perturbed initial value problem

In order to find a solution to BVP (3.3) - (3.4), a formulation is made using a perturbation of the corresponding IVP:

$$ {}_0\mathrm{D}_t^{\alpha,\beta}\mathbf{x}(t) = \mathbf{f}(t, \mathbf{x}(t)) + \Delta(\tilde{\mathbf{x}}_0), \tag{3.5}$$

$$ {}_0\mathrm{I}_t^{1-\gamma}\mathbf{x}(0) = \tilde{\mathbf{x}}_0, \tag{3.6}$$

with $\Delta(\tilde{\mathbf{x}}_0) \in \mathbb{R}^d$. By Theorem 3.1.1, every solution $\mathbf{x} \in C_{1-\gamma}^{\gamma}[0, T]$ to the perturbed IVP (3.5)- (3.6) must satisfy the perturbed integral equation

$$\mathbf{x}(t) = \frac{\tilde{\mathbf{x}}_0}{\Gamma(\gamma)} t^{\gamma-1} + {}_0\mathrm{I}_t^{\alpha}\left[\mathbf{f}(t, \mathbf{x}(t)) + \Delta(\tilde{\mathbf{x}}_0)\right]. \tag{3.7}$$

Now, as in Equation 13 of Theorem 23 of [11], this gives a fractional integral of

$$\begin{aligned} {}_0\mathrm{I}_t^{1-\gamma}\mathbf{x}(t) &= {}_0\mathrm{I}_t^{1-\gamma}\left[\frac{\tilde{\mathbf{x}}_0}{\Gamma(\gamma)} t^{\gamma-1} + {}_0\mathrm{I}_t^{\alpha}\left[\mathbf{f}(t, \mathbf{x}(t)) + \Delta(\tilde{\mathbf{x}}_0)\right]\right], \\ &= \tilde{\mathbf{x}}_0 + {}_0\mathrm{I}_t^{1-\gamma+\alpha}\mathbf{f}(t, \mathbf{x}(t)) + {}_0\mathrm{I}_t^{1-\gamma+\alpha}\Delta(\tilde{\mathbf{x}}_0). \end{aligned}$$

Computing the limit, using Lemma 13 of [11] gives

$$\lim_{t\to 0} {}_0\mathrm{I}_t^{1-\gamma}\mathbf{x}(t) = \tilde{\mathbf{x}}_0.$$

Then, (3.4) yields

$$\begin{aligned}\tilde{\mathbf{x}}_0 &= \tilde{\mathbf{x}}_0 + \left[{}_0\mathrm{I}_t^{1-\gamma+\alpha}\mathbf{f}(t,\mathbf{x}(t)) + {}_0\mathrm{I}_t^{1-\gamma+\alpha}\Delta(\tilde{\mathbf{x}}_0)\right]_{t=T},\\ &= \tilde{\mathbf{x}}_0 + \left[{}_0\mathrm{I}_t^{1-\gamma+\alpha}\mathbf{f}(t,\mathbf{x}(t))\right]_{t=T} + \frac{\Delta(\tilde{\mathbf{x}}_0)T^{1-\gamma+\alpha}}{\Gamma(2-\gamma+\alpha)},\end{aligned}$$

where the final expression follows from writing out the Riemann-Liouville integral of a constant. This, writing out the integral operators and solving for $\Delta(\tilde{\mathbf{x}}_0)$ gives

$$\begin{aligned}\Delta(\tilde{\mathbf{x}}_0) &= -\frac{\Gamma(2-\gamma+\alpha)}{T^{1-\gamma+\alpha}}\left[{}_0\mathrm{I}_t^{1-\gamma+\alpha}\mathbf{f}(t,\mathbf{x}(t))\right]_{t=T},\\ &= -\frac{1-\gamma+\alpha}{T^{1-\gamma+\alpha}}\int_0^T (T-s)^{-\gamma+\alpha}\mathbf{f}(s,\mathbf{x}(s))\,\mathrm{d}s,\\ &= -\frac{1-\gamma+\alpha}{T^{1-\gamma+\alpha}}\int_0^T (T-s)^{-\gamma+\alpha}\mathbf{f}(s,\mathbf{x}(s))\,\mathrm{d}s.\end{aligned}$$

Substituting the expression for $\Delta(\tilde{\mathbf{x}}_0)$ back in (3.7) yields the integral equation of:

$$\begin{aligned}\mathbf{x}(t) =& \frac{\tilde{\mathbf{x}}_0}{\Gamma(\gamma)}t^{\gamma-1} + \frac{1}{\Gamma(\alpha)}\Bigg[\int_0^t (t-s)^{\alpha-1}\mathbf{f}(s,\mathbf{x}(s))\,\mathrm{d}s\\ &- \left(\frac{1-\gamma}{\alpha}+1\right)T^{\gamma-1}\left(\frac{t}{T}\right)^{\alpha}\int_0^T (T-s)^{\alpha-\gamma}\mathbf{f}(s,\mathbf{x}(s))\,\mathrm{d}s\Bigg],\end{aligned} \tag{3.8}$$

which is the equivalent integral equation of the perturbed IVP (3.5) - (3.6) satisfying BVP (3.3) - (3.4). Since both the left-hand and right-hand side expressions contain the solution $\mathbf{x}$, this implicit formulation cannot be used to directly obtain the solution in a closed-form expression. Thus, in the next section, this integral equation will be used as a starting point to obtain iterative solutions for the integral boundary value problem.

3.2.2. Existence and uniqueness results and approximations

Now, assume that for BVP (3.3) - (3.4), the following conditions hold:

A.1 The function $\mathbf{f} : [0,T]\times D \mapsto \mathbb{R}^d$ satisfies $\mathbf{f} \in C_{1-\gamma}[0,T]$ and the componentwise inequality:

$$||t \mapsto \mathbf{f}(.,\mathbf{u})||_{1-\gamma} \leq \mathbf{m}, \tag{3.9}$$

for some nonnegative $\mathbf{m} \in \mathbb{R}^d$ and $\mathbf{f}$ satisfies the Lipschitz condition in $\mathbf{x}$ component wise, hence, there exists a nonnegative $d \times d$ matrix $\mathbf{K}$ such that:

$$|\mathbf{f}(t,\mathbf{u}(t)) - \mathbf{f}(t,\mathbf{v}(t))| \leq \mathbf{K}|\mathbf{u}(t) - \mathbf{v}(t)|, \tag{3.10}$$

for all $t \in (0,T]$ for $\mathbf{u}(t), \mathbf{v}(t) \in D$.

A.2 The set

$$D_\beta = \left\{\frac{\tilde{\mathbf{x}}_0}{\Gamma(\gamma)}t^{\gamma-1} \in D : \left\{\mathbf{u} \in C_{1-\gamma}[0,T] : \left|\left|\mathbf{u} - \frac{\tilde{\mathbf{x}}_0}{\Gamma(\gamma)}t^{\gamma-1}\right|\right| \leq \beta\right\} \subset D\right\},$$

is non-empty, where $\beta := \Xi\mathbf{m}$, with $\Xi \in \mathbb{R}$ satisfying

$$\begin{aligned}\Xi = \sup_{t\in[0,T]}\Bigg(&\frac{\mathrm{B}(\alpha,\gamma)\,t^{\alpha}}{\Gamma(\alpha)} + \frac{t^{\alpha+1-\gamma}}{\Gamma(\alpha)T^{1-\gamma}}\Bigg[-\mathrm{B}_{t/T}(\gamma,\alpha-\gamma+1) + \mathrm{B}_{1-t/T}(\alpha-\gamma+1,\gamma)\\ &+ \left(\frac{1-\gamma}{\alpha}\right)\mathrm{B}(\alpha-\gamma+1,\gamma)T^{-1}\Bigg]\Bigg),\end{aligned} \tag{3.11}$$

where B denotes the (incomplete) beta function as defined in Definition 2.2.2 and 2.2.3.

A.3 The matrix $\mathbf{Q}$ defined as

$$\mathbf{Q} := \Xi \mathbf{K} \tag{3.12}$$

satisfies the spectral radius requirement of

$$\rho(\mathbf{Q}) < 1. \tag{3.13}$$

Then, we can approximate a solution to the problem (3.3)-(3.4) in the space $C_{1-\gamma}[0,T]$ as a sequence of functions

$$\begin{aligned}\mathbf{x}_{m+1}(t) =& \frac{\tilde{\mathbf{x}}_0}{\Gamma(\gamma)} t^{\gamma-1} + \frac{1}{\Gamma(\alpha)} \left[\int_0^t (t-s)^{\alpha-1} \mathbf{f}(s, \mathbf{x}_m(s)) \, \mathrm{d}s \right. \\ & \left. - \left(\frac{1-\gamma}{\alpha} + 1 \right) T^{\gamma-1} \left(\frac{t}{T} \right)^{\alpha} \int_0^T (T-s)^{\alpha-\gamma} \mathbf{f}(s, \mathbf{x}_m(s)) \, \mathrm{d}s \right]. \end{aligned} \tag{3.14}$$

The convergence of sequence (3.14) and its relation to BVP (3.3)-(3.4) will be proven in Theorem 3.2.1 and 3.2.2, with preceding Lemma's 3.2.1 and 3.2.2 providing required preliminary results.
Remark 3.2.1. For $\beta = 1$, which gives $\gamma = \alpha + \beta - \alpha\beta = 1$, expression (3.11) can be computed explicitly, yielding:

$$\Xi = \sup_{t \in [0,T]} \frac{2(t - t^2/T)^{\alpha}}{\Gamma(\alpha+1)} = \left[\frac{2(t - t^2/T)^{\alpha}}{\Gamma(\alpha+1)} \right]_{t=T/2} = \frac{2(T/4)^{\alpha}}{\Gamma(\alpha+1)} = \frac{T^{\alpha}}{2^{2\alpha-1}\Gamma(\alpha+1)},$$

providing the bounds as in [8] as expected for the Caputo derivative case $\beta = 1$.

However, for $\beta < 1$, it is in general not possible to yield a closed-form expression for Ξ because of the incomplete Beta function. The supremum can be numerically approximated using numerical optimization techniques with built-in expressions for the incomplete beta function in numerical software. If an explicit error bound is required however, a less tightly bounded but explicitly available expression for Ξ of the form:

$$\Xi = T^{\alpha} \left[\frac{\left(\frac{\alpha}{2\alpha-\gamma+1} \right)^{\alpha} \left(1 - \frac{\alpha}{2\alpha-\gamma+1} \right)^{\alpha-\gamma+1}}{(\alpha-\gamma+1)\,\Gamma(\alpha)} + \frac{\left(\frac{\alpha\gamma}{\alpha+1} \mathrm{B}(\alpha,\gamma) \right)^{\alpha} \Gamma(\gamma)}{(\alpha+1)\,\Gamma(\alpha+\gamma)} + \frac{(1-\gamma)\,\mathrm{B}(\alpha-\gamma+1,\gamma)}{\Gamma(\alpha+1)} \right],$$

of which the derivation is given in Appendix A.
Lemma 3.2.1. *Let* $\mathbf{f}(t) \in C_{1-\gamma}[0,T]$. *Then for all* $t \in [0,T]$, *we have*

$$\left| \frac{t^{1-\gamma}}{\Gamma(\alpha)} \left[\int_0^t (t-s)^{\alpha-1} \mathbf{f}(s) \, \mathrm{d}s - \left(\frac{1-\gamma}{\alpha} + 1 \right) T^{\gamma-1} \left(\frac{t}{T} \right)^{\alpha} \int_0^T (T-s)^{\alpha-\gamma} \mathbf{f}(s) \, \mathrm{d}s \right] \right| \leq \xi_1(t) ||\mathbf{f}||_{1-\gamma},$$

where

$$\begin{aligned}\xi_1(t) =& \frac{\mathrm{B}(\alpha,\gamma)\, t^{\alpha}}{\Gamma(\alpha)} + \frac{t^{\alpha+1-\gamma}}{\Gamma(\alpha) T^{1-\gamma}} \left[-\mathrm{B}_{t/T}(\gamma, \alpha-\gamma+1) + \mathrm{B}_{1-t/T}(\alpha-\gamma+1, \gamma) \right. \\ & \left. + \left(\frac{1-\gamma}{\alpha} \right) \mathrm{B}(\alpha-\gamma, \gamma) T^{-1} \right]. \end{aligned} \tag{3.15}$$

Here, B *denotes the beta function and* B_z *denotes the incomplete beta function up to* z *as introduced in Definition 2.2.2 and 2.2.3 respectively. The inequalities on both* $|\,.\,|$ *and* $||\,.\,||_{1-\gamma}$ *can be seen component wise.*

Proof. First, writing out the expression to three nonnegative integrals gives:

$$\begin{aligned}& \left| \frac{t^{1-\gamma}}{\Gamma(\alpha)} \left[\int_0^t (t-s)^{\alpha-1} \mathbf{f}(s) \, \mathrm{d}s - \left(\frac{1-\gamma}{\alpha} + 1 \right) T^{\gamma-1} \left(\frac{t}{T} \right)^{\alpha} \int_0^T (T-s)^{\alpha-\gamma} \mathbf{f}(s) \, \mathrm{d}s \right] \right|, \\ &= \left| \frac{t^{1-\gamma}}{\Gamma(\alpha)} \left[\int_0^t \frac{(t-s)^{\alpha-1}}{s^{1-\gamma}} s^{1-\gamma} \mathbf{f}(s) \, \mathrm{d}s - \left(\frac{1-\gamma}{\alpha} + 1 \right) T^{\gamma-1} \left(\frac{t}{T} \right)^{\alpha} \int_0^T \frac{(T-s)^{\alpha-\gamma}}{s^{1-\gamma}} s^{1-\gamma} \mathbf{f}(s) \, \mathrm{d}s \right] \right|. \end{aligned}$$

This gives, after rearranging:

$$= \left| \frac{t^{1-\gamma}}{\Gamma(\alpha)} \left[\int_0^t \frac{(t-s)^{\alpha-1} - T^{\gamma-1}\left(\frac{t}{T}\right)^{\alpha}(T-s)^{\alpha-\gamma}}{s^{1-\gamma}} s^{1-\gamma}\mathbf{f}(s)\,\mathrm{d}s \right.\right.$$
$$\left.\left. - T^{\gamma-1}\left(\frac{t}{T}\right)^{\alpha} \int_t^T \frac{(T-s)^{\alpha-\gamma}}{s^{1-\gamma}} s^{1-\gamma}\mathbf{f}(s)\,\mathrm{d}s - \left(\frac{1-\gamma}{\alpha}\right) T^{\gamma-1}\left(\frac{t}{T}\right)^{\alpha} \int_0^T \frac{(T-s)^{\alpha-\gamma}}{s^{1-\gamma}} s^{1-\gamma}\mathbf{f}(s)\,\mathrm{d}s \right] \right|,$$

to which the following upper bound can be given:

$$\leq \frac{t^{1-\gamma}}{\Gamma(\alpha)} \Bigg[\underbrace{\int_0^t \frac{(t-s)^{\alpha-1} - T^{\gamma-1}\left(\frac{t}{T}\right)^{\alpha}(T-s)^{\alpha-\gamma}}{s^{1-\gamma}} \mathrm{d}s}_{:=\mathrm{I}_1}$$
$$+ T^{\gamma-1}\left(\frac{t}{T}\right)^{\alpha} \underbrace{\int_t^T \frac{(T-s)^{\alpha-\gamma}}{s^{1-\gamma}} \mathrm{d}s}_{:=\mathrm{I}_2} + \left(\frac{1-\gamma}{\alpha}\right) T^{\gamma-1}\left(\frac{t}{T}\right)^{\alpha} \underbrace{\int_0^T \frac{(T-s)^{\alpha-\gamma}}{s^{1-\gamma}} \mathrm{d}s}_{:=\mathrm{I}_3} \Bigg] ||\mathbf{f}||_{1-\gamma}. \quad (3.16)$$

Here, (3.16) follows from the triangle inequality and Hölder's inequality applied to L^1 and L^∞, since all integrals are nonnegative. Indeed, for I_1 we have:

$$\begin{aligned}
(t-s)^{\alpha-1} - T^{\gamma-1}\left(\frac{t}{T}\right)^{\alpha}(T-s)^{\alpha-\gamma} &= (t-s)^{\alpha-1} - T^{\gamma-1}\left(\frac{t}{T}\right)^{\alpha}(T-s)^{\alpha-1+1-\gamma}, \\
&= (t-s)^{\alpha-1} - \left(\frac{T-s}{T}\right)^{1-\gamma}\left(\frac{t}{T}\right)^{\alpha}(T-s)^{\alpha-1}, \\
&\geq (t-s)^{\alpha-1} - \left(\frac{t}{T}\right)^{\alpha}(T-s)^{\alpha-1}, \\
&\geq (t-s)^{\alpha-1}\frac{T-t}{T} \geq 0,
\end{aligned}$$

for $s \in [0,t]$, $\alpha \in (0,1)$, $\gamma \in [0,1]$, where the final line follows from [8]. Now, I_2 and I_3 are nonnegative as well, since

$$\frac{(T-s)^{\alpha-\gamma}}{s^{1-\gamma}} \geq 0 \quad \text{for } s \in [t,T],\ \alpha \in (0,1),\ \gamma \in [0,1].$$

Evaluating each integral in (3.16) using Proposition 2.2.6, 2.2.7 and 2.2.8 gives:

$$\begin{aligned}
\mathrm{I}_1 &= \int_0^t \frac{(t-s)^{\alpha-1} - T^{\gamma-1}\left(\frac{t}{T}\right)^{\alpha}(T-s)^{\alpha-\gamma}}{s^{1-\gamma}} \mathrm{d}s, \\
&= \int_0^t (t-s)^{\alpha-1}s^{\gamma-1}\,\mathrm{d}s - T^{\gamma-1}\left(\frac{t}{T}\right)^{\alpha}\int_0^t (T-s)^{\alpha-\gamma}s^{\gamma-1}\,\mathrm{d}s, \\
&= \mathrm{B}(\alpha,\gamma)t^{\alpha+\gamma-1} - T^{\alpha+\gamma-1}\left(\frac{t}{T}\right)^{\alpha}\mathrm{B}_{t/T}(\gamma,\alpha-\gamma+1).
\end{aligned}$$

$$\mathrm{I}_2 = \int_t^T (T-s)^{\alpha-\gamma}s^{\gamma-1}\,\mathrm{d}s = T^{\alpha}\mathrm{B}_{1-t/T}(\alpha-\gamma+1,\gamma).$$

And finally,

$$\mathrm{I}_3 = \int_0^T (T-s)^{\alpha-\gamma}s^{\gamma-1}\,\mathrm{d}s = \mathrm{B}(\alpha-\gamma+1,\gamma)T^{\alpha-1}.$$

Substituting this back to (3.16) gives a total expression of

$$\begin{aligned}
\xi_1(t) =& \frac{\mathrm{B}(\alpha,\gamma)\,t^{\alpha}}{\Gamma(\alpha)} + \frac{t^{\alpha+1-\gamma}}{\Gamma(\alpha)T^{1-\gamma}}\Big[-\mathrm{B}_{t/T}(\gamma,\alpha-\gamma+1) \\
&+ \mathrm{B}_{1-t/T}(\alpha-\gamma+1,\gamma) + \left(\frac{1-\gamma}{\alpha}\right)\mathrm{B}(\alpha-\gamma+1,\gamma)T^{-1}\Big].
\end{aligned}$$

□

Lemma 3.2.2. *Let* $\{\xi_m(t)\}_{m\in\{\mathbb{N}\cup\{0\}\}}$ *be a sequence of functions in* $C_{1-\gamma}[0,T]$ *as given by*

$$\xi_m(t) := \frac{t^{1-\gamma}}{\Gamma(\alpha)}\left[\int_0^t (t-s)^{\alpha-1}\xi_{m-1}(s)\,\mathrm{d}s - \left(\frac{1-\gamma}{\alpha}+1\right)T^{\gamma-1}\left(\frac{t}{T}\right)^{\alpha}\int_0^T (T-s)^{\alpha-\gamma}\xi_{m-1}(s)\,\mathrm{d}s\right] \tag{3.17}$$

with $\xi_0(t) := 1$ *and* $\xi_1(t)$ *of the form* (3.15)*. Then, for all* $m \in \mathbb{N}$*, the following estimate holds:*

$$\xi_{m+1}(t) \le \Xi^m \xi_1(t) \le \Xi^{m+1}, \tag{3.18}$$

where

$$\begin{aligned}\Xi &= \sup_{t\in[0,T]} \xi_1(t),\\ &= \sup_{t\in[0,T]}\left(\frac{\mathrm{B}(\alpha,\gamma)\,t^{\alpha}}{\Gamma(\alpha)} + \frac{t^{\alpha+1-\gamma}}{\Gamma(\alpha)T^{1-\gamma}}\left[-\mathrm{B}_{t/T}(\gamma,\alpha-\gamma+1) + \mathrm{B}_{1-t/T}(\alpha-\gamma+1,\gamma) + \left(\frac{1-\gamma}{\alpha}\right)\mathrm{B}(\alpha-\gamma,\gamma)T^{-1}\right]\right).\end{aligned}$$

Proof. The proof follows an induction argument. First, for $m = 0$, it holds trivially that

$$\xi_1(t) \le \sup_{t\in[0,T]} \xi_1(t) := \Xi.$$

Now, assume (3.18) holds for some $k-1$, hence

$$\xi_k(t) \le \Xi^{k-1}\xi_1(t) \le \Xi^k. \tag{3.19}$$

Then, for k, we have

$$\begin{aligned}\xi_{k+1}(t) &= \frac{t^{1-\gamma}}{\Gamma(\alpha)}\left[\int_0^t (t-s)^{\alpha-1}\xi_k(s)\,\mathrm{d}s - \left(\frac{1-\gamma}{\alpha}+1\right)T^{\gamma-1}\left(\frac{t}{T}\right)^{\alpha}\int_0^T (T-s)^{\alpha-\gamma}\xi_k(s)\,\mathrm{d}s\right],\\ &\le \frac{t^{1-\gamma}}{\Gamma(\alpha)}\left[\int_0^t (t-s)^{\alpha-1}\Xi^k\,\mathrm{d}s - \left(\frac{1-\gamma}{\alpha}+1\right)T^{\gamma-1}\left(\frac{t}{T}\right)^{\alpha}\int_0^T (T-s)^{\alpha-\gamma}\Xi^k\,\mathrm{d}s\right], \qquad (3.20)\\ &= \Xi^k\xi_1(t),\\ &\le \Xi^{k+1}.\end{aligned}$$

Here, line (3.20) follows from induction hypothesis (3.19), and the final expression from definition (3.17) using the fact that $\xi_0(t) = 1$ combined with the induction hypothesis applied again. Hence, the result holds for $k+1$, and thus we have proven the inequality holds for any $m \in \{\mathbb{N}\cup\{0\}\}$. □

Theorem 3.2.1. *Assume that conditions* ***A.1*** *-* ***A.3*** *hold for BVP* (3.3) - (3.4)*. Then, for all initial solution approximations* $\mathbf{x}_0(t) = \frac{\tilde{\mathbf{x}}_0 t^{\gamma-1}}{\Gamma(\gamma)} \in D_\beta$*,* $\tilde{\mathbf{x}}_0 \in \mathbb{R}^d$*, it holds that*

1. *Functions of the sequence* (3.14) *are in* $C_{1-\gamma}[0,T]$ *and satisfy the generalized integral boundary conditions*

$$ {}_0\mathrm{I}_t^{1-\gamma}\mathbf{x}_m(0) = {}_0\mathrm{I}_t^{1-\gamma}\mathbf{x}_m(T).$$

2. *The sequence of functions* (3.14) *converge uniformly in* $C_{1-\gamma}[0,T]$ *as* $m\to\infty$ *for* $t\in[0,T]$ *to the limit function*

$$\mathbf{x}_\infty(t,\tilde{\mathbf{x}}_0) = \lim_{m\to\infty}\mathbf{x}_m(t,\tilde{\mathbf{x}}_0). \tag{3.21}$$

3. *The limit function satisfies the boundary conditions*

$$ {}_0\mathrm{I}_t^{1-\gamma}\mathbf{x}_\infty(0) = {}_0\mathrm{I}_t^{1-\gamma}\mathbf{x}_\infty(T).$$

4. *The limit function satisfies* $\mathbf{x}_\infty \in C_{1-\gamma}[0,T]$ *in* t *and is the unique solution of the integral equation*

$$\mathbf{x}(t) = \frac{\tilde{\mathbf{x}}_0}{\Gamma(\gamma)} t^{\gamma-1} + \frac{1}{\Gamma(\alpha)} \left[\int_0^t (t-s)^{\alpha-1} \mathbf{f}(s, \mathbf{x}(s))\, \mathrm{d}s \right.$$
$$\left. - \left(\frac{1-\gamma}{\alpha} + 1 \right) T^{\gamma-1} \left(\frac{t}{T} \right)^{\alpha} \int_0^T (T-s)^{\alpha-\gamma} \mathbf{f}(s, \mathbf{x}(s))\, \mathrm{d}s \right]. \tag{3.22}$$

which is the corresponding integral equation to the perturbed Cauchy-type IVP (3.5)-(3.6)*:*

$$ {}_0\mathrm{D}_t^{\alpha,\beta} \mathbf{x}(t) = \mathbf{f}(t, \mathbf{x}(t)) + \Delta(\tilde{\mathbf{x}}_0),$$
$$ {}_0\mathrm{I}_t^{1-\gamma} \mathbf{x}(0) = \tilde{\mathbf{x}}_0,$$

with

$$\Delta(\tilde{\mathbf{x}}_0) := \frac{1-\gamma+\alpha}{T^{1-\gamma+\alpha}} \int_0^T (T-s)^{-\gamma+\alpha} \mathbf{f}(s, \mathbf{x}(s))\, \mathrm{d}s. \tag{3.23}$$

5. *The following error estimate holds:*

$$||\mathbf{x}_\infty(t, \tilde{\mathbf{x}}_0) - \mathbf{x}_m(t, \tilde{\mathbf{x}}_0)||_{1-\gamma} \leq \Xi (\mathbf{I}_n - \mathbf{Q})^{-1} \mathbf{Q}^m \mathbf{m}. \tag{3.24}$$

Proof. Statement 1 follows from construction of our approximating sequence (3.14) and can be shown by direct computation using the weighed boundary conditions. Furthermore, by Lemma 11 of [11] and construction of the approximation sequence, we know that all approximating functions are in $C_{1-\gamma}[0,T]$.

To show the other statements, it will be proven that the sequence $\mathbf{x}_m(t, \mathbf{x}_0)$ as defined by (3.14) is a Cauchy sequence in the Banach space $(C_{1-\gamma}[0,T], ||\,.\,||_{1-\gamma})$, thus showing convergence to the limit function $\mathbf{x}_\infty(t, \mathbf{x}_0)$. First, we show all $\mathbf{x}_m(t, \tilde{\mathbf{x}}_0) \in D$ for all $(t, \mathbf{x}_0(t)) \in [0,T] \times D_\beta$.

$$\begin{aligned}
||\mathbf{x}_1(t, \tilde{\mathbf{x}}_0) - \mathbf{x}_0(t, \tilde{\mathbf{x}}_0)||_{1-\gamma} &= \left|\left| \mathbf{x}_1(t, \tilde{\mathbf{x}}_0) - \frac{\tilde{\mathbf{x}}_0 t^{\gamma-1}}{\Gamma(\gamma)} \right|\right|_{1-\gamma}, \\
&= \sup_{t\in[0,T]} \left| \frac{t^{1-\gamma}}{\Gamma(\alpha)} \left[\int_0^t (t-s)^{\alpha-1} \mathbf{f}(s, \mathbf{x}_0(s, \tilde{\mathbf{x}}_0))\, \mathrm{d}s \right.\right. \\
&\quad \left.\left. - \left(\frac{1-\gamma}{\alpha} + 1 \right) T^{\gamma-1} \left(\frac{t}{T} \right)^{\alpha} \int_0^T (T-s)^{\alpha-\gamma} \mathbf{f}(s, \mathbf{x}_0(s), \tilde{\mathbf{x}}_0)\, \mathrm{d}s \right] \right|, \\
&\leq \sup_{t\in[0,T]} \xi_1(t) ||\mathbf{f}(t, \mathbf{x}_0(t, \tilde{\mathbf{x}}_0))||_{1-\gamma}, \\
&= \sup_{t\in[0,T]} \xi_1(t) \mathbf{m}, \\
&\leq \Xi \mathbf{m} = \beta.
\end{aligned} \tag{3.25}$$

Here, $\mathbf{m}$ is as defined in assumption (3.9) and the final expression follows from Lemma 3.2.1 and 3.2.2. For induction, assume the above holds for some $\mathbf{x}_{k-1}(t, \tilde{\mathbf{x}}_0)$. Then, again by Lemma 3.2.1 and assumption (3.9), we have that for all $k \in \mathbb{N}$,

$$\begin{aligned}
||\mathbf{x}_k(t, \tilde{\mathbf{x}}_0) - \mathbf{x}_0(t, \tilde{\mathbf{x}}_0)||_{1-\gamma} &= \sup_{t\in[0,T]} \left| \frac{t^{1-\gamma}}{\Gamma(\alpha)} \left[\int_0^t (t-s)^{\alpha-1} \mathbf{f}(s, \mathbf{x}_{k-1}(s, \tilde{\mathbf{x}}_0))\, \mathrm{d}s \right.\right. \\
&\quad \left.\left. - \left(\frac{1-\gamma}{\alpha} + 1 \right) T^{\gamma-1} \left(\frac{t}{T} \right)^{\alpha} \int_0^T (T-s)^{\alpha-\gamma} \mathbf{f}(s, \mathbf{x}_{k-1}(s, \tilde{\mathbf{x}}_0))\, \mathrm{d}s \right] \right|, \\
&\leq \sup_{t\in[0,T]} \xi_1(t) ||\mathbf{f}(t, \mathbf{x}_{k-1}(t, \tilde{\mathbf{x}}_0))||_{1-\gamma}, \\
&\leq \Xi \mathbf{m} \leq \beta.
\end{aligned}$$

This gives that for all $k \in \mathbb{N}$, $\mathbf{x}_k(t, \tilde{\mathbf{x}}_0) \in D$ for all $t \in [0,T]$, $\mathbf{x}_0(t) \in D_\beta$. Now, to prove convergence of the sequence, we show that the following estimate holds for all $m \in \mathbb{N}$:

$$||\mathbf{x}_m(t, \tilde{\mathbf{x}}_0) - \mathbf{x}_{m-1}(t, \tilde{\mathbf{x}}_0)||_{1-\gamma} \leq \sup_{t\in[0,T]} \mathbf{K}^{m-1} \mathbf{m} \xi_m(t) \leq \sup_{t\in[0,T]} \mathbf{Q}^{m-1} \mathbf{m} \xi_1(t) = \Xi \mathbf{Q}^{m-1} \mathbf{m}. \tag{3.26}$$

For $m = 1$, this follows from (3.25). Now, assume (3.26) holds for some $k \in \mathbb{N}$. Then, for $k+1$, we have

$$\begin{aligned}
&||\mathbf{x}_{k+1}(t, \tilde{\mathbf{x}}_0) - \mathbf{x}_k(t, \tilde{\mathbf{x}}_0)||_{1-\gamma}, \\
&= \sup_{t\in[0,T]} \left| \frac{t^{1-\gamma}}{\Gamma(\alpha)} \left[\int_0^t (t-s)^{\alpha-1} \left[\mathbf{f}(s, \mathbf{x}_k(s, \tilde{\mathbf{x}}_0)) - \mathbf{f}(s, \mathbf{x}_{k-1}(s, \tilde{\mathbf{x}}_0)) \right] \mathrm{d}s \right. \right. \\
&\quad \left. \left. - \left(\frac{1-\gamma}{\alpha} + 1 \right) T^{\gamma-1} \left(\frac{t}{T} \right)^{\alpha} \int_0^T (T-s)^{\alpha-\gamma} \left[\mathbf{f}(s, \mathbf{x}_k(s, \tilde{\mathbf{x}}_0)) - \mathbf{f}(s, \mathbf{x}_{k-1}(s, \tilde{\mathbf{x}}_0)) \right] \mathrm{d}s \right] \right|, \\
&\leq \sup_{t\in[0,T]} \xi_1(t) ||\mathbf{f}(t, \mathbf{x}_k(t, \tilde{\mathbf{x}}_0)) - \mathbf{f}(t, \mathbf{x}_{k-1}(t, \tilde{\mathbf{x}}_0))||_{1-\gamma}, \qquad (3.27) \\
&\leq \sup_{t\in[0,T]} \xi_1(t) \mathbf{K} ||\mathbf{x}_k(t, \tilde{\mathbf{x}}_0) - \mathbf{x}_{k-1}(t, \tilde{\mathbf{x}}_0)||_{1-\gamma},
\end{aligned}$$

Here, (3.27) follows from Lemma 3.2.1 and $\mathbf{K}$ is as defined in inequality (3.10). Then, by the induction hypothesis (3.26), we have:

$$||\mathbf{x}_{k+1}(t, \tilde{\mathbf{x}}_0) - \mathbf{x}_k(t, \tilde{\mathbf{x}}_0)||_{1-\gamma} \leq \sup_{t\in[0,T]} \xi_1(t) \mathbf{K} \mathbf{m} \xi_m(t) \leq \Xi \mathbf{Q}^m \mathbf{m},$$

where the final expression is derived from the spectral radius assumption (3.12) and Lemma 3.2.2, with $\mathbf{m}$ as given in inequality (3.9). Then, taking some $j \in \mathbb{N}$, we have by telescoping and the triangle inequality that

$$\begin{aligned}
||\mathbf{x}_{m+j}(t, \tilde{\mathbf{x}}_0) - \mathbf{x}_m(t, \tilde{\mathbf{x}}_0)||_{1-\gamma} &= || \sum_{k=1}^{j} \left[\mathbf{x}_{m+k}(t, \tilde{\mathbf{x}}_0) - \mathbf{x}_{m+k-1}(t, \tilde{\mathbf{x}}_0) \right] ||_{1-\gamma}, \qquad (3.28) \\
&\leq \sum_{k=1}^{j} ||\mathbf{x}_{m+k}(t, \tilde{\mathbf{x}}_0) - \mathbf{x}_{m+k-1}(t, \tilde{\mathbf{x}}_0)||_{1-\gamma}, \\
&\leq \sum_{k=1}^{j} \Xi \mathbf{Q}^{m+k-1} \mathbf{m}, \\
&= \Xi \mathbf{Q}^m \sum_{k=0}^{j-1} \mathbf{Q}^k \mathbf{m}.
\end{aligned}$$

Now, since by assumption (3.13), the spectral radius $\rho(\mathbf{Q}) < 1$, we know that $\lim_{m\to\infty} \mathbf{Q}^m = \mathbf{O}$, where $\mathbf{O}$ is the d-dimensional zero-matrix. Hence, by taking the limit as $m \to \infty$, we have a Cauchy sequence $\mathbf{x}_m$ defined by (3.14) with uniform converge in $[0, T] \times D_\beta$, proving claim 2. Since all functions satisfy boundary conditions, so does the limit function, satisfying claim 3 of the proof. For the error estimate (3.24) of statement 5, note that since $\rho(\mathbf{Q}) < 1$, it also holds that

$$\sum_{k=0}^{j-1} \mathbf{Q}^k \leq (\mathbf{I}_d - \mathbf{Q})^{-1},$$

where $\mathbf{I}_d$ is the d-dimensional unit matrix. Thus, taking the limit $j \to \infty$ for (3.28), we have

$$||\mathbf{x}_\infty(t, \tilde{\mathbf{x}}_0) - \mathbf{x}_m(t, \tilde{\mathbf{x}}_0)||_{1-\gamma} \leq \Xi (\mathbf{I}_d - \mathbf{Q})^{-1} \mathbf{Q}^m \mathbf{m},$$

providing the error bounds of claim 5 of Theorem 3.2.1. For uniqueness and the claim of statement 4, take two solutions, $\mathbf{x}_a(t)$ and $\mathbf{x}_b(t)$ of equation (3.22). Then, by Lemma 3.2.1 and **A.1** - **A.3**,

$$\begin{aligned}
||\mathbf{x}_a(t) - \mathbf{x}_b(t)||_{1-\gamma} &\leq \sup_{t\in[0,T]} \xi_1(t) ||\mathbf{f}(t, \mathbf{x}_a(t)) - \mathbf{f}(t, \mathbf{x}_b(t))||_{1-\gamma}, \\
&\leq \sup_{t\in[0,T]} \xi_1(t) \mathbf{K} ||\mathbf{x}_a(t) - \mathbf{x}_b(t)||_{1-\gamma}, \\
&\leq \mathbf{Q} ||\mathbf{x}_a(t) - \mathbf{x}_b(t)||_{1-\gamma}.
\end{aligned}$$

And since $\rho(\mathbf{Q}) < 1$, we must have $||\mathbf{x}_a(t) - \mathbf{x}_b(t)||_{1-\gamma} = \mathbf{0}$, which by property of the norm yields $\mathbf{x}_a(t) = \mathbf{x}_b(t)$. Finally, by [11], we know that the IVP (3.5)-(3.6) is equivalent to the integral equation (3.22), using Theorem 23 and applying the final statement on regularity as in the proof of Theorem 25. Hence, this problem has a unique solution in the space $C^\gamma_{1-\gamma}[0, T]$. Since we have established that $\mathbf{x}_\infty(t, \mathbf{x}_0)$ satisfies (3.22) uniquely, we know this is the unique solution to the initial value problem, proving the theorem. □

3.2.3. Connection to the boundary value problem

Now, again, consider a perturbed Cauchy-type IVP:

$$ {}_0\mathrm{D}_t^{\alpha,\beta}\mathbf{x}(t) = \mathbf{f}(t,\mathbf{x}(t)) + \nu, \tag{3.29} $$

$$ {}_0\mathrm{I}_t^{1-\gamma}\mathbf{x}(0) = \tilde{\mathbf{x}}_0, \tag{3.30} $$

where ${}_0\mathrm{I}_t^{1-\gamma}$ denotes the left-sided Riemann-Liouville fractional integral of order $1-\gamma$, $\nu \in \mathbb{R}^d$ is a control parameter and ${}_0\mathrm{D}_t^{1-\gamma}\tilde{\mathbf{x}}_0 = \frac{\tilde{\mathbf{x}}_0 t^{\gamma-1}}{\Gamma(\gamma)} \in D_\beta$.

Theorem 3.2.2. *Let $\frac{\tilde{\mathbf{x}}_0 t^{\gamma-1}}{\Gamma(\gamma)} \in D_\beta$ and $\nu \in \mathbb{R}^d$. Suppose conditions **A.1** - **A.3** hold for Theorem 3.2.1 for the system* (3.3)*. Then, the solution $\mathbf{x} = \mathbf{x}(t,\tilde{\mathbf{x}}_0,\nu)$ of* (3.29) - (3.30) *also satisfies the weighed periodic condition* (3.4) *if and only if*

$$ \nu = \Delta(\tilde{\mathbf{x}}_0), $$

with $\Delta(\tilde{\mathbf{x}}_0)$ as given by (3.23)*. Furthermore,*

$$ \mathbf{x}(t,\tilde{\mathbf{x}}_0,\nu) = \mathbf{x}_\infty(t,\tilde{\mathbf{x}}_0) \text{ for } t \in [0,T]. $$

Proof. First, note that existence and uniqueness of solutions in $C_{1-\gamma}[0,T]$ for the Cauchy-type IVP (3.29) - (3.30) is given in [11], providing continuous dependence on $\tilde{\mathbf{x}}_0$ and ν.
" $\Longrightarrow$ ". Assume we have $\nu = \Delta(\tilde{\mathbf{x}}_0)$. Then, by the result of Theorem 3.2.1, we know that the limit function $\mathbf{x}_\infty$ as given in (3.21) satisfies the corresponding integral equation (3.8) to the IVP (3.29) - (3.30), which by [11] must imply $\mathbf{x}(t,\tilde{\mathbf{x}}_0,\nu) = \mathbf{x}_\infty(t,\tilde{\mathbf{x}}_0)$ is the unique solution to the problem.
" $\Longleftarrow$ ". To prove uniqueness for ν, assume there exists another $\bar{\nu} \in \mathbb{R}^d$ and $\bar{\mathbf{x}}(t,\tilde{\mathbf{x}}_0,\bar{\nu})$ which satisfies

$$ {}_0\mathrm{D}_t^{\alpha,\beta}\bar{\mathbf{x}}(t,\tilde{\mathbf{x}}_0,\bar{\nu}) = \mathbf{f}(t,\bar{\mathbf{x}}(t,\tilde{\mathbf{x}}_0,\bar{\nu}) + \bar{\nu}, $$

and condition (3.4). By [11], $\bar{\nu}$ must satisfy the integral equation

$$ \bar{\mathbf{x}}(t) = \frac{\tilde{\mathbf{x}}_0}{\Gamma(\gamma)} t^{\gamma-1} + {}_0\mathrm{I}_t^{\alpha}\left[\mathbf{f}(t,\bar{\mathbf{x}}(t,\tilde{\mathbf{x}}_0,\bar{\nu}) + \bar{\nu}\right]. $$

Then, by (3.7) - (3.8), we know that we must have

$$ \bar{\nu} = -\frac{1}{T^{1-\gamma+\alpha}} \int_0^T (T-s)^{-\gamma+\alpha}\mathbf{f}(s,\bar{\mathbf{x}}(s,\tilde{\mathbf{x}}_0,\bar{\nu}))\,\mathrm{d}s = \Delta(\tilde{\mathbf{x}}_0). $$

Since ${}_0\mathrm{D}_t^{1-\gamma}\tilde{\mathbf{x}}_0 \in D_\beta$, we have that $\bar{\mathbf{x}}(t,\tilde{\mathbf{x}}_0,\bar{\nu}) \in D$. Now, comparing (3.8) to (3.22), we must have that by Theorem 3.2.1, $\bar{\mathbf{x}}(t,\tilde{\mathbf{x}}_0,\bar{\nu}) = \mathbf{x}_\infty(t,\tilde{\mathbf{x}}_0)$, and thus $\bar{\nu} = \Delta(\tilde{\mathbf{x}}_0)$ as given by (3.23), finishing the proof. □

Theorem 3.2.3. *Let the BVP* (3.3) - (3.4) *satisfy conditions* (3.9)-(3.13)*. Then, $\mathbf{x}_\infty(t,\tilde{\mathbf{x}}_0)$ is a solution of* (3.3) - (3.4) *if and only if $\tilde{\mathbf{x}}_0 \in \mathbb{R}^d$ is a solution of*

$$ \Delta(\tilde{\mathbf{x}}_0) = \mathbf{0}, \tag{3.31} $$

where Δ is given by (3.23)*.*

Proof. By applying Theorem 3.2.2 and noting that the perturbed Cauchy-type IVP (3.5) equals (3.3) if and only if $\Delta(\tilde{\mathbf{x}}_0) = \mathbf{0}$, we have that $\mathbf{x}_\infty(t,\tilde{\mathbf{x}}_0)$ is a solution of (3.3) - (3.4) if and only if (3.31) holds. □

3.2.4. Systems of mixed fractional derivative type and order

Similar to [9], for a integral boundary value problem system with mixed order derivatives α and derivative type β, formulate a mixed order and type Hilfer-BVP as follows:

$$ {}_0\mathrm{D}_t^{\alpha_1,\beta_1}\mathbf{x}(t) = \mathbf{f}(t,\mathbf{x}(t),\mathbf{y}(t)), $$

$$ {}_0\mathrm{D}_t^{\alpha_2,\beta_2}\mathbf{y}(t) = \mathbf{g}(t,\mathbf{x}(t),\mathbf{y}(t)), $$

subject to boundary conditions

$$
\begin{aligned}
{}_0\mathrm{I}_t^{1-\gamma_1}\mathbf{x}(0) &= {}_0\mathrm{I}_t^{1-\gamma_1}\mathbf{x}(T),\\
{}_0\mathrm{I}_t^{1-\gamma_2}\mathbf{y}(0) &= {}_0\mathrm{I}_t^{1-\gamma_2}\mathbf{y}(T),
\end{aligned}
$$

where $0 < t < T$, $0 < \alpha_i < 1$, $0 \leq \beta_i \leq 1$ and $\gamma_i = \alpha_i + \beta_i - \alpha_i\beta_i$, for $i \in \{1, 2\}$. Furthermore, $\mathbf{f} \in C_{1-\gamma_1}[0, T]$ and $\mathbf{g} \in C_{1-\gamma_2}[0, T]$. Now, assume that

B.1 $\mathbf{f} : [0, T] \times D_f \mapsto \mathbb{R}^{d_1}$ and $\mathbf{g} : [0, T] \times D_g \mapsto \mathbb{R}^{d_2}$, satisfy the following inequalities componentwise:

$$
\begin{aligned}
||t \mapsto \mathbf{f}(., \mathbf{u}, \mathbf{v})||_{1-\gamma_1} &\leq \mathbf{m}_f,\\
||t \mapsto \mathbf{g}(., \mathbf{u}, \mathbf{v})||_{1-\gamma_2} &\leq \mathbf{m}_g,
\end{aligned}
$$

for some nonnegative $\mathbf{m}_f \in \mathbb{R}^{d_1}$, $\mathbf{m}_g \in \mathbb{R}^{d_2}$ and $\mathbf{f}$ satisfies the Lipschitz condition component wise:

$$
\begin{aligned}
|\mathbf{f}(t, \mathbf{u}_1, \mathbf{v}_1) - \mathbf{f}(t, \mathbf{u}_2, \mathbf{v}_2)| &\leq \mathbf{K}_{11}|\mathbf{u}_1 - \mathbf{u}_2| + \mathbf{K}_{12}|\mathbf{v}_1 - \mathbf{v}_2|,\\
|\mathbf{g}(t, \mathbf{u}_1, \mathbf{v}_1) - \mathbf{f}(t, \mathbf{u}_2, \mathbf{v}_2)| &\leq \mathbf{K}_{21}|\mathbf{u}_1 - \mathbf{u}_2| + \mathbf{K}_{22}|\mathbf{v}_1 - \mathbf{v}_2|,
\end{aligned}
$$

for nonnegative matrices $\mathbf{K}_{ij}$ and all $\mathbf{u}_i(t), \mathbf{v}_i(t) \in D$, $t \in [0, T]$.

B.2 The sets

$$
D_{\zeta_1} = \left\{ \frac{\tilde{\mathbf{x}}_0}{\Gamma(\gamma_1)} t^{\gamma_1 - 1} \in D : \left\{ \mathbf{u} \in C_{1-\gamma_1}[0, T] : \left|\left| \mathbf{u} - \frac{\tilde{\mathbf{x}}_0}{\Gamma(\gamma_1)} t^{\gamma_1 - 1} \right|\right|_{1-\gamma_1} < \zeta_1 \right\} \subset D \right\},
$$

$$
D_{\zeta_2} = \left\{ \frac{\tilde{\mathbf{y}}_0}{\Gamma(\gamma_2)} t^{\gamma_2 - 1} \in D : \left\{ \mathbf{v} \in C_{1-\gamma_2}[0, T] : \left|\left| \mathbf{u} - \frac{\tilde{\mathbf{y}}_0}{\Gamma(\gamma_1)} t^{\gamma_1 - 1} \right|\right|_{1-\gamma_2} < \zeta_2 \right\} \subset D \right\},
$$

are non-empty, where $\zeta_1 := \Xi_1 \mathbf{m}_f$ and $\zeta_2 := \Xi_2 \mathbf{m}_g$, with $\Xi_i \in \mathbb{R}$ satisfying

$$
\begin{aligned}
\Xi_i = \sup_{t \in [0,T]} \Bigg(& \frac{\mathrm{B}(\alpha_i, \gamma_i)\, t^{\alpha_i}}{\Gamma(\alpha_i)} + \frac{t^{\alpha_i + 1 - \gamma_i}}{\Gamma(\alpha_i) T^{1-\gamma_i}} \Bigg[-\mathrm{B}_{t/T}(\gamma_i, \alpha_i - \gamma_i + 1) + \mathrm{B}_{1-t/T}(\alpha_i - \gamma_i + 1, \gamma_i) \\
& + \left(\frac{1 - \gamma_i}{\alpha_i} \right) \mathrm{B}(\alpha_i - \gamma_i + 1, \gamma_i) T^{-1} \Bigg] \Bigg), i \in \{1, 2\},
\end{aligned}
$$

Here, B, B_x denote the standard and incomplete beta function as defined in Definition 2.2.2 and 2.2.3 respectively. For an explicit calculation of Ξ, see Remark 3.2.1.

B.3 The matrix $\mathbf{Q}$ defined as

$$
\mathbf{Q} := \Omega \mathbf{K},
$$

with

$$
\Omega := \max\{\Xi_1, \Xi_2\},
$$

satisfies the spectral radius requirement of

$$
\rho(\mathbf{Q}) < 1.
$$

Now, consider the sequence of functions

$$
\begin{aligned}
\mathbf{x}_{m+1}(t, \tilde{\mathbf{x}}_0) =& \frac{\tilde{\mathbf{x}}_0}{\Gamma(\gamma_1)} t^{\gamma_1 - 1} + \frac{1}{\Gamma(\alpha_1)} \Bigg[\int_0^t (t - s)^{\alpha_1 - 1} \mathbf{f}(s, \mathbf{x}_m(s, \tilde{\mathbf{x}}_0), \mathbf{y}_m(s, \tilde{\mathbf{y}}_0))\, \mathrm{d}s \\
& - \left(\frac{1 - \gamma_1}{\alpha_1} + 1 \right) T^{\gamma_1 - 1} \left(\frac{t}{T} \right)^{\alpha_1} \int_0^T (T - s)^{\alpha_1 - \gamma_1} \mathbf{f}(s, \mathbf{x}_m(s, \tilde{\mathbf{x}}_0), \mathbf{y}_m(s, \tilde{\mathbf{y}}_0))\, \mathrm{d}s \Bigg], \\
\mathbf{y}_{m+1}(t, \tilde{\mathbf{y}}_0) =& \frac{\tilde{\mathbf{y}}_0}{\Gamma(\gamma_2)} t^{\gamma_2 - 1} + \frac{1}{\Gamma(\alpha_2)} \Bigg[\int_0^t (t - s)^{\alpha_2 - 1} \mathbf{g}(s, \mathbf{x}_m(s, \tilde{\mathbf{x}}_0), \mathbf{y}_m(s, \tilde{\mathbf{y}}_0))\, \mathrm{d}s \\
& - \left(\frac{1 - \gamma_2}{\alpha_2} + 1 \right) T^{\gamma_2 - 1} \left(\frac{t}{T} \right)^{\alpha_2} \int_0^T (T - s)^{\alpha_2 - \gamma_2} \mathbf{g}(s, \mathbf{x}_m(s, \tilde{\mathbf{x}}_0), \mathbf{y}_m(s, \tilde{\mathbf{y}}_0))\, \mathrm{d}s \Bigg].
\end{aligned}
$$

Taking the same argumentation as in [9] and using the inequalities from Lemma 3.2.1 and Lemma 3.2.2 from the previous sections, one can show existence and uniqueness for the solution under requirements **B.1**-**B.3**. Hence, for a mixed system, this can be interpreted as existence and uniqueness on the interval and solution space satisfying the strictest of both component-wise requirements. Furthermore, note that using the assumption $\mathbf{f} \in C_{1-\gamma_1}$, $\mathbf{g} \in C_{1-\gamma_2}$, one obtains solutions $\mathbf{x}$ and $\mathbf{y}$ in these respective function spaces, where $\gamma_1 \neq \gamma_2$ in general for a mixed system with different fractional derivative types and/or orders.

4

Bernstein splines approximations and fractional integration

This chapter serves as an introduction to Bernstein splines, which will be used in the following chapters to build function spaces approximating the analytical solutions to the fractional differential equation problems of Chapter 3. First, an introduction is given to Bernstein basis polynomials in Section 4.1. These basis polynomials will serve to construct *splines*, a collection of locally-supported polynomials, as outlined in Section 4.2. Fractional integration theory applied to splines is then established in Section 4.3, with a note on implementation in Section 4.4.

4.1. Bernstein polynomials

In numerical analysis, polynomial function approximations are ubiquitously used. A main advantage is the ability to reduce approximation problems to a linear parametrization of the function space using a polynomial basis. In other words: given a function $f : [a, b] \to \mathbb{R}$ to approximate, a corresponding n'th order polynomial approximation is written by

$$\tilde{f}(t) = \sum_{i=0}^{m} a_i \, b_i(t) \approx f(t), \tag{4.1}$$

where a_i are its coefficients and $b_i : [a, b] \to \mathbb{R}$ for $i \in \{0, ..., m\}$ are basis polynomials of degree at most n.

One such set of basis polynomials are given by the Bernstein basis polynomials:

Definition 4.1.1 (Bernstein basis polynomial [21])**.** The $n + 1$ Bernstein basis functions of order n denoted by $b_{j,n} : [0, 1] \to \mathbb{R}$ for $j \in \{0, 1, ...n\}$ are defined as

$$b_{j,n}(s) = \binom{n}{j} s^j (1 - s)^{n-j}.$$

Here, $\binom{n}{j} = \frac{n!}{j!\,(n-j)!}$ denotes the binomial coefficient. A graphical example of the Bernstein basis polynomials is provided in Figure 4.1.

Remark 4.1.1 (Bernstein basis polynomials in monomial form)*.* By using the binomial theorem, all Bernstein basis functions can be written in monomial form:

$$b_{j,n}(s) = \sum_{\ell=j}^{n} \binom{n}{\ell} \binom{\ell}{j} (-1)^{\ell-j} s^{\ell}, \quad \text{for } j \in \{0, ..., n\}.$$

To use the Bernstein basis polynomials for any arbitrary real domain $[a, b]$ and not just the domain $[0, 1]$, one can define a transformation $s_{[a,b]} : [a, b] \to [0, 1]$, and hence

$$b_{j,n} \circ s_{[a,b]} : [a, b] \to \mathbb{R}.$$

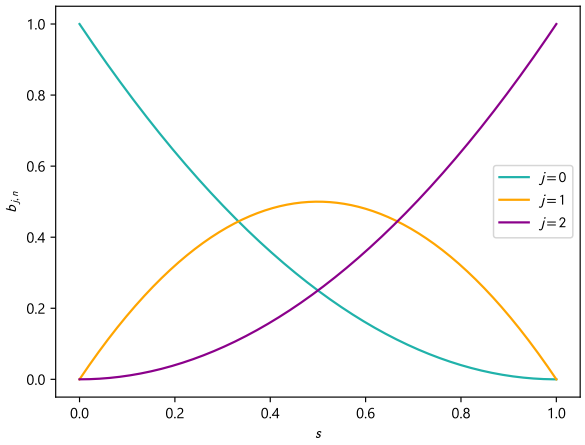

Figure 4.1: Bernstein basis polynomials $b_{j,n}$ for $n = 2$.

Taking a linear transformation, this can be defined as

$$s_{[a,b]}(t) = \frac{t-a}{b-a}.$$

Now that the building blocks for the basis polynomials are in place, this just leaves the choice for coefficients a_j, $j \in \{0, ..., n\}$ as in (4.1). A useful property of the order n-Bernstein polynomials is the fact that, taking the standard $n+1$ basis functions and a function $g : [0,1] \to \mathbb{R}$ to approximate, a good choice of coefficients is provided by

$$a_i = g(i/n), \quad \text{for } i \in \{0, ..., n\}.$$

Taking transformed basis elements $b_{j,n} \circ s_{[a,b]}$ and an arbitrary function $f : [a,b] \to \mathbb{R}$ gives

$$a_i = f\left(s^{-1}_{[a,b]}(i/n)\right) = f\left(a + \frac{i(b-a)}{n}\right), \quad \text{for } i \in \{0, ..., n\}.$$

Using this choice of coefficients, an operator approximating functions using Bernstein polynomials can be provided as follows:

Definition 4.1.2 (Bernstein operator [21])**.** For a function $f : [a,b] \to \mathbb{R}$, define the Bernstein operator of order n as:

$$B^n f(t) = \sum_{j=0}^{n} f\left(a + \frac{j(b-a)}{n}\right) \binom{n}{j} \left(\frac{t-a}{b-a}\right)^j \left(\frac{b-t}{b-a}\right)^{n-j}.$$

Let us first establish some basic and easy to check properties:

Proposition 4.1.1 (Bernstein operator at endpoints)**.** *For a function $f : [a,b] \to \mathbb{R}$, direct calculation using Definition 4.1.2 gives*

$$B^n f(a) = f(a), \quad \text{and} \quad B^n f(b) = f(b).$$

This property will be useful later on when taking multiple locally supported polynomials. Furthermore, for the result $B^n f$, note that:

Proposition 4.1.2 (Continuity of the Bernstein operator polynomial)**.** *For $f : [a,b] \to \mathbb{R}$ continuous, $B^n f(t) : [a,b] \to \mathbb{R}$ is continuous since it is the finite sum of continuous polynomials of order ≥ 0.*

Now that we have established a way to approximate functions using Bernstein polynomials, a first question is the accuracy of this approximation. For this, let us establish the so-called *modulus of continuity* ω:

Definition 4.1.3 (Modulus of continuity ([21], Section 1.6))**.** For a continuous function $f : [a, b] \to \mathbb{R}$, the modulus of continuity ω is defined as

$$\omega(f; \delta) = \sup_{|t-s| \leq \delta} |f(t) - f(s)|, \quad \text{for } t, s \in [a, b].$$

Intuitively, this can be seen as the largest attainable difference in function values in a domain of neighborhood size δ. For continuously differentiable functions, this is equal to the derivative. Now, we can provide a bound on the accuracy of the approximation of a continuous function $f : [a, b] \to \mathbb{R}$:
Theorem 4.1.1 (Bernstein operator error bound [31, 21])**.** *For a continuous function $f : [a, b] \to \mathbb{R}$, the following error estimate holds:*

$$|f(t) - B^n f(t)| \leq \frac{5}{4} \omega\left(f; \frac{(b-a)}{\sqrt{n}}\right), \quad \textit{for all } t \in [a, b].$$

Hence, the error of the Bernstein polynomial is dependent on the maximum attainable difference of f in a neighborhood of size $\frac{b-a}{\sqrt{n}}$. Note that as discussed in the proof of the theorem, the constant $\frac{5}{4}$ might be non-optimal, however, no theoretical optimum has been found [31, 21].

4.2. A collection of local polynomials: Bernstein splines

However, for many practical applications, this polynomial approximation is not satisfactory. It follows from Theorem 4.1.1 that, to have the same upper error bound for the Bernstein operator on a twice as large interval, the polynomial order n would need to be four times greater. However, this is not possible for general practical implementations as the Runge-effect poses a problem when increasing the polynomial order. This effect can cause the numerical approximation approach to become unstable [31]. To overcome numerical stability problem, we want a method to look further in time while keeping the same complexity. This is done by taking a *splines* approach. A spline is a piecewise-defined polynomial, in which all polynomial components have limited support. Consider the following:

Say we want to approximate a function $f : [0, T] \to \mathbb{R}$. First, spline "knots" are defined by subdividing the interval $[0, T]$ into $k + 1$ subintervals, taking $t_i \in [0, T]$ for $i \in \{0, ..., k + 1\}$ such that:

$$[0, T] = \bigcup_{i=0}^{k-1} [t_i, t_{i+1}) \cup [t_k, t_{k+1}].$$

The choice of values for t_i can be made in any way. One of the most standard approaches is an equidistant choice, in which for all $i \in \{0, ..., k\}$, $t_{i+1} - t_i = h$ for some $h > 0$. Now, denoting the intervals in the time domain by:

$$A_i = \begin{cases} [t_i, t_{i+1}), & \text{for } i \in \{0, ..., k-1\}, \\ [t_k, t_{k+1}], & \text{for } i = k, \end{cases}$$

one can define the spline $S : [0, T] \to \mathbb{R}$ as:

$$S(t) = \sum_{i=0}^{k} \mathbb{1}_{A_i} P_i(t),$$

where $P_i : A_i \to \mathbb{R}$ is a polynomial with local support. Hence, in the case of a standard Bernstein polynomial $B : [0, 1] \to \mathbb{R}$, one can take the transformation $s_i : [t_i, t_{i+1}] \to [0, 1]$ as

$$s_i(t) = \frac{t - t_i}{t_{i+1} - t_i},$$

and thus

$$S(t) = \sum_{i=0}^{k} \mathbb{1}_{A_i}(t)\, B_i(s_i(t)),$$

where $B_i : [0, 1] \to \mathbb{R}$ represents the i'th Bernstein polynomial with corresponding coefficients.

Now, using Definition 4.1.2, we can establish a Bernstein splines operator as follows

Definition 4.2.1 (Bernstein spline operator)**.** For a function $f : [0, T] \to \mathbb{R}$, and a collection of disjoint knot intervals $\mathcal{A} = \{A_0, ..., A_k\} = \{[t_0, t_1), ..., [t_{k-1}, t_k), [t_k, t_{k+1}]\}$, such that $\bigcup_{A_i \in \mathcal{A}} A_i = [0, T]$, define the order q Bernstein spline operator as:

$$S^q_{\mathcal{A}} f(t) = \sum_{i=0}^{k} \mathbb{1}_{A_i}(t)\, B^q\{\mathbb{1}_{\bar{A}_i} f\}(t),$$

where $\bar{A}_i$ denotes the closure of A_i.
Proposition 4.2.1 (Continuity of the Bernstein splines operator)**.** *If $f : [0, T] \to \mathbb{R}$ is continuous, $S^q_{\mathcal{A}} f$ is continuous as well.*

Proof. First, note that for every $t \in A_i \in \mathcal{A}$, we have that $S^q_{\mathcal{A}} f : A_i \to \mathbb{R}$ is continuous by continuity of the Bernstein polynomials (Proposition 4.1.2). Now, to prove $S^q_{\mathcal{A}} f$ is not merely piecewise continuous but continuous on the whole interval $[0, T]$, take an arbitrary internal knot point t_j with $j \in \{1, ...k\}$. Then,

$$\begin{aligned}
\lim_{t \uparrow t_j} S^q_{\mathcal{A}} f(t) &= \lim_{t \uparrow t_j} \sum_{i=0}^{k} \mathbb{1}_{A_i}(t)\, B^q\{\mathbb{1}_{A_i} f\}(t), \\
&= \lim_{t \uparrow t_j} B^q\{\mathbb{1}_{\bar{A}_{j-1}} f\}(t), \\
&= \lim_{t \uparrow t_j} B^q\{\mathbb{1}_{[t_{j-1}, t_j]} f\}(t), \\
&= f(t_j).
\end{aligned}$$

Here, the last line follows from the result of Proposition 4.1.1. Similarly, we have

$$\lim_{t \downarrow t_j} S^q_{\mathcal{A}} f(t) = \lim_{t \downarrow t_j} B^q\{\mathbb{1}_{[t_j, t_{j+1}]} f\}(t) = f(t_j).$$

Thus resulting in

$$\lim_{t \downarrow t_j} S^q_{\mathcal{A}} f(t) = \lim_{t \uparrow t_j} S^q_{\mathcal{A}} f(t),$$

proving continuity at internal knot points, giving continuity on the whole interval $[0, T]$. □

To provide an error bound, we can use the result of Theorem 4.1.1:
Theorem 4.2.1 (Bernstein splines error bound)**.** *Let $f : [0, T] \to \mathbb{R}$ be a continuous function with a defined modulus of continuity ω. Let $h = \sup_{A_i \in \mathcal{A}} |A_i|$ be the largest knot size of knot collection $\mathcal{A}$. Then, for the Bernstein spline operator of order q, it holds that*

$$|f(t) - S^q_{\mathcal{A}} f(t)| = \leq \frac{5}{4}\, \omega\left(f; \frac{h}{\sqrt{q}}\right).$$

Proof. First of all, using the definition of the splines operator as given in Definition 4.2.1, one can write:

$$\begin{aligned}
|f(t) - S^q_{\mathcal{A}} f(t)| &= \left| f(t) - \sum_{i=0}^{k} \mathbb{1}_{A_i}(t)\, B^q\{\mathbb{1}_{A_i} f\}(t) \right|, \\
&= \left| \sum_{i=0}^{k} \mathbb{1}_{A_i} f(t) - \sum_{i=0}^{k} \mathbb{1}_{A_i}(t)\, B^q\{\mathbb{1}_{A_i} f\}(t) \right|, \\
&= \left| \sum_{i=0}^{k} \mathbb{1}_{A_i}(t)[\mathbb{1}_{A_i} f(t) - B^q\{\mathbb{1}_{A_i} f\}(t)] \right|.
\end{aligned}$$

Now, using the triangle inequality and the result of Theorem 4.1.1 gives:

$$\begin{aligned}\left|\sum_{i=0}^{k} \mathbb{1}_{A_i}(t)[\mathbb{1}_{A_i} f(t) - B^q\{\mathbb{1}_{A_i} f\}(t)]\right| &\leq \sum_{i=0}^{k} \mathbb{1}_{A_i}(t)\,|\mathbb{1}_{A_i} f(t) - B^q\{\mathbb{1}_{A_i} f\}(t)|\,,\\ &\leq \sum_{i=0}^{k} \mathbb{1}_{A_i}(t)\,\frac{5}{4}\,\omega\left(\mathbb{1}_{A_i} f, (t_{i+1}-t_i)q^{-1/2}\right),\\ &\leq \frac{5}{4}\,\omega\left(f; \frac{h}{\sqrt{q}}\right),\end{aligned}$$

since $t_{i+1} - t_i \leq h$ for all $i \in \{0, ..., k\}$. □

One important property of the splines operator $S_{\mathcal{A}}^q$ is that the spline of a continuously differentiable function is not in general continuously differentiable:
Remark 4.2.1 (Differentiability of the spline operator). For $f \in C^1[0,T]$, in general one has $S_{\mathcal{A}}^q f \notin C^1[0,T]$. A demonstration of this property is provided in Figure 4.2. This effect is most apparent in the case of a piecewise linear spline ($q = 1$), of which the derivative results in a piecewise constant spline ($q = 0$). It can quickly be seen that this derivative can only be continuous if the derivative of the original spline is constant, and thus only satisfied when $S_{\mathcal{A}}^q f = \alpha t + \beta$ for $\alpha, \beta \in \mathbb{R}$.

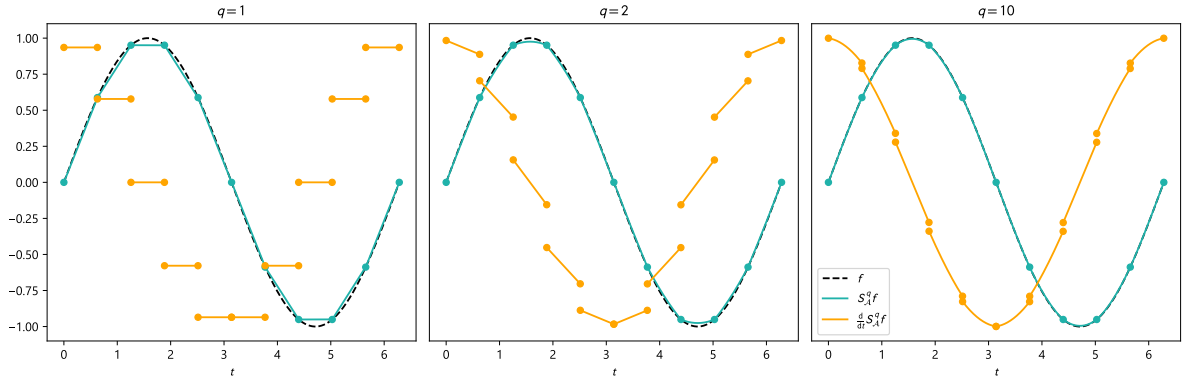

Figure 4.2: A Bernstein splines approximation $S_{\mathcal{A}}^q$ of $f = \sin(t)$ using 10 knots on $t \in [0, 2\pi]$ for $q \in \{1, 2, 10\}$. Dotted markers denote the knot boundaries. As stated in Remark 4.2.1, the derivative of the splines approximation is not continuous. However, for higher values of q and more accurate splines approximations $S_{\mathcal{A}}^q f$, the discontinuities decrease in magnitude.

4.3. Fractional integration and Bernstein splines

A major advantage of using Bernstein polynomials and splines is the closed-form expression for integrating a Bernstein basis function because of its polynomial form. This can be used to form a closed-form expression of integrating a Bernstein spline $S(t)$. First of all, we use Remark 4.1.1 to write all Bernstein basis polynomials as a finite sum of monomials. We know that for the j'th Bernstein basis polynomial of order n, we have $b_{j,n}(t) = \sum_{\ell=j}^{n} \binom{n}{\ell}\binom{\ell}{j}(-1)^{\ell-j} t^{\ell}$. And hence, for a Bernstein spline $S(t)$ with Bernstein coefficients $a_{i,j}$ for knots $i \in \{0, ..., k\}$ and Bernstein polynomial orders $j \in \{0, ..., q\}$ respectively, this yields:

$$\begin{aligned}S(t) &= \sum_{i=0}^{k} \mathbb{1}_{A_i}(t)\, B_i(s_i(t)),\\ &= \sum_{i=0}^{k} \mathbb{1}_{A_i}(t) \sum_{j=0}^{q} a_{i,j} b_{j,q}(s_i(t)),\\ &= \sum_{i=0}^{k}\sum_{j=0}^{q}\sum_{\ell=j}^{q} a_{i,j}\binom{q}{\ell}\binom{\ell}{j}(-1)^{\ell-j}\,\mathbb{1}_{A_i}(t)\, s_i(t)^{\ell}.\end{aligned} \tag{4.2}$$

Although the expression of (4.2) might not appear to be very elegant at first sight, it gives a very useful formulation for expressing the fractional integral by using its linearity property:

$$ {}_0\mathrm{I}_t^\alpha S(t) = \sum_{i=0}^{k} \sum_{j=0}^{q} \sum_{\ell=j}^{q} a_{i,j} \binom{q}{\ell} \binom{\ell}{j} (-1)^{\ell-j} \, {}_0\mathrm{I}_t^\alpha \{ \mathbb{1}_{A_i}(t) \, s_i(t)^\ell \}(t). \tag{4.3} $$

Thus, fractionally integrating the spline $S : [0,T] \to \mathbb{R}$ can be reduced to fractionally integrating a monomial of order ℓ with limited support $A_i = [t_i, t_{i+1}] \to \mathbb{R}$. This gives us our final challenge in writing a closed form solution. First, note that for $t < t_i$, the integral must be zero as the fractional integral of a zero function is zero. Now, for $t \geq t_i$, the integral can be written out as follows:

$$ \begin{aligned} {}_0\mathrm{I}_t^\alpha \{ \mathbb{1}_{A_i}(t) \, s_i(t)^\ell \}(t) &= \frac{1}{\Gamma(\alpha)} \int_0^t (t-x)^{\alpha-1} \mathbb{1}_{A_i}(x) \, s_i(x)^\ell \, \mathrm{d}x, \\ &= \frac{1}{\Gamma(\alpha)} \int_{t_i}^{t \wedge t_{i+1}} (t-x)^{\alpha-1} s_i(x)^\ell \, \mathrm{d}x, \\ &= \frac{(t_{i+1}-t_i)}{\Gamma(\alpha)} \int_0^{s_i(t) \wedge 1} (t - s_i^{-1}(z))^{\alpha-1} z^\ell \, \mathrm{d}z, \\ &= \frac{(t_{i+1}-t_i)^\alpha}{\Gamma(\alpha)} \int_0^{s_i(t) \wedge 1} \left(\frac{t-t_i}{t_{i+1}-t_i} - z \right)^{\alpha-1} z^\ell \, \mathrm{d}z, \\ &= \frac{(t_{i+1}-t_i)^\alpha}{\Gamma(\alpha)} \int_0^{s_i(t) \wedge 1} (s_i(t) - z)^{\alpha-1} \, z^\ell \, \mathrm{d}z. \end{aligned} \tag{4.4} $$

Where $a \wedge b$ denotes $\min(a,b)$. Here, a substitution transformation $z := s_i(x)$ is taken in (4.4), yielding $\mathrm{d}x = (t_{i+1} - t_i) \, \mathrm{d}z$. Note that the notation $s^{-1} : [0,1] \to [t_i, t_{i+1}]$ is used for the inverse function of s_i as given by $s^{-1}(s) = s(t_{i+1} - t_i) + t_i$. Now, for the final step, using the transformation $\vartheta := z / s_i(t)$, giving $\mathrm{d}z = s_i(t) \, \mathrm{d}\vartheta$, yields

$$ \begin{aligned} {}_0\mathrm{I}_t^\alpha \{ \mathbb{1}_{A_i}(t) \, s_i(t)^\ell \}(t) &= \frac{(t_{i+1}-t_i)^\alpha}{\Gamma(\alpha)} \int_0^{s_i(t) \wedge 1} (s_i(t) - z)^{\alpha-1} \, z^\ell \, \mathrm{d}z, \\ &= \frac{(t_{i+1}-t_i)^\alpha s_i(t)^{\alpha+\ell}}{\Gamma(\alpha)} \int_0^{1 \wedge 1/s_i(t)} (1-\vartheta)^{\alpha-1} \, \vartheta^\ell \, \mathrm{d}\vartheta, \\ &= \frac{(t-t_i)^{\alpha+\ell}}{(t_{i+1}-t_i)^\ell \, \Gamma(\alpha)} \mathrm{B}_{1 \wedge 1/s_i(t)}(\ell+1, \alpha). \end{aligned} \tag{4.5} $$

Here, $\mathrm{B}_x(a,b) = \int_0^x t^{a-1} \, (1-t)^{b-1} \, \mathrm{d}t$ denotes the incomplete Beta function as defined in Definition 2.2.3.

Now, going back to equation (4.3) and taking the result of (4.5) combined with linearity of the integral, we finally have an expression in the form

$$ {}_0\mathrm{I}_t^\alpha S(t) = \frac{1}{\Gamma(\alpha)} \sum_{i=0}^{k} \sum_{j=0}^{q} \sum_{\ell=j}^{q} a_{i,j} \binom{q}{\ell} \binom{\ell}{j} (-1)^{\ell-j} \frac{(t-t_i)^{\alpha+\ell}}{(t_{i+1}-t_i)^\ell} \mathrm{B}_{1 \wedge 1/s_i(t)}(\ell+1, \alpha). \tag{4.6} $$

This gives an exact expression for the fractional integral of a Bernstein spline.

Finally, for the use in numerical approximations, one also requires properties of the opposite operation: the Bernstein spline of a fractional integral. This cannot be expressed exactly for fractional integrals of general functions f. However, certain bounds on this approximation can be given. Let us study the properties of this operation.

Definition 4.3.1 (Spline fractional integration operator)**.** For $\alpha \in (0,1)$, a knot collection $\mathcal{A}$ such that $\cup_{A_i \in \mathcal{A}} A_i = [0,T]$ and the spline operator $S_{\mathcal{A}}^q$ as defined in Definition 4.2.1, introduce the splines fractional integration operator ${}_0^q\Phi_t^\alpha : C([0,T]) \to C([0,T])$ as:

$$ {}_0^q\Phi_t^\alpha u(t) = S_{\mathcal{A}}^q \, {}_0\mathrm{I}_t^\alpha u(t), \quad \text{for } t \in [0,T]. $$

To provide error bounds, we can use our previously established error estimates as follows:
Lemma 4.3.1 (Error of the spline integration operator)**.** *Take $u : [0, T] \to \mathbb{R}$ continuous. Then,*

$$||{}_0\mathrm{I}_t^\alpha u - {}_0^q\Phi_t^\alpha u||_\infty \leq \left(\frac{h}{\sqrt{q}}\right)^\alpha \frac{5\,||u||_\infty}{2\,\Gamma(\alpha+1)},$$

where h represents the maximum knot size $h = \sup_{A_i \in \mathcal{A}} |A_i|$ and q is the order of Bernstein basis polynomial splines.

Proof. First, by the definition of ${}_0^q\Phi_t^\alpha$ and Theorem 4.2.1 we have

$$|{}_0\mathrm{I}_t^\alpha u(t) - {}_0^q\Phi_t^\alpha u(t)| = \left|{}_0\mathrm{I}_t^\alpha\, u(t) - S_{\mathcal{A}}^q\, {}_0\mathrm{I}_t^\alpha u(t)\right| \leq \frac{5}{4}\,\omega\left({}_0\mathrm{I}_t^\alpha u(t); \frac{h}{\sqrt{q}}\right).$$

Then, taking the intermediate result in the proof of Proposition 2.2.4 of the continuity of the Riemann-Liouville integral, we have

$$\omega\left({}_0\mathrm{I}_t^\alpha u(t); hq^{-1/2}\right) = \frac{2(hq^{-1/2})^\alpha}{\Gamma(\alpha+1)}||u||_\infty,$$

resulting in the error bound. □

We can use this result to give a bound for the operator:
Lemma 4.3.2 (Bound of the spline integration operator)**.** *Take a continuous function $u : [a, T] \to \mathbb{R}$. Then, for $a < t < T$, the spline integration operator ${}_a^q\Phi_t^\alpha$ is bounded. Hence,*

$$||{}_a^q\Phi_t^\alpha u||_\infty \leq \Psi||u||_\infty,$$

with $\Psi = \frac{\frac{5}{2}\left(\frac{h}{\sqrt{q}}\right)^\alpha + (t-a)^\alpha}{\Gamma(\alpha+1)}$. Here, $||u||_\infty := \sup_{t\in[a,t]} |u(t)|$, where h is the maximum knot size $h = \sup_{A_i \in \mathcal{A}} |A_i|$ and q the order of Bernstein basis polynomial splines.

Proof. Taking the result from Lemma 4.3.1 and the proof of Proposition 2.2.3, write

$$\begin{aligned}
||{}_a^q\Phi_t^\alpha u||_\infty &\leq ||{}_a^q\Phi_t^\alpha u - {}_a\mathrm{I}_t^\alpha u + {}_a\mathrm{I}_t^\alpha u||_\infty, \\
&\leq ||{}_a^q\Phi_t^\alpha u - {}_a\mathrm{I}_t^\alpha u||_\infty + ||{}_a\mathrm{I}_t^\alpha u||_\infty, \\
&\leq \left(\frac{h}{\sqrt{q}}\right)^\alpha \frac{5\,||u||_\infty}{2\,\Gamma(\alpha+1)} + \frac{(t-a)^\alpha}{\Gamma(\alpha+1)}||u||_\infty \\
&= \frac{\frac{5}{2}\left(\frac{h}{\sqrt{q}}\right)^\alpha + (t-a)^\alpha}{\Gamma(\alpha+1)}||u||_\infty.
\end{aligned}$$

□

Now that all ingredients are in place to calculate integrals of splines and to approximate splines of integrals, let us establish applications of these operators to fractional differential equations.

4.4. A note on implementation

One major computational advantage of the technique as outlined in Section 4.3 is the opportunity for vectorization of the code. Recall equation (4.6), which will be stated again for convenience:

$${}_0\mathrm{I}_t^\alpha S(t) = \frac{1}{\Gamma(\alpha)} \sum_{i=0}^{k} \sum_{j=0}^{q} \sum_{\ell=j}^{q} a_{i,j} \binom{q}{\ell} \binom{\ell}{j} (-1)^{\ell-j} \frac{(t-t_i)^{\alpha+\ell}}{(t_{i+1}-t_i)^\ell} \mathrm{B}_{1\wedge 1/s_i(t)}(\ell+1, \alpha).$$

Now, given a spline of order q with a size k knot collection $\mathcal{A} = \{[t_0, t_1), [t_1, t_2), ...[t_{k-1}, t_k]\}$ and a $k \times (q+1)$ coefficient matrix $\mathbf{A}$ as given by:

$$\mathbf{A} = \begin{bmatrix} a_0 & ... & a_q \\ a_q & ... & a_{2q} \\ a_{2q} & ... & a_{3q} \\ \vdots & \vdots & \vdots \\ a_{(k-1)q} & ... & a_{kq} \end{bmatrix},$$

we are interested in computing expression (4.6) for $h+1$ desired evaluation points $\mathbf{t} = \begin{bmatrix} \tau_0 & \tau_1 & ... & \tau_h \end{bmatrix}$. In all notations of vectors, no distinction is given between a "column" or "row" vector. First, vectorize the expression for the binomial coeffients by writing the $(q+1) \times (q+1)$-matrix $\mathbf{B}$ as:

$$B_{j,\ell} = \begin{cases} \binom{q}{\ell}\binom{\ell}{j}(-1)^{\ell-j} & \text{if } \ell \geq j, \\ 0 & \text{else,} \end{cases} \quad \text{for } j, \ell \in \{0, ..., q\}.$$

Now, the most import part comes down to computing the tensor $\mathbf{J}$ of size $k \times (q+1) \times (h+1)$. The entries are provided by:

$$J_{i,\ell,m} = \frac{1}{\Gamma(\alpha)} \frac{(\tau_m - t_i)^{\alpha+\ell}}{(t_{i+1} - t_i)^{\ell}} \mathrm{B}_{1 \wedge 1/s_i(\tau_m)}(\ell + 1, \alpha), \quad \text{for} \quad \begin{cases} i \in \{0, ..., k\}, \\ \ell \in \{0, ..., q\}, \\ h \in \{0, ..., h\}. \end{cases}$$

Here, B denotes the incomplete beta function as introduced in Definition 2.2.3, which is installed in most software as a callable function. In Python for instance, this is provided by `scipy.special.betainc`[1]. Furthermore, as before,

$$s_i(\tau_m) = \frac{\tau_m - t_i}{t_{i+1} - t_i}.$$

Now, the result of the fractional integral of spline S at points $\mathbf{t}$ can be given as

$$\begin{bmatrix} {}_0\mathrm{I}^{\alpha}_{\tau_0} S(\tau_0) & {}_0\mathrm{I}^{\alpha}_{\tau_1} S(\tau_1) & ... & {}_0\mathrm{I}^{\alpha}_{\tau_h} S(\tau_h) \end{bmatrix} = (\mathbf{AB}) \cdot \mathbf{J},$$

where the operation "$\cdot$" can be seen as a tensor dot product with the first two dimensions of $\mathbf{J}$, thus yielding a total resulting vector of size $h+1$ as required.

There are two main advantages to this approach. First of all, all computations are reduced to matrix multiplications, which are much more efficiently optimized in most computer hardware and software. Second of all, the matrices $\mathbf{B}$ and $\mathbf{J}$ can be stored in memory for fractional integrals of the same type of splines. This reduces the problem to merely updating coeffients $\mathbf{A}$, without the need to call any special functions per iteration.

[1] Note however that this function is "regularized" by default and should thus be multiplied by $\frac{\Gamma(\ell+1+\alpha)}{\Gamma(\ell+1)\Gamma(\alpha)}$.

5

Bernstein splines applied to fractional initial value problems (IVP's)

In this section, the spline theory of the previous chapter will be applied to fractional-order IVP's as discussed in Section 3.1. Results are provided first for the Caputo-derivative in Section 5.1, before developing methods for the Hilfer-fractional derivative in Section 5.2. Source code for all methods is provided in `https://github.com/ngoedegebure/fracnum`.

5.1. Methods for Caputo-derivative initial value problems

Consider the fractional IVP with Caputo-derivative (Definition 2.3.2) as follows:

$$\begin{cases} {}_0^{\mathrm{C}}\mathrm{D}_t^{\alpha}\mathbf{x}(t) = \mathbf{f}(t,\mathbf{x}), \\ \mathbf{x}(0) = \tilde{\mathbf{x}}_0, \end{cases} \tag{5.1}$$

for $t \in [0,T]$, $\mathbf{f} : [0,T] \times D_f \to \mathbb{R}^d$ continuous with $D_f \subset \mathbb{R}^d$ closed and bounded and $\tilde{\mathbf{x}}_0 \in \mathbb{R}^d$. Note that the Caputo IVP (5.1) is equivalent to the Hilfer IVP (3.1) for $\beta = 1$. Existence and uniqueness and intermediate results are proven in Section 3.1. As shown in Theorem 3.1.1, a solution $\mathbf{x}(t)$ to (5.1) must satisfy the integral equation:

$$\mathbf{x}(t) = \tilde{\mathbf{x}}_0 + {}_0\mathrm{I}_t^{\alpha}\mathbf{f}(t,\mathbf{x}(t)), \quad \text{for all} \quad 0 \le t \le T. \tag{5.2}$$

For the proof see e.g. [11] with $\beta = 1$ or Appendix B for more detail. For many practical implications, it can be difficult to establish an analytic sequence of functions using computational software. Now that we have established the building blocks of integration on splines, we can establish convergence results using iterations of Bernstein splines. Three main methods will be outlined, starting with one of the most commonly used methods in literature:

5.1.1. Diethelm's predictor-corrector time integration method

The *predictor-corrector* method of Diethelm, Ford, and Freed [6] is one of the most popular time-integration methods, used extensively in literature for IVP's. The core of the method is to approach the fractional integral using quadrature integration rules in a "predictor" and "corrector" step, constructing a piecewise linear spline solution. A short overview of the method will be provided here, together with a discussion of the method's strengths and shortcomings.

In essence, the predictor-corrector approach is taken from the Adam-Bashfort-Moulton-like methods in an aim to overcome the *implicit* nature of the iterative equation. That is to say, on every step, solving the equation $\mathbf{x}(t_{n+1}) = {}_0\mathrm{I}_{t_{n+1}}^{\alpha}\mathbf{f}(t,\mathbf{x}(t))$ amounts to solving an implicit equation as $\mathbf{x}(t_{n+1})$ is needed for both the left and right hand side. The solution to this equation is approached by a piecewise linearly interpolated approximation $\mathbf{x}_h(t)$, using a two-step explicit predictor-corrector approach.

The predictor step amounts to solving:

$$\mathbf{x}_h^{\mathrm{P}}(t_{n+1}) = \tilde{\mathbf{x}}_0 + \frac{1}{\Gamma(\alpha)} \sum_{j=0}^{n} b_{j,n+1} \mathbf{f}(t_j, \mathbf{x}_h(t_j)),$$

where the quadrature weights are given by

$$b_{j,n+1} = \frac{h^\alpha}{\alpha} \left((n+1-j)^\alpha - (n-j)^\alpha \right).$$

This essentially makes it a fractional product left-side rectangle quadrature rule. Here, h is the step size in the time discretization. Hence, one has $t_{i+1} - t_i = h$ for all $i \in \{0, ..., N-1\}$.

In the corrector step, the final to-be-computed solution value is taken with a trapezoidal quadrature rule:

$$\mathbf{x}_h(t_{n+1}) = \tilde{\mathbf{x}}_0 + \frac{h^\alpha}{\Gamma(\alpha+2)} \mathbf{f}(t_{n+1}, \mathbf{x}_h^{\mathrm{P}}(t_{n+1})) + \frac{h^\alpha}{\Gamma(\alpha+2)} \sum_{j=0}^{n} a_{j,n+1} \mathbf{f}(t_j, \mathbf{x}_h(t_j)),$$

where

$$a_{j,n+1} = \begin{cases} n^{\alpha+1} - (n-\alpha)(n+1)^\alpha, & \text{if } j = 0, \\ (n-j+2)^{\alpha+1} + (n-j)^{\alpha+1} - 2(n-j+1)^{\alpha+1}, & \text{if } 1 \leq j \leq n, \\ 1 & \text{if } j = n+1. \end{cases}$$

A detailed error analysis is carried out in [7], where it is shown that under the assumption $\mathbf{x} \in C^2[0,T]$, the global error is expected to behave as

$$\max_{j \in \{0,\ldots,N\}} |\mathbf{x}(t_j) - \mathbf{x}_h(t_j)| = \mathcal{O}(h^p), \quad \text{with} \quad p = \min(2, 1+\alpha). \tag{5.3}$$

The main benefits of the approach are its simplicity, computational efficiency when vectorized and its numerical stability [6]. However, a number of considerations can be made:

- The method assumes a piecewise linear interpolation of the solution $\mathbf{x}$ in a uniformly spaced time-discretization grid and is not flexible for more general interpolation setups taking higher-order effects into account.
- The two-step quadrature approach is efficient but does not give a clear sense of error introduction and propagation on every step. As outlined in [6], a multistep corrector iteration setup could also be implemented, possibly beneficial for more “stiff” nonlinear equations.
- Finally, although the error order as shown in (5.3) proves convergence of the method, as noted by the authors themselves in [7], it is in general not possible to find exact constants describing the global error of the method.

Let us address some of the main concerns by establishing new methods.

5.1.2. Bernstein spline iterations: the "global approach"

A direct and “naive” approach to applying Bernstein splines theory to numerical methods for solving fractional differential equations is taken by replacing the integral operator in (5.2) by the splines integral operator of Definition 4.3.1. This approach is taken similar to that of Satmari [30], of which the error analysis is worked out in detail by Bica [2]. Let us analyze the iterative method this creates:

Theorem 5.1.1 (Convergence of fractional splines iterations for IVP’s)**.** *Given the analytical IVP* (5.1)*, assume the requirements of Theorem B.0.1 hold. Thus, the sequence*

$$\mathbf{x}_{m+1}(t) = \tilde{\mathbf{x}}_0 + {}_0\mathrm{I}_t^\alpha \mathbf{f}(t, \mathbf{x}_m(t)), \tag{5.4}$$

converges to a continuous solution $\mathbf{x}_\infty : [0,T] \to \mathbb{R}^d$ *satisfying IVP* (5.1) *and equivalent integral equation* (5.2)*. Assume there exists a nonnegative vector*

$$\mathbf{r} = ||\tilde{\mathbf{x}}_0 - \mathbf{x}_0^q||_\infty + \frac{5/2 \left(\frac{h}{\sqrt{q}} \right)^\alpha + T^\alpha}{\Gamma(\alpha+1)} \mathbf{m},$$

such that

$$D_{\mathbf{r}} := \{\{\mathbf{u} \in D_{\mathbf{b}} : ||\mathbf{u} - \mathbf{x}_0||_\infty \leq \mathbf{r}\} \subset D_{\mathbf{b}}\},$$

is non-empty and $\mathbf{f}$ *is Lipschitz with coefficients* K *for every* $\mathbf{u}, \mathbf{v} \in D_{\mathbf{r}}$*, where* $\mathbf{K}$ *and* $D_{\mathbf{b}}$ *are as given in Theorem B.0.1. Then, for a knot collection* $\mathcal{A}$ *such that* $\cup_{A_i \in \mathcal{A}} A_i = [0, T]$ *and the spline operator* $S^q_{\mathcal{A}}$ *and spline integration operator* ${}^q_0\Phi^\alpha_t$ *as defined in Definition 4.2.1 and 4.3.1 respectively, the iterative sequence using Bernstein splines as defined by*

$$\begin{aligned} \mathbf{x}^q_0(t) :&= S^q_{\mathcal{A}}\mathbf{x}_0(t), \\ \mathbf{x}^q_{m+1}(t) &= \tilde{\mathbf{x}}_0 + {}^q_0\Phi^\alpha_t \mathbf{f}(t, \mathbf{x}^q_m(t)), \end{aligned} \tag{5.5}$$

converges. Furthermore, we have:

1. *The sequence* $\mathbf{x}^q_m(t)$ *satisfies the initial conditions for every iteration. Hence,*

$$\mathbf{x}^q_m(0) = \tilde{\mathbf{x}}_0, \quad \textit{for all } m, q \geq 0.$$

2. *The sequence* $\mathbf{x}^q_m(t)$ *converges uniformly to the solution of the IVP* $\mathbf{x}_\infty(t)$*. Hence*

$$\lim_{q,m\to\infty} \mathbf{x}^q_m(t) = \mathbf{x}_\infty(t), \textit{ for all } t \in [0, T].$$

3. *On every iteration, the following estimate holds for all* $t \in [0, T]$*:*

$$|\mathbf{x}_\infty(t) - \mathbf{x}^q_m(t)| \leq \mathbf{Q}^m(\mathbf{I} - \mathbf{Q})^{-1}\mathbf{b} + \mathbf{Q}^m\mathbf{e}_0 + (\mathbf{I} - \mathbf{Q}^m)(\mathbf{I} - \mathbf{Q})^{-1}\mathbf{n},$$

   Here, $\mathbf{Q} = \frac{T^\alpha \mathbf{K}}{\Gamma(\alpha+1)}$*,* $\Xi = \frac{T^\alpha}{2^{2\alpha-1}\Gamma(\alpha+1)}$*,* $\mathbf{b} = \frac{T^\alpha \mathbf{m}}{\Gamma(\alpha+1)} + ||\tilde{\mathbf{x}}_0 - \mathbf{x}_0||_\infty$*,* $\mathbf{e}_0 = \frac{5}{4}\omega\left(\mathbf{x}_0(t); \frac{h}{\sqrt{q}}\right)$*,* $\mathbf{n} = \left(\frac{h}{\sqrt{q}}\right)^\alpha \frac{5\,\mathbf{m}}{2\,\Gamma(\alpha+1)}$ *with* $\mathbf{m}, \mathbf{K}$ *are as in the assumptions of Theorem B.0.1,* h *is the maximum knot size* $h = \sup_{A_i \in \mathcal{A}} |A_i|$ *and* q *the order of Bernstein basis polynomial splines.*
4. *The approximation has a convergence order in knot size* h *of:*

$$\sup_{t\in[0,T]} |\mathbf{x}^q_\infty(t) - \mathbf{x}_\infty(t)| = \mathcal{O}(h^\alpha),$$

   and a convergence in polynomial order q *of:*

$$\sup_{t\in[0,T]} |\mathbf{x}^q_\infty(t) - \mathbf{x}_\infty(t)| = \mathcal{O}(q^{-\alpha/2}).$$

Proof. Item 1 follows quickly from (5.5) and the fact that $\mathbf{f}$ is continuous, yielding

$$\mathbf{x}^q_m(0) = \tilde{\mathbf{x}}_0 + \left[{}^q_0\Phi^\alpha_t \mathbf{f}(t, \mathbf{x}^q_{m-1})\right]_{t=0} = \tilde{\mathbf{x}}_0.$$

For items 2 and 3, write:

$$\begin{aligned} |\mathbf{x}^q_m(t) - \mathbf{x}^q_0(t)| &= |\tilde{\mathbf{x}}_0 - \mathbf{x}^q_0(t) + {}^q_0\Phi^\alpha_t \mathbf{f}(t, \mathbf{x}^q_{m-1}(t))| \\ &\leq |\tilde{\mathbf{x}}_0 - \mathbf{x}^q_0(t)| + |{}^q_0\Phi^\alpha_t \mathbf{f}(t, \mathbf{x}^q_{m-1}(t)) - {}_0\mathrm{I}^\alpha_t \mathbf{f}(t, \mathbf{x}^q_{m-1}(t))| + |{}_0\mathrm{I}^\alpha_t \mathbf{f}(t, \mathbf{x}^q_{m-1}(t))|. \end{aligned}$$

And thus by Lemma 4.3.1 and Proposition 2.2.3 we have, after taking the supremum:

$$||\mathbf{x}^q_m - \mathbf{x}^q_0||_\infty \leq ||\tilde{\mathbf{x}}_0 - \mathbf{x}^q_0||_\infty + \frac{5/2\left(\frac{h}{\sqrt{q}}\right)^\alpha + T^\alpha}{\Gamma(\alpha+1)}||f||_\infty := \mathbf{r}.$$

Now, take the sequence (5.4) satisfying requirements for convergence as established in [11]. Hence $||\mathbf{Q}|| := ||\frac{T^\alpha \mathbf{K}}{\Gamma(\alpha+1)}|| < 1$, for the Lipschitz coefficient matrix $\mathbf{K}$. We prove that the Bernstein splines

iterations converge to the analytical solution as $q \to \infty$. First, for $m = 0$, we have

$$\begin{aligned}
||\mathbf{x}_1^q - \mathbf{x}_1||_\infty &\leq ||{}_0^q\Phi_t^\alpha \mathbf{f}(t, \mathbf{x}_0^q(t)) - {}_0\mathrm{I}_t^\alpha \mathbf{f}(t, \mathbf{x}_0(t))||_\infty, \\
&\leq ||{}_0\mathrm{I}_t^\alpha [\mathbf{f}(t, \mathbf{x}_0(t)) - \mathbf{f}(t, \mathbf{x}_0^q(t))]||_\infty + ||({}_0\mathrm{I}_t^\alpha - {}_0^q\Phi_t^\alpha)\mathbf{f}(t, \mathbf{x}_0^q(t))||_\infty, \\
&\leq ||{}_0\mathrm{I}_t^\alpha [\mathbf{K}|\mathbf{x}_0(t) - \mathbf{x}_0^q(t)|]||_\infty + ||({}_0\mathrm{I}_t^\alpha - {}_0^q\Phi_t^\alpha)\mathbf{f}(t, \mathbf{x}_0^q(t))||_\infty, \\
&\leq \frac{T^\alpha \mathbf{K}}{\Gamma(\alpha+1)} ||\mathbf{x}_0(t) - S_{\mathcal{A}}^q \mathbf{x}_0(t)||_\infty + \left(\frac{h}{\sqrt{q}}\right)^\alpha \frac{5\,||f||_\infty}{2\,\Gamma(\alpha+1)}, \\
&\leq \underbrace{\frac{T^\alpha \mathbf{K}}{\Gamma(\alpha+1)}}_{=\mathbf{Q}} \underbrace{\frac{5}{4}\omega\left(\mathbf{x}_0(t); \frac{h}{\sqrt{q}}\right)}_{:=\mathbf{e}_0} + \underbrace{\left(\frac{h}{\sqrt{q}}\right)^\alpha \frac{5\,\mathbf{m}}{2\,\Gamma(\alpha+1)}}_{:=\mathbf{n}},
\end{aligned}$$

Now, for general $m+1$, we have

$$\begin{aligned}
||\mathbf{x}_{m+1}^q - \mathbf{x}_{m+1}||_\infty &\leq ||{}_0^q\Phi_t^\alpha \mathbf{f}(t, \mathbf{x}_m^q(t)) - {}_0\mathrm{I}_t^\alpha \mathbf{f}(t, \mathbf{x}_m(t))||_\infty, \\
&\leq ||{}_0\mathrm{I}_t^\alpha [\mathbf{f}(t, \mathbf{x}_m(t)) - \mathbf{f}(t, \mathbf{x}_m^q(t))]||_\infty + ||({}_0\mathrm{I}_t^\alpha - {}_0^q\Phi_t^\alpha)\mathbf{f}(t, \mathbf{x}_m^q(t))||_\infty, \\
&\leq ||{}_0\mathrm{I}_t^\alpha [\mathbf{K}|\mathbf{x}_m(t) - \mathbf{x}_m^q(t)|]||_\infty + ||({}_0\mathrm{I}_t^\alpha - {}_0^q\Phi_t^\alpha)\mathbf{f}(t, \mathbf{x}_m^q(t))||_\infty, \\
&\leq \frac{T^\alpha \mathbf{K}}{\Gamma(\alpha+1)} ||\mathbf{x}_m - \mathbf{x}_m^q||_\infty + \left(\frac{h}{\sqrt{q}}\right)^\alpha \frac{5\,||f||_\infty}{2\,\Gamma(\alpha+1)}, \\
&= \mathbf{Q}||\mathbf{x}_m - \mathbf{x}_m^q||_\infty + \mathbf{n}.
\end{aligned}$$

And thus,

$$\begin{aligned}
||\mathbf{x}_{m+1}^q - \mathbf{x}_{m+1}||_\infty &\leq \mathbf{Q}[\mathbf{Q}||\mathbf{x}_{m-1}(t) - \mathbf{x}_{m-1}^q(t)||_\infty + \mathbf{n}] + \mathbf{n}, \qquad (5.6) \\
&\leq \mathbf{Q}[\mathbf{Q}(\mathbf{Q}||\mathbf{x}_{m-2}(t) - \mathbf{x}_{m-2}^q(t)||_\infty + \mathbf{n}) + \mathbf{n}] + \mathbf{n}, \\
&\ldots \\
&\leq \mathbf{Q}^{m+1}\mathbf{e}_0 + \sum_{j=0}^{m} \mathbf{Q}^j \mathbf{n}, \\
&= \mathbf{Q}^{m+1}\mathbf{e}_0 + (\mathbf{I} - \mathbf{Q}^{m+1})(\mathbf{I} - \mathbf{Q})^{-1}\mathbf{n}. \qquad (5.7)
\end{aligned}$$

This already gives that

$$\lim_{m\to\infty} ||\mathbf{x}_m^q - \mathbf{x}_m||_\infty = \lim_{m\to\infty} \mathbf{Q}^m\mathbf{e}_0 + (\mathbf{I} - \mathbf{Q})^{-1}\mathbf{n} = (\mathbf{I} - \mathbf{Q})^{-1}\mathbf{n},$$

since $||\mathbf{Q}|| < 1$. This implies that the error of the iterative splines limit compared to the analytical solution is given by:

$$||\mathbf{x}_\infty^q - \mathbf{x}_\infty||_\infty = (\mathbf{I} - \mathbf{Q})^{-1}\mathbf{n} = \frac{5}{2\,\Gamma(\alpha+1)} \left(\frac{h}{\sqrt{q}}\right)^\alpha \left(\mathbf{I} - \frac{T^\alpha \mathbf{K}}{\Gamma(\alpha+1)}\right)^{-1} \mathbf{m}.$$

Furthermore, this gives us the convergence orders of

$$\sup_{t\in[0,T]} |\mathbf{x}^q(t) - \mathbf{x}(t)| = \mathcal{O}(h^\alpha), \quad \text{and} \quad \sup_{t\in[0,T]} |\mathbf{x}^q(t) - \mathbf{x}(t)| = \mathcal{O}(q^{-\alpha/2}).$$

Then, convergence is obtained as

$$\lim_{q\to\infty} ||\mathbf{x}_m^q - \mathbf{x}_m||_\infty = \lim_{q\to\infty} \left[\mathbf{Q}^m\mathbf{e}_0 + (\mathbf{I} - \mathbf{Q}^m)(\mathbf{I} - \mathbf{Q})^{-1}\mathbf{n}\right] = \mathbf{0}, \qquad (5.8)$$

since both $\mathbf{n} \to \mathbf{0}$ and $\mathbf{e}_0 \to \mathbf{0}$ as $q \to \infty$. Using these results, it can be shown that

$$\lim_{m,q\to\infty} ||\mathbf{x}_m^q - \mathbf{x}_m||_\infty = \lim_{m,q\to\infty} ||\mathbf{x}_m^q - \mathbf{x}_m||_\infty = \mathbf{0}.$$

Finally, to establish an error estimate on every iteration compared to the analytical solution, we use the result of Theorem B.0.1, stating $||\mathbf{x}_\infty - \mathbf{x}_m||_\infty \leq (\mathbf{I} - \mathbf{Q})^{-1}\mathbf{Q}^m\mathbf{b}$. Then, combining this with (5.7) gives:

$$\begin{aligned}
||\mathbf{x}_\infty - \mathbf{x}_m^q||_\infty &\leq ||\mathbf{x}_\infty - \mathbf{x}_m||_\infty + ||\mathbf{x}_m - \mathbf{x}_m^q||_\infty, \\
&\leq \mathbf{Q}^m(\mathbf{I} - \mathbf{Q})^{-1}\mathbf{b} + \mathbf{Q}^m\mathbf{e}_0 + (\mathbf{I} - \mathbf{Q}^m)(\mathbf{I} - \mathbf{Q})^{-1}\mathbf{n}.
\end{aligned}$$

□

Results show satisfactory convergence, with error convergence orders corresponding to the results of Bica [2]. However, one issue is the convergence requirements dependence on T^α in $\mathbf{Q}, \Xi, \mathbf{b}$. For general problems, this makes obtaining solutions impossible for larger T, as the convergence criteria cannot be satisfied. Luckily, there is a way to overcome this problem. Let us look at a way to obtain convergence criteria in h instead of T.

5.1.3. A new local splines approach

Once again, consider the initial-value problem (5.1). Now, for a local time-integration approach, instead of directly iterating to the integral equation (5.2), the aim is to satisfy

$$\mathbf{x}(t_i) = \tilde{\mathbf{x}}_0 + {}_0\mathrm{I}^\alpha_{t_i}\mathbf{f}(t, \mathbf{x}(t)), \quad \text{for all } i \in \{0, ..., N\}.$$

As noted in Remark 2.2.3, every $\mathbf{x}(t_i)$ is in general influenced by all previous values $\mathbf{x}(s)$, $s < t_i$ due to the nonlocal nature of the fractional integral. However, since values $\mathbf{x}(t_i)$ are independent of future values $\mathbf{x}(s)$, $s > t_i$, an iterative strategy is possible, creating a sequence of equations to satisfy:

$$\begin{cases} \mathbf{x}(t_0) &= \tilde{\mathbf{x}}_0, \\ \mathbf{x}(t_1) &= \tilde{\mathbf{x}}_0 + {}_0\mathrm{I}^\alpha_{t_1}\mathbf{f}(t, \mathbf{x}(t)), \\ \quad \vdots & \\ \mathbf{x}(t_N) &= \tilde{\mathbf{x}}_0 + {}_0\mathrm{I}^\alpha_{t_N}\mathbf{f}(t, \mathbf{x}(t)). \end{cases}$$

Using this setup, the main challenge becomes approximating the fractional integral ${}_0\mathrm{I}^\alpha_{t_n}\mathbf{f}(t, \mathbf{x}(t))$ by using the values of $\mathbf{x}(t_0), ..., \mathbf{x}(t_{n-1})$. Using the theory as developed in Chapter 4, a new local time-integration approach is developed, addressing the main concerns of existing time-integration approaches as established above.

A local analytical existence and uniqueness proof

First, let us establish an analytical approach to establish the "local" solution method and establish some notation. For more details, see Furati, Kassim, and Tatar [11] (where $\beta = 1$ yields the Caputo case). Consider the Caputo IVP (5.1) Already, one element of the splines-approach can be taken into account: the division of the time-domain. Take a knot collection $\mathcal{A} = \{A_0, A_1, ..., A_k\} = \{[0, t_1), [t_1, t_2), ..., [t_k, T]\}$ such that $\bigcup_{i=0}^k A_k = [0, T]$.

Then, we construct a solution function $\mathbf{x}_{j,\mathbf{n}} : [0, t_{j+1}] \to \mathbb{R}^d$ consisting of locally supported functions $\mathbf{u}_{i,n_i} : A_i \to \mathbb{R}^d$ such that:

$$\mathbf{x}_{j,\mathbf{n}}(t) = \sum_{i=0}^{j} \mathbf{u}_{i,n_i}\mathbb{1}_{A_i}(t) = \begin{cases} \mathbf{u}_{0,n_0}(t), & \text{if} \quad t \in A_0, \\ \mathbf{u}_{1,n_1}(t), & \text{if} \quad t \in A_1, \\ \quad \vdots & \\ \mathbf{u}_{j,n_j}(t), & \text{if} \quad t \in A_j. \end{cases}$$

Note that for the whole domain we have $\mathbf{x}_{k,\mathbf{n}} : [0, T] \to \mathbb{R}^d$. Now, define the recursive sequence

$$(\mathbf{u}_{i,n+1})_{n\geq 0} = \tilde{\mathbf{x}}_0 + {}_0\mathrm{I}^\alpha_t\mathbf{f}(t, \mathbf{x}_{i,\mathbf{n}}(t)), \quad \mathbf{n}_i = n, \quad t \in A_i,$$

where

$$\begin{cases} \mathbf{u}_{0,0} := \tilde{\mathbf{x}}_0, \\ \mathbf{u}_{i,0} := \lim\limits_{n\to\infty} \mathbf{u}_{i-1,n}, & \text{if} \quad i \geq 1. \end{cases}$$

Now, we can obtain a limit to approximate the solution $\mathbf{x} : [0, T] \to \mathbb{R}^d$:

$$\mathbf{x}(t) := \mathbf{x}_{k,\infty}(t) = \sum_{i=0}^{k} \lim_{n\to\infty} \mathbf{u}_{i,n}\mathbb{1}_{A_i}(t) \tag{5.9}$$

Convergence to the solution of the IVP can easily be obtained by the work of Furati, Kassim, and Tatar [11]:

Theorem 5.1.2 ("Local" approach analytical convergence for initial value problems)**.** *Given IVP* (5.1) *under the requirement that* $\mathbf{f}$ *is Lipschitz with coefficients* $\mathbf{K}$ *where* $\mathbf{K}$ *is as given in Theorem B.0.1. If knot collection* $\mathcal{A}$ *satisfies* $||\frac{\mathbf{K}}{\Gamma(\alpha)}(t_{i+1}-t_i)||_\infty < 1$ *for all* $i \in \{0,...,k\}$*, then, the limit of* (5.9) *converges to the unique solution of the Caputo IVP* (5.1)*. Furthermore, the solution* $\mathbf{x}$ *satisfies the integral equation* (5.2)*.*

Proof. See the proof of Theorem 25 of [11] for $\beta = 1$. □

A local splines approximation

Now that we have established an analytical result, let us approximate the solution using splines. Define the solution spline approximation $\mathbf{x}^q_{j,\mathbf{n}} : [0, t_{j+1}] \to \mathbb{R}^d$ as

$$\mathbf{x}^q_{j,\mathbf{n}}(t) = \sum_{i=0}^{j} \mathbf{u}^q_{i,n_i} \mathbb{1}_{A_i}(t) = \begin{cases} \mathbf{u}^q_{0,n_0}(t), & \text{if} \quad t \in A_0, \\ \mathbf{u}^q_{1,n_1}(t), & \text{if} \quad t \in A_1, \\ \quad \vdots & \\ \mathbf{u}^q_{j,n_j}(t), & \text{if} \quad t \in A_j. \end{cases} \tag{5.10}$$

and

$$(\mathbf{u}^q_{i,n+1}(t))_{n\geq 0} = \tilde{\mathbf{x}}_0 + {}^q_0\Phi^\alpha_t \mathbf{f}(t, \mathbf{x}^q_{i,\mathbf{n}}(t)), \quad \mathbf{n}_i = n, \quad t \in A_i, \tag{5.11}$$

where ${}^q_0\Phi^\alpha_t := S^q_{\mathcal{A}0}\mathrm{I}^\alpha_t$ is the splines integration operator as defined in Definition 4.3.1 and using

$$\begin{cases} \mathbf{u}^q_{0,0} := \tilde{\mathbf{x}}_0, \\ \mathbf{u}^q_{i,0} := \lim_{n\to\infty} \mathbf{u}^q_{i-1,n}, \quad \text{if} \quad i \geq 1, \end{cases}$$

for initial convergence points. Then, the local splines approximation is given by:

$$\mathbf{x}^q(t) := \mathbf{x}^q_{k,\infty}(t) = \sum_{i=0}^{k} \lim_{n\to\infty} \mathbf{u}^q_{i,n} \mathbb{1}_{A_i}(t). \tag{5.12}$$

Theorem 5.1.3 ("Local" approach spline convergence for initial value problems)**.** *Take IVP* (5.1) *with continuity and Lipschitz requirements for* $\mathbf{f}$ *with coefficients* $\mathbf{K}$ *and let* $\Psi = \frac{\frac{5}{2}\left(\frac{h}{\sqrt{q}}\right)^\alpha + h^\alpha}{\Gamma(\alpha+1)}$*. If knot collection* $\mathcal{A}$ *with max. knot size* h *satisfies* $||\Psi\mathbf{K}||_\infty < 1$*, then, the limit of* (5.12) *converges. Furthermore, we have:*

- ***Convergence in polynomial order.*** *The function* $\mathbf{x}_\infty := \lim_{q\to\infty} \mathbf{x}^q$ *converges to the unique solution* $\mathbf{x}$ *of IVP* (5.1) *with order*

$$\sup_{t\in[0,T]} |\mathbf{x}^q(t) - \mathbf{x}(t)| = \mathcal{O}(q^{-\alpha/2})$$

- ***Convergence in knot size.*** *The limit* $\lim_{h\to 0} \mathbf{x}^q$ *converges to the unique solution* $\mathbf{x}$ *of IVP* (5.1) *with order*

$$\sup_{t\in[0,T]} |\mathbf{x}^q(t) - \mathbf{x}(t)| = \mathcal{O}(h^\alpha)$$

Proof. Recall from Lemma 4.3.2 that ${}^q_{t_i}\Phi^\alpha_t$ is bounded. Using the proof of this lemma, we have that for $t > t_i$ such that $t - t_i < h$, this gives:

$$||{}^q_{t_i}\Phi^\alpha_t u||_\infty \leq \Psi ||u||_\infty,$$

with

$$\Psi = \frac{\frac{5}{2}\left(\frac{h}{\sqrt{q}}\right)^\alpha + h^\alpha}{\Gamma(\alpha+1)}.$$

Using this, we can construct a construction similar to the proof of the analytical sequence. For $i \in \{0, ..., k\}$, write

$$\begin{aligned}
||\mathbf{u}^q_{i,n+1} - \mathbf{u}^q_{i,n}||_\infty &= ||{}^q_0\Phi^\alpha_t\{\mathbf{f}(t, \mathbf{x}^q_{i,\mathbf{n}}(t)) - \mathbf{f}(t, \mathbf{x}^q_{i,\mathbf{n}-1}(t))\}||_\infty, \\
&= ||{}^q_{t_i}\Phi^\alpha_t\{\mathbf{f}(t, \mathbf{u}^q_{i,n}(t)) - \mathbf{f}(t, \mathbf{u}^q_{i,n-1}(t))\}||_\infty, \\
&\leq {}^q_{t_i}\Phi^\alpha_t||\mathbf{f}(t, \mathbf{u}^q_{i,n}(t)) - \mathbf{f}(t, \mathbf{u}^q_{i,n-1}(t))||_\infty, \\
&\leq \Psi||\mathbf{f}(t, \mathbf{u}^q_{i,n}(t)) - \mathbf{f}(t, \mathbf{u}^q_{i,n-1}(t))||_\infty, \\
&\leq \Psi\mathbf{K}||\mathbf{u}^q_{i,n} - \mathbf{u}^q_{i,n-1}||_\infty.
\end{aligned}$$

Hence, we have convergence for every sequence $(\mathbf{u}^q_{i,n})_{n\geq 0}$. Furthermore, from (5.11) and (5.10) it now follows that $\mathbf{x}^q : [0, T] \to \mathbb{R}^d$ satisfies:

$$\mathbf{x}^q(t) = \tilde{\mathbf{x}}_0 + {}^q_0\Phi^\alpha_t\mathbf{f}(t, \mathbf{x}^q(t)).$$

We prove that $\mathbf{x}_\infty := \lim_{q\to\infty} \mathbf{x}^q$ converges to the unique solution of the IVP by using the analytical integral equation formulation (5.2). We can write:

$$\begin{aligned}
\mathbf{x}^q(t) &= \tilde{\mathbf{x}}_0 + {}^q_0\Phi^\alpha_t\mathbf{f}(t, \mathbf{x}^q(t)) - {}_0\mathrm{I}^\alpha_t\mathbf{f}(t, \mathbf{x}^q(t)) + {}_0\mathrm{I}^\alpha_t\mathbf{f}(t, \mathbf{x}^q(t)), \\
&= \tilde{\mathbf{x}}_0 + ({}^q_0\Phi^\alpha_t - {}_0\mathrm{I}^\alpha_t)\mathbf{f}(t, \mathbf{x}^q(t)) + {}_0\mathrm{I}^\alpha_t\mathbf{f}(t, \mathbf{x}^q(t)),
\end{aligned} \tag{5.13}$$

and by Lemma 4.3.1 we have:

$$|\mathbf{x}^q(t) - \tilde{\mathbf{x}}_0 - {}_0\mathrm{I}^\alpha_t\mathbf{f}(t, \mathbf{x}^q(t))| \leq \left(\frac{h}{\sqrt{q}}\right)^\alpha \frac{5\,||\mathbf{f}||_\infty}{2\,\Gamma(\alpha+1)}.$$

Now, taking the limit on both sides yields

$$\lim_{q\to\infty} |\mathbf{x}^q(t) - \tilde{\mathbf{x}}_0 - {}_0\mathrm{I}^\alpha_t\mathbf{f}(t, \mathbf{x}^q(t))| = \mathbf{0},$$

which by the continuity of the absolute value, the continuity of the Riemann-Liouville integral with regards to $\mathbf{f}$ (see Remark 2.2.1) and of $\mathbf{f}$ in its second argument by Lipschitz continuity yields that

$$\mathbf{x}_\infty(t) = \tilde{\mathbf{x}}_0 + {}_0\mathrm{I}^\alpha_t\mathbf{f}(t, \mathbf{x}_\infty(t)).$$

This satisfies the Caputo-IVP integral equation (5.2) and hence the IVP. The same line of argumentation can be given for convergence in knot size h.

Finally, we use the above result to obtain a convergence order estimate in q and h. Taking an analytical solution $\mathbf{x} : [0, T] \to \mathbb{R}^d$ of the IVP (5.1) and integral equation (5.2), write:

$$\mathbf{x}^q(t) - \mathbf{x}(t) = ({}^q_0\Phi^\alpha_t - {}_0\mathrm{I}^\alpha_t)\mathbf{f}(t, \mathbf{x}^q(t)) + {}_0\mathrm{I}^\alpha_t\{\mathbf{f}(t, \mathbf{x}^q(t)) - \mathbf{f}(t, \mathbf{x})\}$$

And thus

$$\overline{|\mathbf{x}^q(t) - \mathbf{x}(t)|} \leq \left(\frac{h}{\sqrt{q}}\right)^\alpha \frac{5\,\overline{||\mathbf{f}||}_\infty}{2\,\Gamma(\alpha+1)} + ||\mathbf{K}||_\infty\,{}_0\mathrm{I}^\alpha_t\overline{|\mathbf{x}^q(t) - \mathbf{x}(t)|}, \tag{5.14}$$

where $\overline{\mathbf{v}} := \sup_{i\in\{1,...,d\}} v_i$ denotes the supremum over all dimension vector components and $||\mathbf{K}||_\infty$ denotes the supremum-matrix norm as the sum over each row. This makes (5.14) a scalar equation. Furthermore, since $\left(\frac{h}{\sqrt{q}}\right)^\alpha \frac{5\,\overline{||\mathbf{f}||}_\infty}{2\,\Gamma(\alpha+1)}$ does not depend on t, we can apply Grönwall's inequality for the fractional case: Corollary 2 of [41] gives:

$$\overline{|\mathbf{x}^q(t) - \mathbf{x}(t)|} \leq \left(\frac{h}{\sqrt{q}}\right)^\alpha \frac{5\,\overline{||\mathbf{f}||}_\infty}{2\,\Gamma(\alpha+1)}\mathrm{E}_\alpha(t^\alpha||\mathbf{K}||_\infty), \tag{5.15}$$

where $\mathrm{E}_\alpha(z) = \sum_{j=0}^\infty \frac{z^j}{\Gamma(j\alpha+1)}$ denotes the Mittag-Leffer function. Since $\mathrm{E}_\alpha(t^\alpha||\mathbf{K}||_\infty)$ is independent of q and h, and since the supremum is taken over all dimensions, one has convergence orders of:

$$\sup_{t\in[0,T]} |\mathbf{x}^q(t) - \mathbf{x}(t)| = \mathcal{O}(h^\alpha), \quad \text{and} \quad \sup_{t\in[0,T]} |\mathbf{x}^q(t) - \mathbf{x}(t)| = \mathcal{O}(q^{-\alpha/2}).$$

This concludes the proof by providing the final statement. □

In essence, the same integral equation is satisfied as when using the global solution method. Two main differences can be seen as compared to the global method. First of all, there is a spectral radius convergence requirement in h instead of T, as desired. However, another improvement is the absence of conditions on the initial approximation $\mathbf{x}_0^q$ since the local method only needs an initial value $\tilde{\mathbf{x}}_0$ for $t = 0$.

Remark 5.1.1 (A note on mixed-order systems). If a selection is taken of $\alpha = (\alpha_1, \alpha_2, ..., \alpha_d)$ with $\alpha_k \neq \alpha_m$ for $k \neq m$ in general, (5.14) can be adapted to take the supremum over all α_i, $i \in \{1, ..., d\}$, resulting in a convergence order of $\mathcal{O}(\sup_{i\in\{1,...,d\}} h_i^{\alpha})$ and $\mathcal{O}(\sup_{i\in\{1,...,d\}} q^{-\alpha_i/2})$.

5.1.4. An interpretation of global error

Remark 5.1.2 (An indication of the absolute global error). Although the order of convergence is a useful result, for nonlinear $\mathbf{f}$, this gives no useful indication of the absolute global error as the error propagates near-exponentially over time as shown in (5.15). However, both for the global and local method it is possible to give such an indication based on the results established above. Using again (5.13):

$$\mathbf{x}^q(t) = \tilde{\mathbf{x}}_0 + {}_0\mathrm{I}_t^{\alpha}\mathbf{f}(t, \mathbf{x}^q(t)) + ({}_0^q\Phi_t^{\alpha} - {}_0\mathrm{I}_t^{\alpha})\mathbf{f}(t, \mathbf{x}^q(t)),$$

taking the final expression in one function, we can write this as

$$\mathbf{x}^q(t) = \tilde{\mathbf{x}}_0 + {}_0\mathrm{I}_t^{\alpha}\mathbf{f}(t, \mathbf{x}^q(t)) + \mathbf{e}_s(t).$$

Furthermore, assume there is a certain tolerance ε in satisfying the equation above numerically, say $\mathbf{e}_{\varepsilon} \leq \varepsilon$. This yields the overall expression

$$\mathbf{x}^q(t) = \tilde{\mathbf{x}}_0 + {}_0\mathrm{I}_t^{\alpha}\mathbf{f}(t, \mathbf{x}^q(t)) + \mathbf{e}_s(t) + \mathbf{e}_{\varepsilon}(t).$$

Then, since the values at $t = 0$ are known as initial values, taking $\mathbf{e}_s(0) = \mathbf{e}_{\varepsilon}(0) = \mathbf{0}$, the expression can be rewritten as

$$\mathbf{x}^q(t) = \tilde{\mathbf{x}}_0 + {}_0\mathrm{I}_t^{\alpha}\left\{\mathbf{f}(t, \mathbf{x}^q(t)) + {}_0\mathrm{D}_t^{\alpha}\mathbf{e}_s(t) + {}_0\mathrm{D}_t^{\alpha}\mathbf{e}_{\varepsilon}(t)\right\},$$

where ${}_0\mathrm{D}_t^{\alpha}$ represents the Riemann-Liouville fractional derivative. Finally, assuming $\mathbf{e}_s(t) := \mathbf{c}$ and $\mathbf{e}_{\varepsilon}(t) := \varepsilon$ constant for $t > 0$, this gives

$$\mathbf{x}^q(t) = \tilde{\mathbf{x}}_0 + {}_0\mathrm{I}_t^{\alpha}\left\{\mathbf{f}(t, \mathbf{x}^q(t)) + \frac{\varepsilon + \mathbf{c}}{\Gamma(1-\alpha)}t^{-\alpha}\right\}.$$

The constant $\mathbf{c}$ can for instance be taken as $\mathbf{c} := \left(\frac{h}{\sqrt{q}}\right)^{\alpha}\frac{5\,||f||_{\infty}}{2\,\Gamma(\alpha+1)}$, representing a "worst case" for the spline integration error. This shows how the introduced error can be interpreted as decaying "forcing" on the system of differential equations.

5.1.5. Numerical results and convergence validation

In this section, the spline integration methods as outlined in Sections 5.1.2 and 5.1.3 are compared to their analytical solutions for simple problems. Furthermore, the error convergence and behavior is compared to Diethelm's predictor-corrector method [6] as outlined in Section 5.1.1.

Take the following IVP as a test problem:

$$\begin{cases} {}_0^{\mathrm{C}}\mathrm{D}_t^{\alpha}x(t) = t^k, & \alpha \in (0,1), \quad k > 0, \quad 0 < t < T, \\ x(0) = \tilde{x}_0, & \tilde{x}_0 \in \mathbb{R}. \end{cases} \tag{5.16}$$

By the equivalent integral equation and Proposition 2.2.6, the analytical solution can be given as the exact expression

$$x(t) = \frac{\Gamma(k+1)}{\Gamma(\alpha+k+1)}t^{\alpha+k} + \tilde{x}_0.$$

Note that in this example, since f only depends on t, f can be seen as Lipschitz in x with coefficient $\mathbf{K} = 0$. Now, the global solution method of Section 5.1.2 is applied for a linear polynomial structure

($q = 1$). Afterwards, it is compared to both the analytical solution and Diethelm's predictor-corrector method. Selected results are shown in Figure 5.1 and 5.2 and computational times are shown in Table 5.1.

Results in Figure 5.2 show good convergence, with a very quickly obtained sufficient convergence to the analytical solution compared to Diethelm's method. The splines method stays well below the analytical error order of $\mathcal{O}(h^{\alpha})$, whereas interestingly, Diethelms predictor-corrector shows higher errors than its upper bound of $\mathcal{O}(h^{\min(2,1+\alpha)})$ suggest. Furthermore, in the splines method, global error stabilizes after an initial peak right after $t = 0$, whereas in Diethelm's method, errors continue to grow approximately linearly.

Figure 5.2 shows a "worst-case" example for the splines method, with the error bound approximating the theoretical error bound. Hence, convergence is slower compared to the case above. Diethelm's method also performs worse for this problem. However, the error of Diethelm's method does appear to stabilize, which might also be attributed to the concave nature of the analytical solution. Finally, Table 5.1 shows a higher computational time for the spline method, which is as expected since more calculations are ran every timestep. For this example, satisfactory results are reached in two spline iterations per knot. However, it should be noted that for more complex and nonlinear problems, many more iterations can be required to solve the knot-wise iterations.

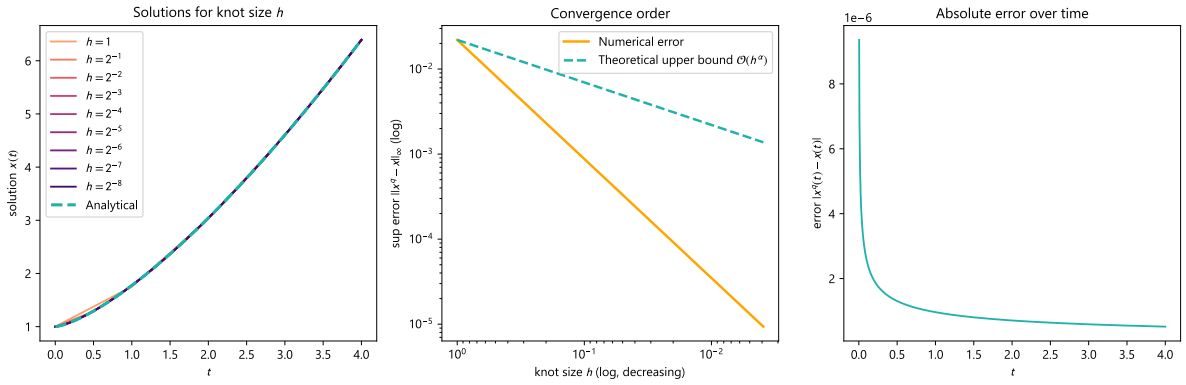

(a) Linear Bernstein splines $q = 1$.

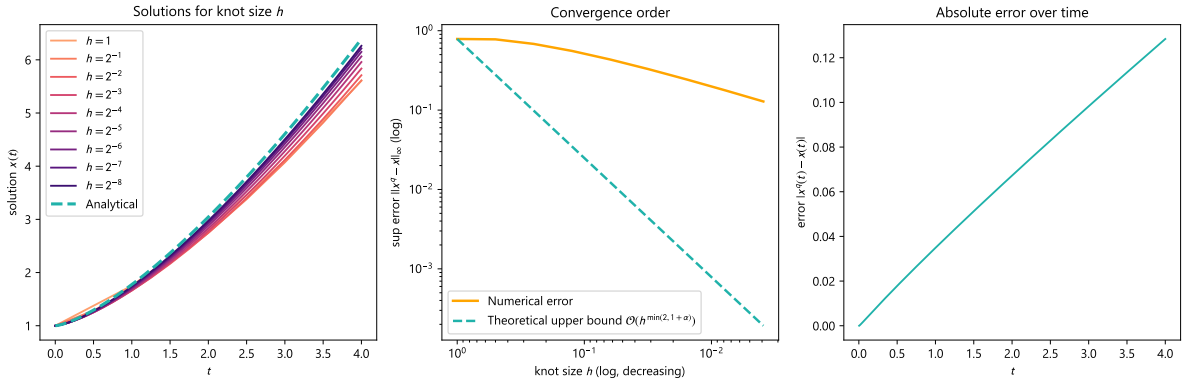

(b) Diethelm predictor-corrector.

Figure 5.1: Results of both the linear spline-integration method $q = 1$ (a) and Diethelm's predictor-corrector method (b) for IVP (5.16) with $\alpha = \frac{1}{2}$, $k = 0.9$, $\tilde{x}_0 = 1$, $T = 4$. The error over time is shown for the smallest respective knot sizes.

h	Diethelm time (s)	Splines time (s)	Spline iterations per knot
2^{-1}	6.990×10^{-3}	2.027×10^{-3}	2.0
2^{-2}	7.511×10^{-3}	2.066×10^{-3}	2.0
2^{-3}	1.081×10^{-2}	4.647×10^{-4}	2.0
2^{-4}	2.918×10^{-2}	4.184×10^{-3}	2.0
2^{-5}	4.174×10^{-2}	1.571×10^{-2}	2.0
2^{-6}	7.429×10^{-2}	3.163×10^{-2}	2.0
2^{-7}	1.248×10^{-1}	4.78×10^{-2}	2.0
2^{-8}	2.079×10^{-1}	1.567×10^{-1}	2.0

Table 5.1: Computational times for IVP (5.16) with $\alpha = \frac{1}{2}$, $k = 0.01$, $\tilde{x}_0 = 1$, $T = 4$, using the local splines approach ($q = 1$) and Diethelm's predictor-corrector method.

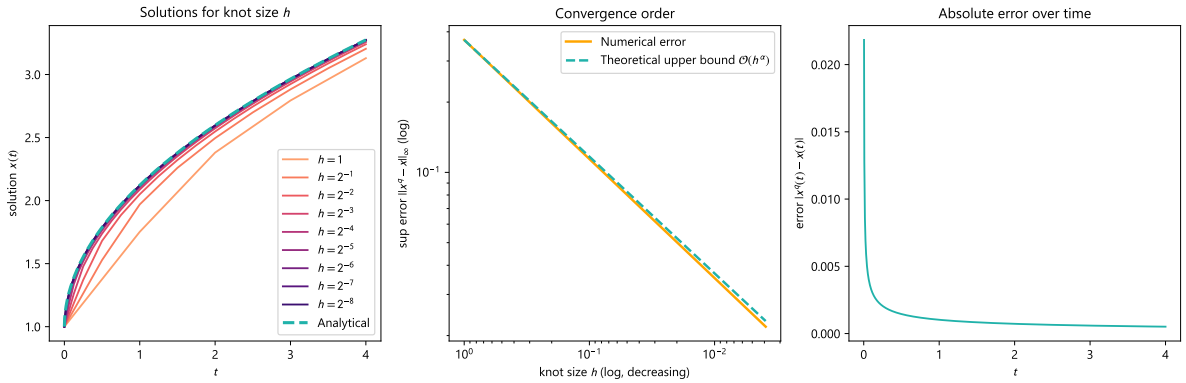

(a) Linear Bernstein splines $q = 1$.

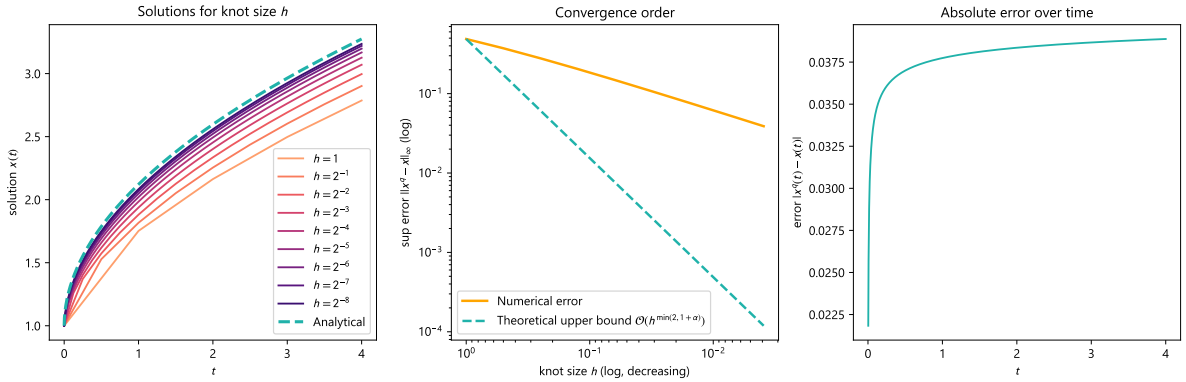

(b) Diethelm predictor-corrector.

Figure 5.2: Results of both the linear spline-integration method $q = 1$ (a) and Diethelm's predictor-corrector method (b) for IVP (5.16) with $\alpha = \frac{1}{2}$, $k = 0.01$, $\tilde{x}_0 = 1$, $T = 4$. The error over time is shown for the smallest respective knot sizes.

5.2. Methods for Hilfer-derivative initial value problems

Now, instead of merely taking the Caputo fractional derivative case, let us look at the more general Hilfer derivative. This introduces some problems in implementation, which are attempted to be addressed in the following sections.

5.2.1. Hilfer implementation problems

Instead of the Caputo fractional derivative, take the general Hilfer operator for IVP (3.1), restated below:

$$\begin{cases} {}_0\mathrm{D}_t^{\alpha,\beta}\mathbf{x}(t) = \mathbf{f}(t, \mathbf{x}(t)) & t > 0, \quad 0 < \alpha < 1, \quad 0 \leq \beta \leq 1, \\ {}_0\mathrm{I}_t^{1-\gamma}\mathbf{x}(0) = \tilde{\mathbf{x}}_0, & \gamma = \alpha + \beta - \alpha\beta. \end{cases}$$

Again, we have the assumptions $\mathbf{x} : [0,T] \mapsto D \subset \mathbb{R}^d$, $\mathbf{f} : [0,T] \times D \mapsto \mathbb{R}^d$ and $\mathbf{x}, \mathbf{f} \in C_{1-\gamma}[0,T] := \{g : [0,T] \to \mathbb{R}^d, t^{1-\gamma} g \in C[0,T]\}$, where D is a closed and bounded domain in the norm $||g||_{1-\gamma} := \sup_{t\in[0,b]} \left|t^{1-\gamma} g(t)\right|$. As provided in Section 3.1, solutions can be obtained using the equivalent integral equation (3.2), restated below:

$$\mathbf{x}(t) = \frac{\tilde{\mathbf{x}}_0}{\Gamma(\gamma)} t^{\gamma-1} + {}_0\mathrm{I}_t^\alpha \mathbf{f}(t, \mathbf{x}(t)).$$

However, since $0 < \gamma \leq 1$, with $\gamma = 1$ only satisfied for the Caputo case of $\beta = 1$, this gives in general a singular solution with $\mathbf{x}(t) \to \infty$ for $t \to 0$. This is also represented by the fact that as shown in section 3.1, the solutions to the Hilfer IVP are in the space $\mathbf{x} \in C_{1-\gamma}$.

In numerical implementation, this results in the following problems for the general Hilfer case of $\beta \neq 1$ and $\tilde{\mathbf{x}}_0 \neq \mathbf{0}$:

- Since $\lim_{t\to 0} x(t) = \infty$, one cannot evaluate the first knot, requiring the value of $\mathbf{x}(0)$ as coefficient (see Proposition 4.1.1).
- The Bernstein operator, and thus also the Bernstein spline operator, assume continuity on the function it operates on (Definition 4.1.2 and 4.2.1), which is not satisfied as $\mathbf{f}, \mathbf{x} \in C_{1-\gamma}[0,T] \not\subset C[0,T]$.
- As shown in Section 3.1, convergence is in the norm $||.||_{1-\gamma}$, providing no easily interpretable bounds for global errors and knot iteration stopping criteria, especially close to $t = 0$.

To overcome these challenges, a different approach is taken, making use of the flexible knot selection properties of the implementation as provided above.

5.2.2. Approximation methods for Hilfer-derivative initial value problems

Again, consider the problem setting and assumptions corresponding to IVP (3.1). However, now take the following integral equation:

$$\mathbf{x}_\varepsilon(t) = \frac{\tilde{\mathbf{x}}_0}{\Gamma(\gamma)} t^{\gamma-1} + {}_\varepsilon\mathrm{I}_t^\alpha \mathbf{f}(t, \mathbf{x}_\varepsilon(t)), \quad 0 < \varepsilon \leq t \leq T. \tag{5.17}$$

Thus, instead of starting from $t_0 = 0$, $t_0 = \varepsilon > 0$ is taken. Let us prove that we can come arbitrarily close to the original Hilfer IVP:

Theorem 5.2.1 (Epsilon time-shifted Hilfer IVP convergence)**.** *Take the Hilfer IVP with the existence and uniqueness assumptions of Theorem* (3.1.2)*. Additionaly, assume* $\alpha + \gamma > 1$*. Now, assume the shifted integral equation* (5.17) *has a solution* $\mathbf{x}_\varepsilon : (\varepsilon, T] \to D \subset \mathbb{R}^d$*. Then,*

$$\lim_{\varepsilon\downarrow 0} \sup_{t\in(\varepsilon,T]} |\mathbf{x}(t) - \mathbf{x}_\varepsilon(t)| = \mathbf{0},$$

where $\mathbf{x}$ *is the solution of the analytical integral equation* (3.2) *and IVP* (3.1)*. Furthermore,*

$$\sup_{t\in(\varepsilon,T]} |\mathbf{x}(t) - \mathbf{x}_\varepsilon(t)| = \mathcal{O}(\varepsilon^{\alpha+\gamma-1}).$$

Proof. Take $\mathbf{x} : (0,T] \to \mathbb{R}^d$ satisfying the Hilfer integral equation (3.2) and $\mathbf{x} : [\varepsilon, T] \to \mathbb{R}^d$ satisfying the shifted Hilfer integral equation (5.17) for the same problem. Then, for $\varepsilon \leq t \leq T$ write:

$$\begin{aligned}\mathbf{x}(t) - \mathbf{x}_\varepsilon(t) &= {}_0\mathrm{I}_t^\alpha \mathbf{f}(t, \mathbf{x}(t)) - {}_\varepsilon\mathrm{I}_t^\alpha \mathbf{f}(t, \mathbf{x}_\varepsilon(t)), \\ &= {}_0\mathrm{I}_\varepsilon^\alpha \mathbf{f}(t, \mathbf{x}(t)) + {}_\varepsilon\mathrm{I}_t^\alpha [\mathbf{f}(t, \mathbf{x}(t)) - \mathbf{f}(t, \mathbf{x}_\varepsilon(t))].\end{aligned}$$

By the Lipschitz condition on $\mathbf{f}$ and the triangle inequality, we have

$$|\mathbf{x}(t) - \mathbf{x}_\varepsilon(t)| \leq |{}_0\mathrm{I}_\varepsilon^\alpha \mathbf{f}(t, \mathbf{x}(t))| + {}_\varepsilon\mathrm{I}_t^\alpha \mathbf{K} |\mathbf{x}(t) - \mathbf{x}_\varepsilon(t)|. \tag{5.18}$$

The first term in (5.18), arising from the time shifting, can be written out as follows by making use of the Hölder inequality:

$$\begin{aligned}|{}_0\mathrm{I}_\varepsilon^\alpha \mathbf{f}(t,\mathbf{x}(t))| &\leq \frac{1}{\Gamma(\alpha)}\int_0^\varepsilon |(t-s)^{\alpha-1}\mathbf{f}(t,\mathbf{x}(t))|\,\mathrm{d}s,\\ &= \frac{1}{\Gamma(\alpha)}\int_0^\varepsilon |(t-s)^{\alpha-1}s^{\gamma-1}\mathbf{f}(t,\mathbf{x}(t))s^{1-\gamma}|\,\mathrm{d}s,\\ &\leq \frac{1}{\Gamma(\alpha)}\int_0^\varepsilon (t-s)^{\alpha-1}s^{\gamma-1}\,\mathrm{d}s\,||\mathbf{f}||_{1-\gamma}.\end{aligned}$$

Then, by Proposition 2.2.7, we know

$$\frac{1}{\Gamma(\alpha)}\int_0^\varepsilon (t-s)^{\alpha-1}s^{\gamma-1}\,\mathrm{d}s = \frac{t^{\alpha+\gamma-1}}{\Gamma(\alpha)}\mathrm{B}_{\varepsilon/t}(\gamma,\alpha),$$

where $\mathrm{B}_z(a,b)$ denotes the incomplete beta function (Definition 2.2.3). Hence, we can write:

$$|{}_0\mathrm{I}_\varepsilon^\alpha \mathbf{f}(t,\mathbf{x}(t))| \leq \frac{t^{\alpha+\gamma-1}}{\Gamma(\alpha)}\mathrm{B}_{\varepsilon/t}(\gamma,\alpha)||\mathbf{f}||_{1-\gamma}.$$

Furthermore, as will be used later in the proof, this function is decreasing in $t > \varepsilon$, since

$$\begin{aligned}\frac{\mathrm{d}}{\mathrm{d}t}\left(\frac{1}{\Gamma(\alpha)}\int_0^\varepsilon (t-s)^{\alpha-1}s^{\gamma-1}\,\mathrm{d}s\right) &= \frac{1}{\Gamma(\alpha)}\int_0^\varepsilon \frac{\mathrm{d}}{\mathrm{d}t}(t-s)^{\alpha-1}s^{\gamma-1}\,\mathrm{d}s,\\ &= (\alpha-1)\frac{1}{\Gamma(\alpha)}\int_0^\varepsilon (t-s)^{\alpha-2}s^{\gamma-1}\,\mathrm{d}s < 0,\end{aligned}$$

as $(t-s)^{\alpha-2}s^{\gamma-1} \geq 0$ for $\alpha \in (0,1)$, $\gamma \in (0,1]$, $0 \leq s \leq \varepsilon$ and furthermore $(\alpha-1) < 0$. Thus, the supremum must be attained at $t = \varepsilon$, and hence:

$$|{}_0\mathrm{I}_\varepsilon^\alpha \mathbf{f}(t,\mathbf{x}(t))| \leq \frac{\varepsilon^{\alpha+\gamma-1}}{\Gamma(\alpha)}\mathrm{B}(\gamma,\alpha)||\mathbf{f}||_{1-\gamma}, = \varepsilon^{\alpha+\gamma-1}\underbrace{\frac{\Gamma(\gamma)}{\Gamma(\alpha+\gamma)}}_{:=\Theta}||\mathbf{f}||_{1-\gamma}.$$

Here, B denotes the regular beta function (Definition 2.2.2), equal to the incomplete beta function B_z for $z = 1$. Then, substituting back to (5.18), we have

$$|\mathbf{x}(t) - \mathbf{x}_\varepsilon(t)| \leq \varepsilon^{\alpha+\gamma-1}\Theta + {}_\varepsilon\mathrm{I}_t^\alpha \mathbf{K}|\mathbf{x}(t) - \mathbf{x}_\varepsilon(t)|.$$

Now, writing $\mathbf{u}(t) := |\mathbf{x}(t) - \mathbf{x}_\varepsilon(t)|\mathbb{1}_{[\varepsilon,T]}(t)$, we have

$$\overline{\mathbf{u}}(t) \leq \varepsilon^{\alpha+\gamma-1}\Theta + \frac{||\mathbf{K}||_\infty}{\Gamma(\alpha)}\int_0^t (t-s)^{\alpha-1}\overline{\mathbf{u}}(s)\,\mathrm{d}s.$$

Here, $\overline{\mathbf{v}} := \sup_{i\in\{1,\dots,d\}} v_i$ denotes the supremum over all dimension vector components and $||\mathbf{K}||_\infty$ denotes the supremum-matrix norm as the sum over each row. Now, by the fractional Grönwall inequality as proven in Corollary 2 of Ye, Gao, and Ding [41], we have:

$$\overline{\mathbf{u}}(t) \leq \varepsilon^{\alpha+\gamma-1}\Theta\mathrm{E}_\alpha(t^\alpha||\mathbf{K}||_\infty),$$

where $\mathrm{E}_\alpha(z) = \sum_{j=0}^\infty \frac{z^j}{\Gamma(j\alpha+1)}$ denotes the Mittag-Leffler function. Writing this back as an upper bound to the components of $\mathbf{x}$ and taking the limit over the supremum now gives:

$$\lim_{\varepsilon\to 0}\left(\sup_{t\in(\varepsilon,T]}|\mathbf{x}(t) - \mathbf{x}_\varepsilon(t)|\right) \leq \lim_{\varepsilon\to 0}\varepsilon^{\alpha+\gamma-1}\Theta\mathrm{E}_\alpha(T^\alpha||\mathbf{K}||_\infty) = \mathbf{0},$$

since $\alpha+\gamma-1 > 0$. Furthermore, since $\Theta\mathrm{E}_\alpha(T^\alpha||\mathbf{K}||_\infty)$ is independent of ε, we know:

$$\sup_{t\in(\varepsilon,T]}|\mathbf{x}(t) - \mathbf{x}_\varepsilon(t)| = \mathcal{O}(\varepsilon^{\alpha+\gamma-1}),$$

concluding the proof. □

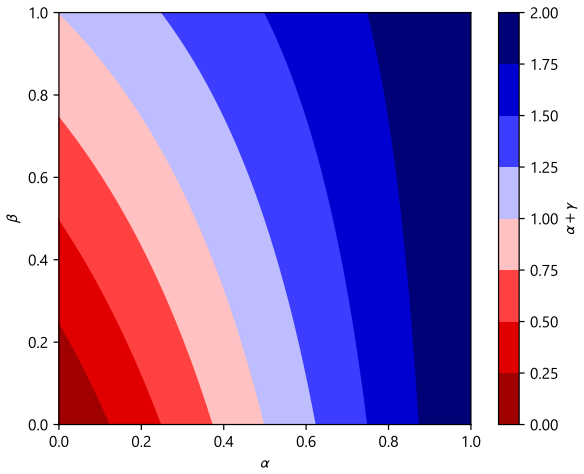

Figure 5.3: $\alpha + \gamma$ for values of integration order α and Hilfer integral type β. Values for which convergence condition $\alpha + \gamma > 1$ of Theorem 5.2.1 is satisfied are shown in shades of blue and other values in shades of red.

Remark 5.2.1 (Hilfer order and type requirements). The requirement of $\alpha + \gamma > 1$ introduces a dependency on the integral type and order. Recalling that $\gamma = \alpha + \beta - \alpha\beta$, this gives $\alpha > \frac{1-\beta}{2-\beta}$. With the further requirement, $\alpha \in (0, 1)$, $\beta \in [0, 1]$, this gives a dependency as illustrated in Figure 5.3. This implies for instance that for the Riemann-Liouville-derivative ($\beta = 0$), the condition $\alpha > 0.5$ must be satisfied.

Now that we have established the connection to the analytical Hilfer IVP of Theorem 5.2.1, the goal is to obtain a splines approximation $\mathbf{x}_\varepsilon^q$ to the shifted integral equation (5.17). However, in implementation this may cause problems, as for low values of ε, we have that $\mathbf{x}_\varepsilon \sim \varepsilon^{\gamma-1}$, which yields very high values around $t = \varepsilon$ since $0 < \gamma \leq 1$. Raising the value of ε however gives worse approximations to the exact solution, as seen in the results of Theorem 5.2.1.

To overcome this problem, a new strategy is taken for implementation. Note that by Theorem 3.1.2, we know $t^{1-\gamma}\mathbf{x} \in C[0, T]$. Now, instead of solving for $\mathbf{x}_\varepsilon$ of integral equation (5.17), consider the transformation

$$\mathbf{v}_\varepsilon(t) := t^{1-\gamma}\mathbf{x}_\varepsilon(t). \tag{5.19}$$

Then, substituting in (5.17) gives

$$\mathbf{v}_\varepsilon(t) = \frac{\mathbf{x}_0}{\Gamma(\gamma)} + t^{1-\gamma}{}_\varepsilon\mathrm{I}_t^\alpha \mathbf{f}(t, t^{\gamma-1}\mathbf{v}_\varepsilon(t)), \quad 0 < \varepsilon \leq t \leq T.$$

Finally, the original result can then be obtained by the inverse transformation of (5.19), taking:

$$\mathbf{x}_\varepsilon(t) = t^{\gamma-1}\mathbf{v}_\varepsilon(t).$$

Now, it is only left to show is for which conditions (5.17) admits a spline solution:
Proposition 5.2.1 (Spline solutions for ε-shifted Hilfer integral equation)**.** *Consider integral equation* (5.17) *on the transformation* (5.19)*. Assume the conditions of existence and uniqueness of Theorem 3.1.2 hold for IVP* (3.1) *and* $\mathbf{x}_\varepsilon \in C_{1-\gamma}[0, T]$*. Then, if*

$$||\mathbf{\Psi}\mathbf{K}_\varepsilon||_\infty < 1,$$

where $\mathbf{\Psi}$ *is as given in Theorem 5.1.3 and* $\mathbf{K}_\varepsilon := \left(\frac{T}{\varepsilon}\right)^{1-\gamma}\mathbf{K}$*, a splines solution* $\mathbf{v}_\varepsilon^q(t) \in C[0, T]$ *to integral equation* (5.19) *can be found, providing* $\mathbf{x}_\varepsilon^q := t^{\gamma-1}\mathbf{v}_\varepsilon^q(t)$*.*

Proof. Rewriting (5.19) gives:

$$\mathbf{v}_\varepsilon(t) = \frac{\mathbf{x}_0}{\Gamma(\gamma)} + {}_\varepsilon\mathrm{I}_t^\alpha t^{1-\gamma}\mathbf{f}(s, s^{\gamma-1}\mathbf{v}_\varepsilon(s)) := \frac{\mathbf{x}_0}{\Gamma(\gamma)} + {}_\varepsilon\mathrm{I}_t^\alpha \mathbf{g}(s, \mathbf{v}_\varepsilon(s)).$$

Here, s is used as variable of integration instead of t to avoid confusion with $t^{1-\gamma}$. Now, since by assumption $\mathbf{x}_\varepsilon, \mathbf{f} \in C_{1-\gamma}[0,T]$ one has $\mathbf{v}_\varepsilon, t^{1-\gamma}\mathbf{f} \in C[0,T]$. Furthermore, recall $|t^{1-\gamma}\mathbf{f}| \leq \mathbf{m}$ for all $\varepsilon < t < T$. Now, it goes to show that $\mathbf{g}$ satisfies the Lipschitz condition in $\mathbf{v}_\varepsilon$. Using the assumption of $\mathbf{f}$ being Lipschitz with coefficients $\mathbf{K}$, take $\varepsilon \leq t \leq T$. Then, for all $\varepsilon \leq s \leq t$ and $s^{\gamma-1}\mathbf{y}, s^{\gamma-1}\mathbf{z} \in D$:

$$\begin{aligned}
|\mathbf{g}(s,\mathbf{y}(s)) - \mathbf{g}(s,\mathbf{z}(s))| &= |t^{1-\gamma}\mathbf{f}(s, s^{\gamma-1}\mathbf{y}(s)) - t^{1-\gamma}\mathbf{f}(s, s^{\gamma-1}\mathbf{z}(s))|, \\
&\leq t^{1-\gamma}\mathbf{K}|s^{\gamma-1}\mathbf{y}(s) - s^{\gamma-1}\mathbf{z}(s)|, \\
&= \left(\frac{t}{s}\right)^{1-\gamma} \mathbf{K}|\mathbf{y}(s) - \mathbf{z}(s)|, \\
&\leq \left(\frac{t}{\varepsilon}\right)^{1-\gamma} \mathbf{K}|\mathbf{y}(s) - \mathbf{z}(s)|.
\end{aligned}$$

And hence, for all $\varepsilon \leq t \leq$, the Lipschitz condition on $\mathbf{g}$ is satisfied for $\mathbf{K}_\varepsilon = \left(\frac{T}{\varepsilon}\right)^{1-\gamma}$. Then, following the proof of Theorem 5.1.3, we can find a splines solution to the integral equation (5.17) for $\mathbf{v}_\varepsilon$ since by assumption, $||\Psi\mathbf{K}_\varepsilon||_\infty < 1$. Furthermore, since by the result of Theorem 5.1.3 $\sup_{t\in(\varepsilon,T]} |\mathbf{v}_\varepsilon(t) - \mathbf{v}(t)| = \mathcal{O}(h^\alpha, q^{-\alpha/2})$, we have:

$$\begin{aligned}
\sup_{t\in(\varepsilon,T]} |\mathbf{x}_\varepsilon(t) - \mathbf{x}(t)| &= \sup_{t\in(\varepsilon,T]} |t^{1-\gamma}\mathbf{v}_\varepsilon(t) - t^{1-\gamma}\mathbf{v}(t)|, \\
&\leq T^{1-\gamma} \sup_{t\in(\varepsilon,T]} |\mathbf{v}_\varepsilon(t) - \mathbf{v}(t)| \\
&= \mathcal{O}(h^\alpha, q^{-\alpha/2}).
\end{aligned}$$

□

Now, we can finally establish a convergence result for the Hilfer derivative IVP:
Corollary 5.2.1 (Hilfer derivative IVP splines convergence)**.** *Take IVP 3.1 with Hilfer derivative. Assume the conditions for Theorem 5.2.1 and Proposition 5.2.1 hold. Then,*

$$\lim_{\varepsilon\downarrow 0,\ h\to 0,\ q\to\infty} \sup_{t\in(\varepsilon,T]} |\mathbf{x}(t) - \mathbf{x}_\varepsilon^q(t)| = \mathbf{0},$$

where $\mathbf{x}$ *is the analytical solution as obtained in Theorem 3.1.2 and* $\mathbf{x}_\varepsilon^q$ *the corresponding splines approximation as in Proposition 5.2.1.*

Proof. By the triangle inequality,

$$\sup_{t\in(\varepsilon,T]} |\mathbf{x}(t) - \mathbf{x}_\varepsilon^q(t)| \leq \sup_{t\in(\varepsilon,T]} |\mathbf{x}(t) - \mathbf{x}_\varepsilon(t)| + \sup_{t\in(\varepsilon,T]} |\mathbf{x}_\varepsilon(t) - \mathbf{x}_\varepsilon^q(t)|,$$

after which the result follows from the results of Theorem 5.2.1 and Proposition 5.2.1 by taking the limit. □

Remark 5.2.2 (Conditions on $\mathbf{K}_\varepsilon$: the ε-dilemma)*.* The the convergence requirements on $\mathbf{K}_\varepsilon$ in Proposition 5.2.1 are very strict for small ε. However, larger ε results in a larger error from the ε-time shifting in Theorem 5.2.1. Are we stuck between two evils? Theoretically, yes. However, in practice, it appears convergence can be satisfied in most cases. An advantage of the splines approach is that a more accurate knot selection can be chosen closer to ε, where values of $\mathbf{K}$ tend to be higher due to an increase in domain size D because of the singularity in solutions close to ε. In the following section and in Section 7.3.2, some practical convergence examples will be shown.

5.2.3. Implementation and results

Let us apply the above to a simple example, taking the same test problem as in the Caputo case of (5.16) but with Hilfer derivative operator. We will now make approximations using ε-shifting of Theorem 5.2.1 and time transformations of Proposition 5.2.1 of the previous section. Analytical solutions are given by:

$$x(t) = \frac{\Gamma(k+1)}{\Gamma(\alpha+k+1)} t^{\alpha+k} + \tilde{x}_0 t^{\gamma-1}.$$

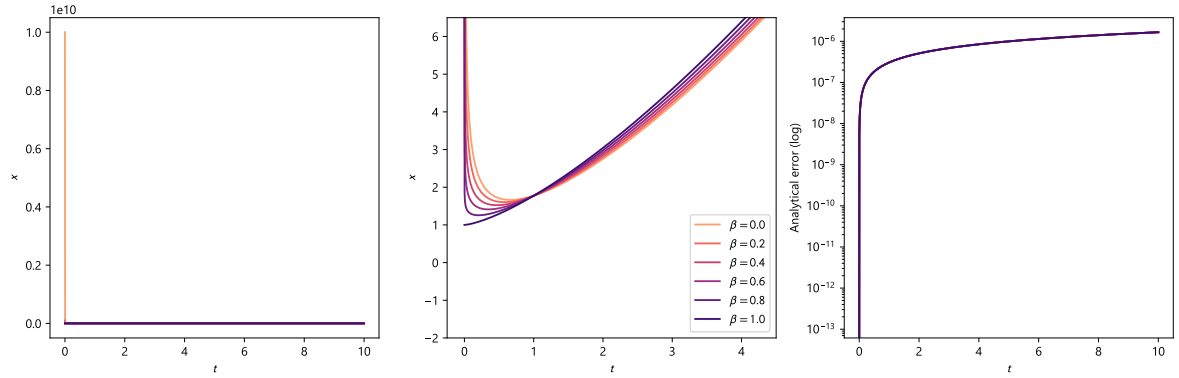

Figure 5.4: Results of the linear spline-integration method with ε-shifting for Hilfer problems for the Hilfer-adaptation of the IVP as in Figure 5.1 in full (left) detail (center) and showing errors (right).

The same values are taken as in the setup shown in Figure 5.1 ($k = 0.9$, $q = 1$, $\tilde{x}_0 = 1$) for different values of β and for $h = 0.01$. A small value of $\varepsilon = 10^{-15}$ is taken. Furthermore, we take $\alpha = \frac{1}{2} + \varepsilon$ to satisfy the requirements of Theorem 5.2.1. Note that in this case, $\mathbf{K} = 0$, hence no problems in ε choices for convergence are present as discussed in Remark 5.2.2. Results are shown in Figure 5.4. Errors are very low, below 10^{-6} in all cases. The behavior of transitioning between Caputo solutions $(\beta = 1)$ and Riemann-Liouville solutions $(\beta = 0)$ can be clearly seen in the results. Errors are roughly identical in all cases, which can be explained by the problem f being fully dependent on t and thus yielding no significant problems in domain size increase D as discussed in Remark 5.2.2. A nonlinear example will be shown in Section 7.3.2.

6

Bernstein splines applied to fractional boundary value problems (BVP's)

In this section, the spline theory of the previous chapter will be applied to fractional-order BVP's as studied in Section 3.2. Results are provided first for the Caputo-derivative in Section 6.1. In Section 6.2, the Hilfer-derivative IVP spline methods of Section 5.2 are applied to Hilfer-fractional derivative BVP's. Source code for all methods is provided in `https://github.com/ngoedegebure/fracnum`.

6.1. Methods for Caputo-derivative boundary value problems

Consider BVP (3.3) -(3.4) for $\beta = 1$, resulting in the Caputo fractional derivative BVP given as:

$$\begin{cases} {}_0^{\mathrm{C}}\mathrm{D}_t^{\alpha}\mathbf{x}(t) = \mathbf{f}(t,\mathbf{x}), \quad 0 < t < T, \quad \alpha \in (0,1), \\ \mathbf{x}(0) = \mathbf{x}(T), \end{cases} \tag{6.1}$$

Requirements on $\mathbf{f}$, T and α for existence and uniqueness of the solution $\mathbf{x}$ are discussed in Section 3.2. Let us formulate a splines solution approach and prove its convergence to the analytical solution.

6.1.1. Bernstein spline iterations: the "global approach"

Theorem 6.1.1 (Convergence of fractional splines iterations for BVP's)**.** *Given BVP* (6.1)*, assume the requirements of Theorem 3.2.1 hold. Hence, the analytical sequence*

$$\mathbf{x}_{m+1}(t) = \tilde{\mathbf{x}}_0 + {}_0\mathrm{I}_t^{\alpha}\mathbf{f}(t,\mathbf{x}_m(t)) - (t/T)^{\alpha}\,{}_0\mathrm{I}_T^{\alpha}\mathbf{f}(t,\mathbf{x}_m(t)),$$

converges to the unique continuous solution $\mathbf{x}_{\infty} : [0,T] \to \mathbb{R}$ *of* (6.1) *for a choice of initial approximation* $\mathbf{x}_0$*. Now, assume there exists a nonnegative vector*

$$\mathbf{r} = ||\tilde{\mathbf{x}}_0 - \mathbf{x}_0^q||_{\infty} + \frac{5\left(\frac{h}{\sqrt{q}}\right)^{\alpha} + T^{\alpha}2^{1-2\alpha}}{\Gamma(\alpha+1)}\mathbf{m},$$

such that for $\mathbf{x}_0$ *we have:*

$$D_{\mathbf{r}} := \{\{\mathbf{u} \in D_{\beta} : ||\mathbf{u} - \mathbf{x}_0||_{\infty} \leq \mathbf{r}\} \subset D_{\beta}\},$$

is non-empty and $\mathbf{f}$ *is Lipschitz with coefficients* $\mathbf{K}$ *for every* $\mathbf{u}, \mathbf{v} \in D_{\mathbf{r}}$*, where* $\mathbf{K}$ *and* D_{β} *are as given in Theorem 3.2.1. Then, for a knot collection* $\mathcal{A}$ *such that* $\cup_{A_i \in \mathcal{A}} A_i = [0,T]$*, spline operator* $S_{\mathcal{A}}^q$ *(Definition 4.2.1) and spline integration operator* ${}_0^q\Phi_t^{\alpha}$ *(Definition 4.3.1), the iterative sequence using Bernstein splines as defined by*

$$\begin{aligned} \mathbf{x}_0^q(t) &:= S_{\mathcal{A}}^q\mathbf{x}_0(t), \\ \mathbf{x}_{m+1}(t) &= \tilde{\mathbf{x}}_0 + {}_0^q\Phi_t^{\alpha}\mathbf{f}(t,\mathbf{x}_m(t)) - S_{\mathcal{A}}^q\,(t/T)^{\alpha}\,{}_0^q\Phi_T^{\alpha}\mathbf{f}(s,\mathbf{x}_m(s)), \end{aligned} \tag{6.2}$$

converges. Furthermore, it holds that:

1. *The sequence $\mathbf{x}_m^q(t)$ satisfies the boundary conditions at every iteration step. Hence,*
$$\mathbf{x}_m(0) = \mathbf{x}_m(T), \quad \textit{for all } m, q \geq 0.$$
2. *The sequence $\mathbf{x}_m^q(t)$ converges uniformly to the solution of the BVP $\mathbf{x}_\infty(t)$. Hence,*
$$\lim_{q,m\to\infty} \mathbf{x}_m^q(t) = \mathbf{x}_\infty(t), \quad \textit{for all } t \in [0,T].$$
3. *On every iteration, the following estimate holds:*
$$||x_\infty - x_m^q||_\infty \leq \mathbf{Q}^m(\mathbf{I}-\mathbf{Q})^{-1}\mathbf{b} + \mathbf{Q}^m\mathbf{e}_0 + (\mathbf{I}-\mathbf{Q}^m)(\mathbf{I}-\mathbf{Q})^{-1}\mathbf{n},$$
Here, $\mathbf{Q} = \Xi\mathbf{K}$, $\Xi = \frac{T^\alpha}{2^{2\alpha-1}\Gamma(\alpha+1)}$, $\mathbf{b} = \Xi\mathbf{m} + ||\tilde{\mathbf{x}}_0 - \mathbf{x}_0||_\infty$, $\mathbf{e}_0 = \frac{5}{4}\omega\left(\mathbf{x}_0(t); \frac{h}{\sqrt{q}}\right)$, $\mathbf{n} = \left(\frac{h}{\sqrt{q}}\right)^\alpha \frac{5}{\Gamma(\alpha+1)}\mathbf{m}$ with $\mathbf{m}, \mathbf{K}$ are as in Theorem 3.2.1, h being the maximum knot size $h = \sup_{A_i\in\mathcal{A}} |A_i|$ and q denotes the order of Bernstein basis polynomial splines.

Proof. First, for notation purposes, define for continuous $\mathbf{u} : [0,T] \to \mathbb{R}^d$ the operator:
$$\Lambda^q\mathbf{u}(t) := \tilde{\mathbf{x}}_0 + {}_0^q\Phi_t^\alpha\mathbf{u}(t) - S_\mathcal{A}^q (t/T)^\alpha {}_0^q\Phi_T^\alpha\mathbf{u}(t).$$
Then, following the notation of Definition 4.3.1, define
$$\Lambda\mathbf{u}(t) := \tilde{\mathbf{x}}_0 + {}_0\mathrm{I}_t^\alpha\mathbf{u}(t) - (t/T)^\alpha {}_0\mathrm{I}_T^\alpha\mathbf{u}(t).$$
Note that we can write $\Lambda^q\mathbf{u} = S_\mathcal{A}^q\Lambda\mathbf{u}$. Thus, by Lemma 4.2.1
$$||\Lambda^q\mathbf{u} - \Lambda\mathbf{u}||_\infty = ||S_\mathcal{A}^q\Lambda\mathbf{u} - \Lambda\mathbf{u}||_\infty \leq \frac{5}{4}\omega\left(\Lambda\mathbf{u}; \left(\frac{h}{\sqrt{q}}\right)\right).$$
Now, proceeding as in [10], we have for $t_1, t_2 \in [0,T]$ that
$$|\Lambda\mathbf{u}(t_2) - \Lambda\mathbf{u}(t_1)| \leq 4\frac{(t_2-t_1)^\alpha}{\Gamma(\alpha+1)}||\mathbf{u}||_\infty.$$
And hence, by the definition of the modulus of continuity 4.1.3,
$$||\Lambda^q\mathbf{u} - \Lambda\mathbf{u}||_\infty = \left(\frac{h}{\sqrt{q}}\right)^\alpha \frac{5}{\Gamma(\alpha+1)}||\mathbf{u}||_\infty.$$
Furthermore, we know from e.g. [8] and Theorem 3.2.1 that
$$||\Lambda f||_\infty \leq \frac{T^\alpha}{2^{2\alpha-1}\Gamma(\alpha+1)}||f||_\infty = \frac{T^\alpha}{2^{2\alpha-1}\Gamma(\alpha+1)}\mathbf{m} := \Xi,$$
where Ξ is as in Theorem 3.2.1. Using this, we can estimate the distance to the initial estimate:
$$\begin{aligned}
||\mathbf{x}_m^q(t) - \mathbf{x}_0^q(t)||_\infty &= ||\tilde{\mathbf{x}}_0 - \mathbf{x}_0^q + \Lambda^q\mathbf{f}(t, \mathbf{x}_{m-1}^q(t))||_\infty \\
&\leq ||\tilde{\mathbf{x}}_0 - \mathbf{x}_0^q||_\infty + ||\Lambda^q\mathbf{f}(t, \mathbf{x}_{m-1}^q(t)) - \Lambda\mathbf{f}(t, \mathbf{x}_{m-1}^q(t))||_\infty + ||\Lambda\mathbf{f}(t, \mathbf{x}_{m-1}^q(t))||, \\
&\leq ||\tilde{\mathbf{x}}_0 - \mathbf{x}_0^q||_\infty + \left(\frac{h}{\sqrt{q}}\right)^\alpha \frac{5}{\Gamma(\alpha+1)}\mathbf{m} + \frac{T^\alpha}{2^{2\alpha-1}\Gamma(\alpha+1)}, \\
&= ||\tilde{\mathbf{x}}_0 - \mathbf{x}_0^q||_\infty + \frac{5\left(\frac{h}{\sqrt{q}}\right)^\alpha + T^\alpha 2^{1-2\alpha}}{\Gamma(\alpha+1)}\mathbf{m} := \mathbf{r}.
\end{aligned}$$
Now, for convergence, let us fix $m = 0$ and evaluate the difference:
$$\begin{aligned}
||\mathbf{x}_1^q - \mathbf{x}_1||_\infty &= ||\Lambda^q\mathbf{f}(t, \mathbf{x}_0^q(t)) - \Lambda\mathbf{f}(t, \mathbf{x}_0(t))||_\infty, \\
&\leq ||\Lambda[\mathbf{f}(t, \mathbf{x}_0(t)) - \mathbf{f}(t, \mathbf{x}_0^q(t))]||_\infty + ||(\Lambda - \Lambda^q)\mathbf{f}(t, \mathbf{x}_0^q(t))||_\infty, \\
&\leq \Lambda||\mathbf{K}|\mathbf{x}_0 - \mathbf{x}_0^q|||_\infty + ||(\Lambda - \Lambda^q)\mathbf{f}(t, \mathbf{x}_0^q(t))||_\infty, \\
&\leq \frac{T^\alpha\mathbf{K}}{2^{2\alpha-1}\Gamma(\alpha+1)}||\mathbf{x}_0 - \mathbf{x}_0^q||_\infty + \left(\frac{h}{\sqrt{q}}\right)^\alpha \frac{5}{\Gamma(\alpha+1)}\mathbf{m} \\
&\leq \underbrace{\frac{T^\alpha\mathbf{K}}{2^{2\alpha-1}\Gamma(\alpha+1)}}_{=\mathbf{Q}:=\Xi\mathbf{K}} \underbrace{\frac{5}{4}\omega\left(\mathbf{x}_0(t); \frac{h}{\sqrt{q}}\right)}_{:=\mathbf{e}_0} + \underbrace{\left(\frac{h}{\sqrt{q}}\right)^\alpha \frac{5}{\Gamma(\alpha+1)}\mathbf{m}}_{:=\mathbf{n}}.
\end{aligned}$$

Now, proceeding as in (5.6), this gives

$$||\mathbf{x}_{m+1}^q - \mathbf{x}_{m+1}||_\infty \leq \mathbf{Q}||\mathbf{x}_m - \mathbf{x}_m^q||_\infty + \mathbf{n}.$$

And thus, as in (5.7), we have

$$||\mathbf{x}_m^q - \mathbf{x}_m||_\infty \leq \mathbf{Q}^m\mathbf{e}_0 + (\mathbf{I} - \mathbf{Q}^m)(\mathbf{I} - \mathbf{Q})^{-1}\mathbf{n}.$$

Similarly, this also yields

$$\lim_{m\to\infty} ||\mathbf{x}_m^q - \mathbf{x}_m||_\infty = (\mathbf{I} - \mathbf{Q})^{-1}\mathbf{n}.$$

And thus the normed difference of the spline and exact solution given by

$$||\mathbf{x}_\infty^q - \mathbf{x}_\infty||_\infty = (\mathbf{I} - \mathbf{Q})^{-1}\mathbf{n} = (\mathbf{I} - \mathbf{Q})^{-1}\mathbf{n} = \left(\mathbf{I} - \frac{T^\alpha \mathbf{K}}{2^{2\alpha-1}\Gamma(\alpha+1)}\right)^{-1}\left(\frac{h}{\sqrt{q}}\right)^\alpha \frac{5}{\Gamma(\alpha+1)}\mathbf{m}.$$

Furthermore, just as in in (5.8), $\lim_{q\to\infty} ||\mathbf{x}_m^q - \mathbf{x}_m||_\infty = \mathbf{0}$, giving convergence in spline order. With the established relations above, it follows that

$$\lim_{m,q\to\infty} ||\mathbf{x}_m^q - \mathbf{x}_m||_\infty = \lim_{m,q\to\infty} ||\mathbf{x}_m^q - \mathbf{x}_m||_\infty = \mathbf{0},$$

proving the convergence statement of item 2. Finally, for the error estimate, we use the result of Theorem 3.2.1 combined with the approach as in Theorem B.0.1, which gives as in (B.5) that

$$||\mathbf{x}_\infty - \mathbf{x}_m||_\infty \leq (\mathbf{I} - \mathbf{Q})^{-1}\mathbf{Q}^m\mathbf{b},$$

with $\mathbf{b} := \Xi\mathbf{m} + ||\tilde{\mathbf{x}}_0 - \mathbf{x}_0||_\infty$. This provides the estimate of

$$\begin{aligned} ||x_\infty - x_m^q||_\infty &\leq ||x_\infty - x_m||_\infty + ||x_m - x_m^q||_\infty, \\ &\leq \mathbf{Q}^m(\mathbf{I} - \mathbf{Q})^{-1}\mathbf{b} + \mathbf{Q}^m\mathbf{e}_0 + (\mathbf{I} - \mathbf{Q}^m)(\mathbf{I} - \mathbf{Q})^{-1}\mathbf{n}, \end{aligned}$$

proving the final statement. Finally, for statement 1, using (6.2) we have by continuity of $\mathbf{f}$ that

$$\begin{aligned} \mathbf{x}_m(0) &= \tilde{\mathbf{x}}_0 + {}_0^q\Phi_0^\alpha\mathbf{f}(t, \mathbf{x}_{m-1}(t)) = \tilde{\mathbf{x}}_0, \\ \mathbf{x}_m(T) &= \tilde{\mathbf{x}}_0 + {}_0^q\Phi_T^\alpha\mathbf{f}(t, \mathbf{x}_{m-1}(t)) - {}_0^q\Phi_T^\alpha\mathbf{f}(s, \mathbf{x}_{m-1}(s)) = \tilde{\mathbf{x}}_0, \end{aligned}$$

and thus $\mathbf{x}_m(0) = \mathbf{x}_m(T)$, proving the claim. □

Numerical results

To assess the corresponding method for BVP-problems, a simple fractional differential equation resulting in oscillating behavior is taken. Consider the harmonic oscillator with one Caputo-fractional derivative, given in system notation as:

$$\begin{cases} {}_0^C\mathrm{D}_t^\alpha x(t) &= y(t), \quad \alpha \in (0,1), \\ \dot{y}(t) &= x(t). \end{cases} \tag{6.3}$$

Note that $\dot{y}(t) = {}_0^C\mathrm{D}_t^1 y(t)$. In later usage, we will denote (6.3) as ${}_0^C\mathrm{D}_t^\alpha\mathbf{x}(t) = \mathbf{f}(\mathbf{x}(t))$. Then, the method of Section 6.1.1 will be applied to find a solution such that for a given $T > 0$ and $\mathbf{x}(0) = \tilde{\mathbf{x}}_0 \in \mathbb{R}$, the system:

$$\begin{cases} {}_0^C\mathrm{D}_t^\alpha\mathbf{x}(t) = \mathbf{f}(\mathbf{x}(t)) + \Delta(\mathbf{x}_0), \\ \mathbf{x}(0) = \mathbf{x}(T). \end{cases} \tag{6.4}$$

is satisfied for $\Delta(\mathbf{x}_0) = \frac{1}{T^\alpha}{}_0\mathrm{I}_T^\alpha\mathbf{f}(\mathbf{x}(t))$. For this example, values are taken of $\alpha = 0.95$ and $\tilde{\mathbf{x}}_0 = (1, 0)$. As context, the system is first ran using the regular IVP approach as established in 6.1, of which results are shown in Figure 6.1. Then, the BVP method is ran with $\mathbf{x}_0(t) = (t/T)\tilde{\mathbf{x}}_0$ as initial guess, taken

non-constant to avoid the trivial solution. Results of this approach are shown in Figure 6.2. Finally, the BVP-method is ran using $\mathbf{x}_0(t) = \mathbf{y}_\infty(t)$, where $\mathbf{y}_\infty(t)$ is the result of the IVP-method (Figure 6.3).

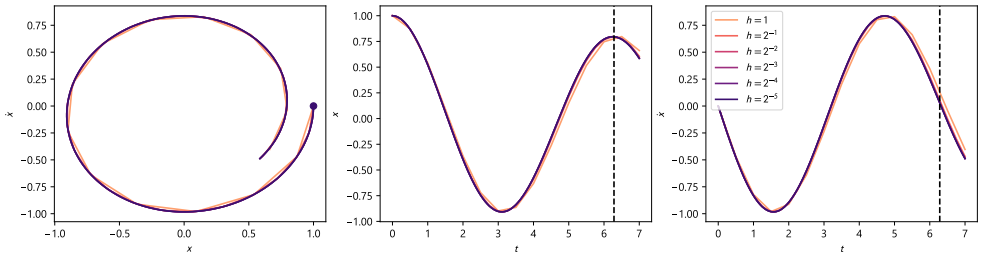

Figure 6.1: IVP results of the fractional harmonic oscillator for $\alpha = 0.95$, $\tilde{\mathbf{x}}_0 = (1, 0)$.

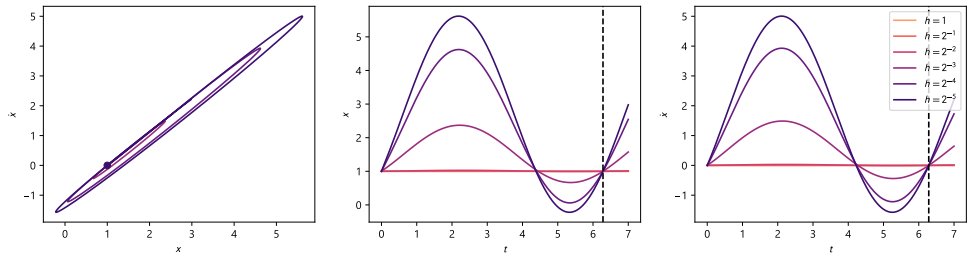

Figure 6.2: Splines BVP results of the fractional harmonic oscillator for $\alpha = 0.95$, $\tilde{\mathbf{x}}_0 = (1, 0)$ using a fixed initial guess of $\mathbf{x}_0(t) = (t/T)\tilde{\mathbf{x}}_0$.

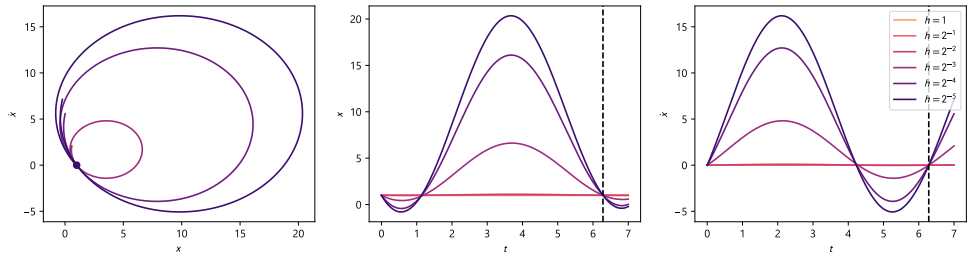

Figure 6.3: Splines BVP results of the fractional harmonic oscillator for $\alpha = 0.95$, $\tilde{\mathbf{x}}_0 = (1, 0)$ using the IVP solution as initial guess $\mathbf{x}_0(t)$.

h	$\Delta(\mathbf{x}_0)$, fixed $\mathbf{x}_0(t)$	$\Delta(\mathbf{x}_0)$, IVP $\mathbf{x}_0(t)$
2^{-0}	$(0.00, -1.00)$	$(0.00, -1.00)$
2^{-1}	$(-0.00, -1.00)$	$(-0.00, -1.00)$
2^{-2}	$(-0.01, -1.02)$	$(0.04, -1.05)$
2^{-3}	$(-0.65, -1.80)$	$(1.80, -3.57)$
2^{-4}	$(-1.78, -3.15)$	$(4.66, -7.95)$
2^{-5}	$(-2.29, -3.76)$	$(5.91, -9.91)$

Table 6.1: Values of Δ for found solutions of the BVP-method.

Results show that both for a fixed initial solution and the IVP initial solution, the higher knot sizes only give the trivial solution to the BVP. Starting from $h = 2^{-3}$ however, nontrivial solutions are found, resulting in oscillations which exactly satisfy the boundary conditions, regardless of knot size h. Whereas the behavior of the IVP initial solution method appears to approach the behavior of the original system

more in terms of structure when looking at the phase portrait, both approaches converge to solutions with fairly high values of $\Delta(\mathbf{x}_0)$, as can be seen in Table 6.1. Furthermore, the values of $\Delta(\mathbf{x}_0)$ do not decrease for more accurate knot values but only appear to increase, providing solution behavior even further from the original system behavior.

A note on delta and convergence
As noted in the existence and uniqueness-proofs of the BVP-method in Theorem 3.2.3, the BVP (6.4) corresponds to the original unperturbed BVP if and only if $\Delta(\mathbf{x}_0) = \mathbf{0}$. As shown for example in Table 6.1, this is not the case in the current setup and cases. To obtain such a value for the system, a method such as root-finding could be applied to the BVP-method, with the aim of finding a value for $T > 0$ and $\tilde{\mathbf{x}}_0 \in \mathbb{R}^d$ such that $\Delta(\mathbf{x}_0) = \mathbf{0}$. However, preliminary results show very unstable convergence to roots of the system as in general, nonzero values of $\Delta(\mathbf{x}_0)$ will be found even when close to systems with periodic behavior $\mathbf{x}(0) = \mathbf{x}(T)$.

Furthermore, the method has stringent convergence criteria. No convergent results could be found for near-limit cycle values of T for nonlinear systems such as the Van der Pol oscillator. To overcome these problems, another solution approach is proposed:

6.1.2. A local IVP approach to BVP's

Taking the local splines IVP-approach as outlined in 5.1.3 with less stringent convergence criteria, an approach can be formulated to approximate solutions to (6.1). By means of numerical root-finding, solve the following system of $d + 1$ equations:

$$\text{given initial guess:} \quad \begin{pmatrix} \tilde{\mathbf{x}}_0 \\ T \end{pmatrix}, \quad \text{solve:} \quad \begin{pmatrix} \Delta(\tilde{\mathbf{x}}_0) \\ p(\tilde{\mathbf{x}}_0) \end{pmatrix} = \mathbf{0}. \tag{6.5}$$

Here, p is a phase condition, such as $f_i(0, \tilde{\mathbf{x}}_0) = 0$ for $i \in \{0, ..., d\}$, and $\Delta(\tilde{\mathbf{x}}_0)$ is calculated using the IVP-splines approach by the observation that:

$$\Delta(\tilde{\mathbf{x}}_0) = \frac{\mathbf{x}(T) - \mathbf{x}(\mathbf{0})}{T^\alpha},$$

where $\mathbf{x}(T)$ is obtained using the IVP-approach. Various phase conditions p can be chosen: see for instance [32], Chapter 6. In the case it can be safely assumed solution $\mathbf{x}$ crosses a certain value $a \in \mathbb{R}$ in coordinate x_i, another option for p is for instance to start from this value, giving $p(\tilde{\mathbf{x}}_0) = \tilde{x}_{i,0} - a$. This essentially reduces the system of equations (6.5) to one of one order lower by removing one free variable.

A major strength of using splines for this setup is the ability to quickly interpolate the obtained solution $\mathbf{x}(T)$ for any $T > 0$ inside of the supported knot intervals by evaluating the corresponding spline knot i for which $t_i < T < t_{i+1}$ at T. Using this approach, one is able to satisfy BVP's for more general problems. Now, as an example, take the nonlinear fractionally damped Van der Pol oscillator system:

$$\begin{cases} {}_0^{\mathrm{C}}\mathrm{D}_t^{\alpha} x(t) & = y(t), \\ {}_0^{\mathrm{C}}\mathrm{D}_t^{2-\alpha} y(t) & = \mu(1 - x(t)^2)y(t) - x(t). \end{cases}$$

This system of equations will be discussed in more detail in Section 7.1.2. Now, taking $\alpha = 0.9$ and applying the approach of (6.5) using the default settings of `scipy.optimize.root` and a phase condition of $p(\tilde{\mathbf{x}}_0) = \tilde{x}_{i,1}$, hence requiring $\tilde{y}_0 = 0$, finds a solution of $\tilde{\mathbf{x}}_\mathbf{0} = (1.929, 0)$ and $T = 5.967$ with tolerance 10^{-13} after 12 iterations, using splines order $q = 2$ and knot size $h = 0.01$. A graphical illustration of results is provided in Figure 6.4

6.2. Methods for Hilfer-derivative boundary value problems

Instead of the Caputo operator BVP, consider the general Hilfer operator BVP (3.3)-(3.4) of Section 3.2, restated below for convenience:

$$\begin{cases} {}_0\mathrm{D}_t^{\alpha,\beta}\mathbf{x}(t) = \mathbf{f}(t, \mathbf{x}(t)), \quad 0 < t < T, \quad 0 < \alpha < 1, \quad 0 \leq \beta \leq 1, \\ {}_0\mathrm{I}_t^{1-\gamma}\mathbf{x}(0) = {}_0\mathrm{I}_t^{1-\gamma}\mathbf{x}(T), \quad \gamma = \alpha + \beta - \alpha\beta.\text{‘} \end{cases}$$

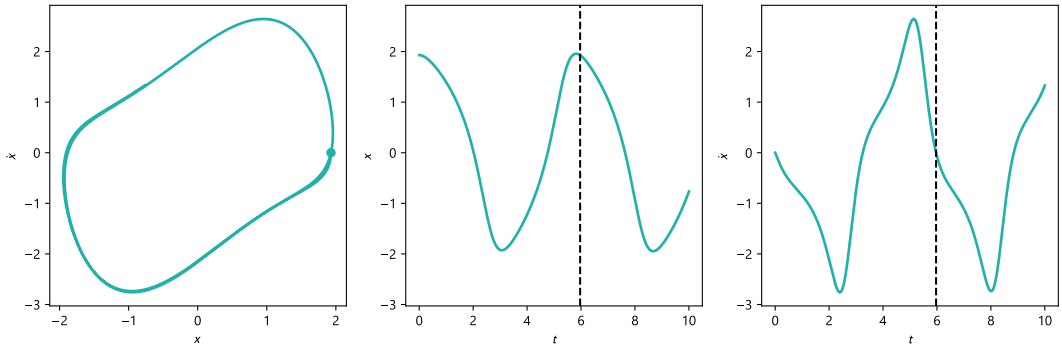

Figure 6.4: Results of the numerical local-IVP-BVP approach, time-integrating with splines from initial condition $\tilde{\mathbf{x}}_\mathbf{0} = (1.929, 0)$. The black dashed line shows the found period $T = 5.967$.

The requirements to existence and uniqueness of a solution to the Hilfer BVP are discussed in Section 3.2. However, similar to Hilfer IVP's, problems arise for numerical implementations, as discussed in Section 5.2.1. These problems can be addressed in the same way as for the initial value case.

6.2.1. Epsilon time-shifting in the global approach

Taking the same approach as for the Hilfer IVP, consider the equivalent integral equation (3.8) for Hilfer-BVP's, ε-shifted in the same way as for IVP (5.17). For $0 < \varepsilon \leq t \leq T$, take:

$$\mathbf{x}(t) = \frac{\tilde{\mathbf{x}}_0}{\Gamma(\gamma)} t^{\gamma-1} + {}_\varepsilon\mathrm{I}_t^\alpha \mathbf{f}(t, \mathbf{x}(t)) - \left(\frac{1-\gamma}{\alpha} + 1\right) T^{\gamma-1} \left(\frac{t}{T}\right)^\alpha \frac{\Gamma(1+\alpha-\gamma)}{\Gamma(\alpha)} {}_\varepsilon\mathrm{I}_T^{1+\alpha-\gamma} \mathbf{f}(t, \mathbf{x}(t))$$

This formulation does not allow for a clear convergence to the original integral equation by Grönwall's inequality as in Theorem 5.2.1. However, assuming convergence for $\varepsilon \downarrow 0$, applying the splines method of Theorem 6.1.1 and the implementation strategy as outlined in Section 5.2.2, this can be numerically implemented for BVP's, as shown in the subsequent section.

6.2.2. Implementation and results

Take the following Hilfer-BVP problem as a test problem:

$$\begin{cases} {}_0\mathrm{D}_t^{\alpha,\beta} x(t) = t^k, & 0 < t < T, \quad 0 < \alpha < 1, \quad 0 \leq \beta \leq 1, \\ {}_0\mathrm{I}_t^{1-\gamma} x(0) = {}_0\mathrm{I}_t^{1-\gamma} x(T), & \gamma = \alpha + \beta - \alpha\beta. \end{cases} \tag{6.6}$$

Results are ran for ${}_0\mathrm{I}_t^{1-\gamma} x(0) = \tilde{x}_0 = 0$, $k = 0.2$, $\alpha = 0.9$, $T = 5$, spline polynomial order $q = 1$, $\varepsilon = 10^{-14}$, $h = 0.05$ in general and $h = 0.005$ for the first 10 knots. The value of β is varied. Results are shown in Figure 6.5, showing a continuous transition to the Hilfer BVP-problem and consistent behavior with the Caputo case for $\beta = 1$. Furthermore, Table 6.2 shows the numerically obtained values for ${}_\varepsilon\mathrm{I}_t^{1-\gamma} x(T)$, showing values consistently close to $\tilde{x}_0 = 1$ as desired.

β	${}_\varepsilon\mathrm{I}_T^{1-\gamma} x(T)$	$\Delta(\tilde{\mathbf{x}}_0)$
0	1.00112	5.15213
0.2	1.00045	5.15213
0.4	1.00016	5.15213
0.6	1.00005	5.15213
0.8	1.00001	5.15213
1.0	1.00000	5.15213

Table 6.2: Numerically obtained weighed period values and Δ for the Hilfer BVP (6.6), using $k = 0.2$, $\alpha = 0.9$, $\tilde{x}_0 = 1$, $T = 5$, $q = 1$, $\varepsilon = 10^{-14}$, $h = 0.05$ in general and $h = 0.005$ for the first 10 knots.

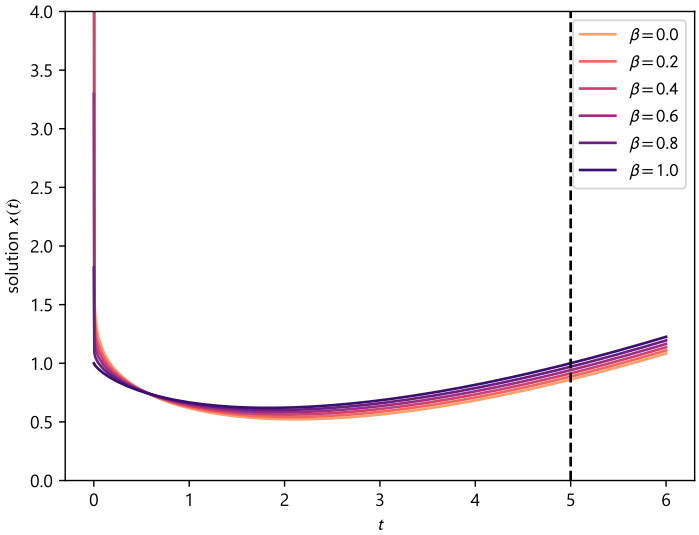

Figure 6.5: Numerical results for various values of β for Hilfer BVP (6.6), using $k = 0.2$, $\alpha = 0.9$, $x(0) = 4$, $T = 5$, $q = 1$, $\varepsilon = 10^{-14}$, $h = 0.05$ in general and $h = 0.005$ for the first 10 knots.

7

The Van der Pol oscillator

The Van der Pol-oscillator is one of the most-studied nonlinear oscillating differential equations. Initially derived from studying electrical circuit oscillations by Dutch Philips engineer Balthasar van der Pol in the early 1920's, the canonical nondimensionalized differential equation as stated in Van der Pol [37] gives:

$$\ddot{x}(t) - \mu(1 - x(t)^2)\dot{x}(t) + x(t) = 0, \quad \mu > 0. \tag{7.1}$$

This is one of the most common examples of a so-called *relaxation oscillation*, providing oscillations with a buildup of "stress" and a sudden "discharge" [34]. Replacing the acting damping term by a fractional derivative, the fractionally damped Van der Pol oscillator is given by

$$\ddot{x}(t) - \mu(1 - x(t)^2){}_0^{\mathrm{C}}\mathrm{D}_t^{\alpha} x(t) + x(t) = 0, \quad \mu > 0, \qquad \alpha \in (0, 1). \tag{7.2}$$

Finally, with external forcing applied, the most complete system formulation of the nondimensionalized fractionally damped, forced Van der Pol oscillator reads:

$$\ddot{x}(t) - \mu(1 - x(t)^2){}_0^{\mathrm{C}}\mathrm{D}_t^{\alpha} x(t) + x(t) = A\sin(\omega t), \quad \mu, A, \omega > 0, \quad \alpha \in (0, 1). \tag{7.3}$$

One main motivation to study the fractionally damped Van der Pol oscillator is its application in control theory. Non-integer order proportional–integral–derivative (PID) control systems have been proposed for instance by Podlubny [28], and several fractional order control approaches have been taken for oscillatory systems with damping [3, 26]. Thus, a better understanding and more efficient numerical approach of the fractionally damped Van der Pol oscillator can be used to improve and develop control approaches for oscillatory systems.

7.1. Physical derivation and application

Before arriving at the fractional Van der Pol equation (7.2), let us start by constructing the integer-order equation (7.1) step-by step from a physical spring-oscillation example.

7.1.1. The classic integer-order derivative Van der Pol oscillator

The harmonic oscillator

To interpret the most basic oscillating system, consider a spring with displacement $x(t)$. Here, we model x such that the spring balances in natural position at $x = 0$. For the example, consider the unit of displacement as $[x] = \mathrm{m}$. Now, by Hooke's law (e.g. [27], Section 10.2), one obtains that the force F required to compress or extend the spring scales linearly with the displacement of the spring with linear relation k. Hence, taking the restoring force that is excited by the spring, we have

$$F_{\text{spring}} = -kx,$$

for some k. In terms of units, we have $[F] = \mathrm{N} = \mathrm{kg} \cdot \mathrm{m} \cdot \mathrm{s}^{-2}$, which implies that one must have $[k] = \mathrm{kg} \cdot \mathrm{s}^{-2}$ since $[x] = \mathrm{m}$. Now, consider Newton's second law of motion, stating the equivalence of

net force to mass times acceleration:

$$F_{\text{net}} = ma. \tag{7.4}$$

Here, m can be seen as the mass of an object on the spring with $[m] = \text{kg}$. Now, note that since F_{spring} is the only force acting on the spring, we must have $F_{\text{spring}} = F_{\text{net}}$. Then, writing $a = \ddot{x}(t)$ gives a balance of forces described by

$$m\ddot{x}(t) + kx(t) = 0.$$

After rearranging, this gives

$$\ddot{x}(t) + \frac{k}{m}x(t) = 0.$$

In commonly used notation, the quantity $\omega := \sqrt{\frac{k}{m}}$ is used with $[\omega] = \text{s}^{-1}$, resulting in the canonical Harmonic oscillator

$$\ddot{x}(t) + \omega^2 x(t) = 0. \tag{7.5}$$

Equation (7.5) is a linear second order differential equation and easily solvable, resulting in solutions of the form

$$x(t) = C_1 \sin(\omega t) + C_2 \cos(\omega t). \tag{7.6}$$

Coefficients C_1 and C_2 can be found by substitution of initial conditions $(x(0), \dot{x}(0))$. Looking at (7.6) and Figure 7.1, it is clear that solutions follow a unique and stable orbit. Furthermore, the system can be seen as "conservative": no energy is dissipated or excited to the spring, and the displacement amplitudes remain constant over time.

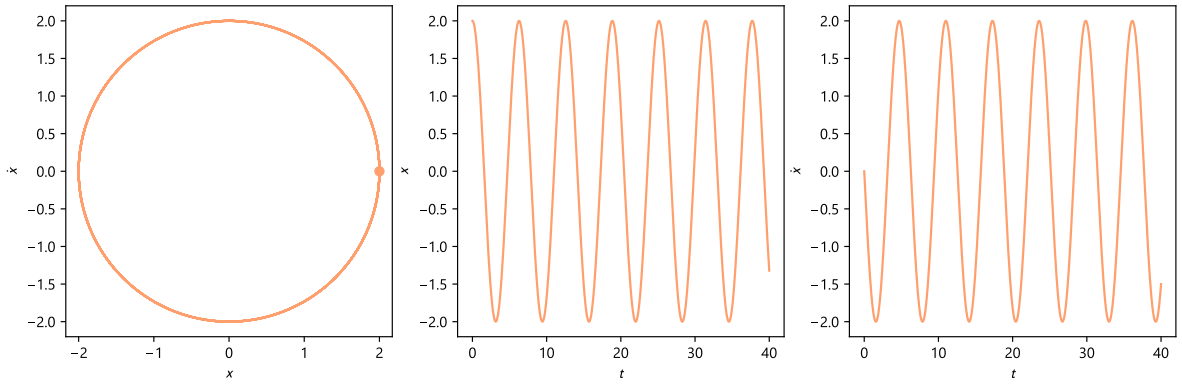

Figure 7.1: Numerical solutions of the harmonic oscillator for $\omega = 1$, with initial value $(x_0, \dot{x}_0) = (2, 0)$.

Oscillation with linear damping and driving

However, in the real world, friction occurs. To model linear friction or *damping*, assume that the spring undergoes a frictional force linearly dependent on the velocity of the spring. Hence, we have

$$F_{\text{net}} = F_{\text{spring}} - F_{\text{friction}}, \quad \text{with} \quad F_{\text{friction}} := b\dot{x}(t), \quad b > 0. \tag{7.7}$$

Unit analysis shows one must have $[b] = \text{kg} \cdot \text{s}^{-1}$. Now again taking Newton's second law of motion (7.4) results in

$$-kx(t) - b\dot{x}(t) = m\ddot{x}(t), \tag{7.8}$$

which, after rearranging gives

$$\ddot{x}(t) + \eta\dot{x}(t) + \omega^2 x(t) = 0, \tag{7.9}$$

with ω as in (7.5) and $\eta := \frac{b}{m}$, with $[\eta] = \mathrm{s}^{-1}$. As shown by Van der Pol [37], one now obtains solutions of the form

$$x(t) = C_1 \mathrm{e}^{-\frac{\eta t}{2}} \sin\left(\sqrt{\omega^2 - \frac{\eta^2}{4}}\, t + \phi\right), \quad \text{for} \quad \frac{\eta^2}{4} < \omega^2. \tag{7.10}$$

As before, constants C_1 and ϕ can be obtained from initial conditions. An illustration of solutions is given in Figure 7.2. For $\eta > 0$, these solutions do not remain in stable orbit as $x(t) \to 0$ for $t \to \infty$. When adding linear resistance, the system becomes dissipative and the spring stops moving after a while, as expected from the real world.

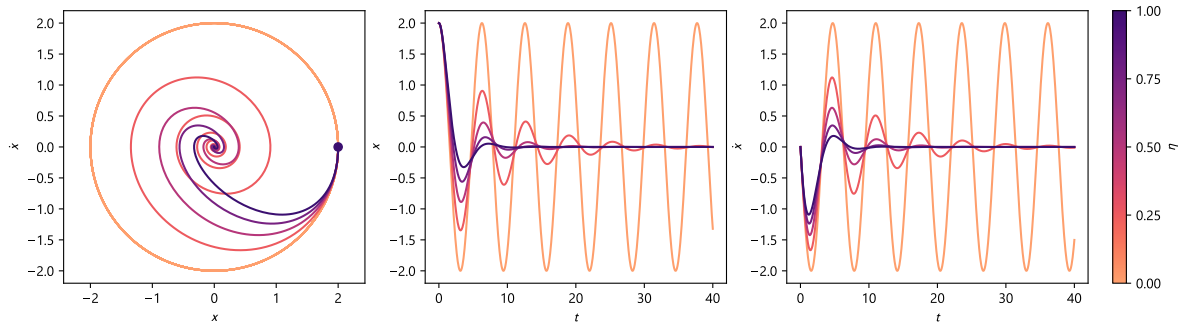

Figure 7.2: Solutions of the linear damped oscillator for $\eta \in \{0, 0.25, 0.5, 0.75, 1\}$ and $\omega = 1$, starting from $(x_0, \dot{x}_0) = (2, 0)$.

Now, what would occur when taking "negative friction" $b < 0$ as a *driving* force? In this case, (7.10) still holds, but since $\eta = \frac{b}{m} < 0$, one obtains solutions oscillating to infinity as can be seen by the exponential term of the solution. The system is thus unstable with $x(t) \to \infty$ for $t \to \infty$, and does not represent real world behavior.

Nonlinear damping and driving: the Van der Pol oscillator

For an oscillator with damping which does not spiral to infinitely large displacements and does not dissipate to zero displacement, Van der Pol proposes replacing η in (7.9) by $-(\eta - 3\rho x(t)^2)$ [37], where ρ is a constant describing the rate of damping. This results in the system

$$\ddot{x}(t) - (\eta - 3\rho x(t)^2)\dot{x}(t) + \omega^2 x(t) = 0. \tag{7.11}$$

In the physical interpretation, this implies:

$$F_{\text{friction}} = -m(\eta - 3\rho x(t)^2)\dot{x}(t) = (3m\rho x(t)^2 - b)\dot{x}(t). \tag{7.12}$$

In other words, the oscillating system is damped with $3m\rho x(t)^2 > 0$ and driven with b relative to the speed of displacement $\dot{x}(t)$. Unit analysis shows $[\rho] = \mathrm{s}^{-1} \cdot \mathrm{m}^{-2}$. Now, Van der Pol proposes the following nondimensionalization:

$$\begin{cases} t' := \omega t, \\ u := \sqrt{\frac{3\rho}{\eta}} x. \end{cases} \tag{7.13}$$

The chain rule gives $\frac{\mathrm{d}}{\mathrm{d}t} = \frac{\mathrm{d}t'}{\mathrm{d}t}\frac{\mathrm{d}}{\mathrm{d}t'} = \omega \frac{\mathrm{d}}{\mathrm{d}t'}$ and $\frac{\mathrm{d}^2}{\mathrm{d}t^2} = \omega^2 \frac{\mathrm{d}^2}{\mathrm{d}t'^2}$, which gives:

$$\ddot{x}(t) = \omega^2 \sqrt{\frac{\eta}{3\rho}} \ddot{u}(t'), \quad -(\eta - 3\rho x(t)^2)\dot{x}(t) = -\omega\left(\eta - \eta u(t')^2\right)\sqrt{\frac{\eta}{3\rho}}\dot{u}(t'), \quad \omega^2 x(t) = \omega^2 \sqrt{\frac{\eta^2}{3\rho}} u(t').$$

Now, writing back to use the old notation again as $x(t) := u(t')$ and substituting in (7.11), we arrive at the nondimensionalized system (7.1) as

$$\ddot{x}(t) - \mu(1 - x(t)^2)\dot{x}(t) + x(t) = 0, \quad \mu = \frac{\eta}{\omega}.$$

Note that when written in the most physical form, $\mu = \frac{b}{\sqrt{km}}$ Furthermore, $[\mu] = 1$ dimensionless. An interpretation for μ can thus be given as the ratio between driving or "negative damping" parameter b and stiffness factor k.

The forced Van der Pol oscillator
Finally, let us examine what would happen when an external force is applied to the system. Taking (7.7) with an external forcing sinusoidal force yields

$$F_{\text{net}} = F_{\text{spring}} - F_{\text{friction}} + F_{\text{forcing}}, \quad \text{with} \quad F_{\text{forcing}} = a\sin(\kappa t), \quad a, \kappa > 0.$$

Here, $[a] = \mathrm{N} = \mathrm{kg}\cdot\mathrm{m}\cdot\mathrm{s}^{-2}$ gives the forcing force and $[\kappa] = \mathrm{s}^{-1}$ the frequency of forcing. Now, proceeding as in (7.8) gives:

$$-kx(t) - b\dot{x}(t) + a\sin(\kappa t) = m\ddot{x}(t),$$

and hence

$$\ddot{x}(t) + \eta\dot{x}(t) + \omega^2 x(t) = \frac{a}{m}\sin(\kappa t).$$

Now, taking the same nondimensionalization (7.13), we have $\sin(\kappa t) = \sin(\frac{\kappa}{\omega}t')$ and thus one arrives at the nondimensionalized system of:

$$\ddot{x}(t) - \mu(1 - x(t)^2)\dot{x}(t) + x(t) = A\sin(\tilde{\omega}t), \quad A := \frac{a}{m\,\omega^2}\sqrt{\frac{3\gamma}{\eta}}, \quad \tilde{\omega} := \frac{\kappa}{\omega}. \tag{7.14}$$

Here, both A and $\tilde{\omega}$ are dimensionless.

Application to electronic systems
The Van der Pol equation as derived from a dimensional system as above is as for a spring-like oscillatory physical system modeling the displacement $x(t)$. However, one of the most important applications and starting grounds by Van der Pol himself of the equations lies in electronic circuits. Proceeding as in [37, 38], one can take $x(t)$ of the van der Pol Equation such as (7.14) to describe the circulation of electricity, one can write for resistance R and capacitator C with $[R] = \Omega$ and $[C] = \mathrm{F}$. Then,

$$\eta \sim \mathrm{R}, \quad \omega^2 \sim \frac{1}{\mathrm{C}}.$$

Furthermore, taking $A = E_0$ for a certain forcing voltage E_0 and applying an alternating current device such as a neon glow lamp (*Ne*) gives a circuit as presented in [38] show in Figure 7.3.

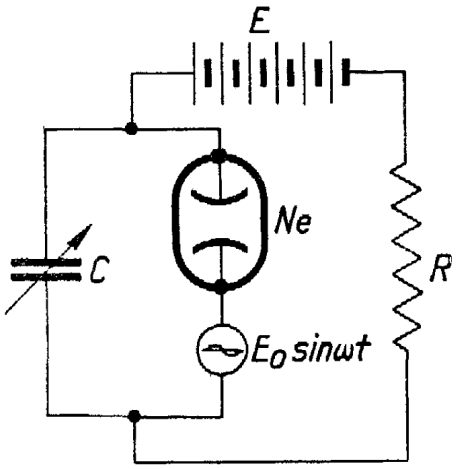

Figure 7.3: Figure 1 of Van der Pol and Van der Mark [38], showing an experimental electrical circuit yielding oscillations as modeled by the forced van der Pol Oscillator.

Note that now, one has in the nondimensionalized system that

$$\mu = \frac{\eta}{\omega} \sim \mathrm{R}\sqrt{\mathrm{C}},$$

yielding an oscillatory period of $T = \mathcal{O}(\mathrm{RC})$ in the dimensional system [38].

Properties of the classic Van der Pol equation
Taking the nondimensionalized system (7.1):

$$\ddot{x}(t) - \mu(1 - x(t)^2)\dot{x}(t) + x(t) = 0, \quad \mu > 0,$$

a few properties are studied in this section. First of all, as can easily be seen by the equation, $\mu = 0$ yields a nondimensionalized harmonic oscillator as discussed in Section 7.1.1, providing solutions in the form of

$$x(t) = C_1 \sin(t) + C_2 \cos(t).$$

When $\mu > 0$, all solutions converge to a unique limit cycle as can be proven by Liènard's theorem (see e.g. [39], Section 4.4). What is the behavior of this limit cycle? For $\mu = \varepsilon > 0$ small, it can be shown ([34], Example 7.6.2) by multiple time-scale perturbation theory that solutions approach a stable limit cycle of the form:

$$\lim_{t\to\infty} x(t) = 2\cos(t + \phi_0) + \mathcal{O}(\varepsilon), \quad \text{for} \quad \phi_0 \in \mathbb{R},$$

with an oscillation frequency of solutions $\omega = 1 + \mathcal{O}(\varepsilon^2)$. Hence, a small parameter μ yields a small adjustment to the long term behavior of the solutions compared to a sinusoidal signal. This is demonstrated in Figure 7.4.

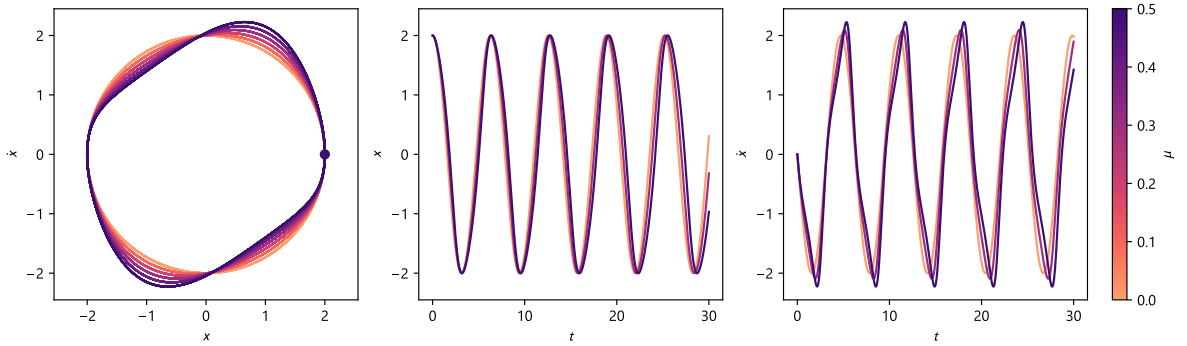

Figure 7.4: Solutions to the integer-order Van der Pol oscillator for $\mu \in \{0, 0.1, ..., 0.5\}$.

Now, for $\mu >> 0$ large, what will happen to the limit cycle and periods of oscillations of the system? In Figure 7.5, results are shown for $1 \leq \mu \leq 5$. While solutions still converge to a stable limit cycle with $-2 \leq x(t) \leq 2$, a clear increase in "steepness" can be seen in the solutions $x(t)$, with a much higher derivative $\dot{x}(t)$ for higher values of μ. As shown by Strogatz [34], the lead-up time before the

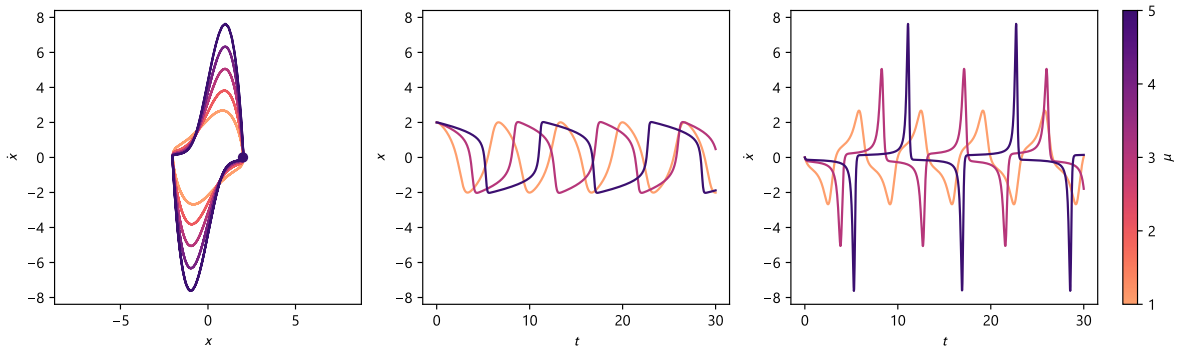

Figure 7.5: Solutions to the integer-order Van der Pol oscillator for $\mu \in \{1, 2, ..., 5\}$.

peaks of x are of $\mathcal{O}(\mu^{-1})$ and the release of the peaks take a time of $\mathcal{O}(\mu)$ (see [34], Figure 7.5.1-7.5.2). Furthermore, an expansion for the period of oscillations can be given as ([34], (6) pp. 216):

$$T = \mu(3 - 2\ln 2) + \mathcal{O}(\mu^{-1/3}).$$

Hence, a higher value of μ leads to a longer period and thus a lower frequency of oscillations. Finally, applying an external sinusoidal forcing such as in (7.14) gives a system of which Van der Pol experimentally found both stable and "transient" oscillations [38]. This phenomenon he analyzed by putting a telephone receiver to listen to the signal of the electrical oscillating circuit (Fig. 1, [38]). When increasing the value of condensation capacitance C (see Section 7.1.1), the forced oscillator "jumps" from one stable oscillation frequency to the other (see [38], Fig. 2). In between two jumps however, another phenomenon occurs. Van der Pol notes that:

> "Often an irregular noise is heard in the telephone receivers before the frequency jumps to the next lower value. However, this is a subsidiary phenomenon, the main effect being the regular frequency multiplication."

It turns out that this subsidiary phenomenon was not at all trivial. Later, in the emerging field of chaos theory, these effects could be recognized as "chaotic" [13], with solutions showing irregular unstable but bounded behavior.

7.1.2. The fractionally damped Van der Pol oscillator

Derivation and dimensional analysis

Extending the oscillator to incorporate non-integer order effects, consider a damping relative to the fractional derivative: Adapting (7.12) and taking the Caputo fractional derivative gives:

$$\tilde{F}^{(\alpha)}_{\text{friction}} = (3m\gamma x(t)^2 - b){}_0^{\text{C}}\mathrm{D}_t^{\alpha} x(t), \quad \alpha \in (0,1).$$

However, this provides a problem with unit correspondence, since $\left[{}_0^{\text{C}}\mathrm{D}_t^{\alpha} x(t)\right] = \mathrm{m}\cdot\mathrm{s}^{-\alpha}$, one has

$$[(3m\gamma x(t)^2 - b){}_0^{\text{C}}\mathrm{D}_t^{\alpha} x(t)] = (\mathrm{kg}\cdot\mathrm{s}^{-1})(\mathrm{m}\cdot\mathrm{s}^{-\alpha}) = \mathrm{kg}\cdot\mathrm{m}\cdot\mathrm{s}^{-(1+\alpha)},$$

but $[F] = \mathrm{kg}\cdot\mathrm{m}\cdot\mathrm{s}^{-2}$. To overcome this discrepancy, introduce a constant ψ with $[\psi] = s$. Then, one can write

$$F^{(\alpha)}_{\text{friction}} = \psi^{\alpha-1}(3m\gamma x(t)^2 - b){}_0^{\text{C}}\mathrm{D}_t^{\alpha} x(t), \quad \alpha \in (0,1).$$

with, as required,

$$[F^{(\alpha)}_{\text{friction}}] = \mathrm{s}^{\alpha-1}(\mathrm{kg}\cdot\mathrm{s}^{-1})(\mathrm{m}\cdot\mathrm{s}^{-\alpha}) = \mathrm{kg}\cdot\mathrm{m}\cdot\mathrm{s}^{-2}.$$

Now, continuing as in the integer order case one has the dimensionfull system

$$\ddot{x}(t) - \psi^{\alpha-1}(\eta - 3\gamma x(t)^2){}_0^{\text{C}}\mathrm{D}_t^{\alpha} x(t) + \omega^2 x(t) = 0,$$

which after using the same nondimensionalization as (7.13) gives the canonical fractionally damped Van der Pol oscillator as in (7.2):

$$\ddot{x}(t) - \mu(1 - x(t)^2){}_0^{\text{C}}\mathrm{D}_t^{\alpha} x(t) + x(t) = 0, \quad \mu = \frac{\psi^{\alpha-1}\,\eta}{\omega}.$$

A vizualization of numerical solutions is given in Figure 7.6. One problem however is the fact that one now has a dimensionfull parameter μ:

$$[\mu] = \mathrm{s}^{\alpha-1}.$$

Let us analyze the dependence on and interpretation of ψ. An insightful result is the case of $\alpha \to 0$, yielding a friction term of

$$\lim_{\alpha\to 0} F^{(\alpha)}_{\text{friction}} = (3m\gamma x(t)^2 - b)\frac{x(t)}{\psi}.$$

Hence, ψ can be seen as a quantity of time with which the displacement $x(t)$ has to be "weighed" for it to act as a substitution for taking the change of the displacement $\dot{x}(t)$.

More research can be done to overcome this nondimensionalization problem and provide a satisfying interpretation. However, already this short insight helps to see where the difficulties lie in fractional calculus applied to real world problems. It is interesting that while many authors discuss physical interpretation on a high-over level, almost no attention appears to be given to thorough unit-analysis, working only with already nondimensionalized systems. Doing so could provide more robust general applications and interpretations of fractional differential equations.

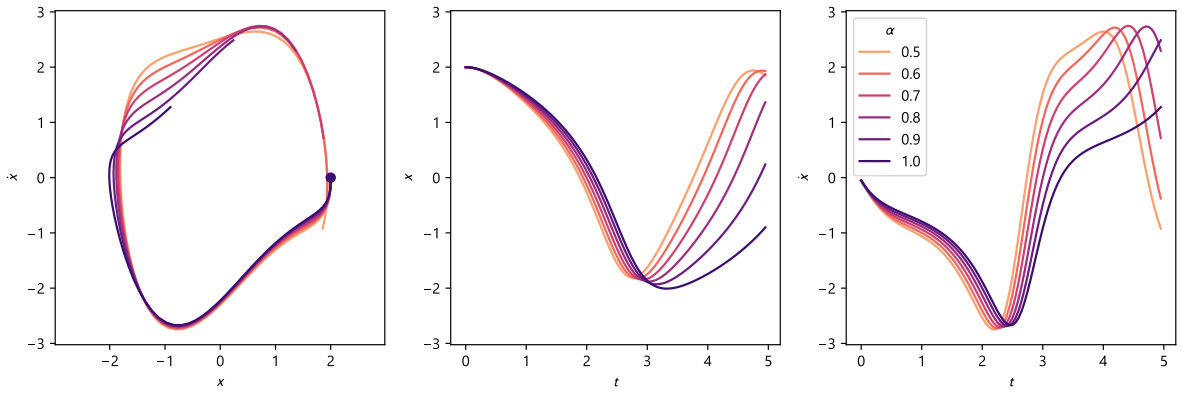

Figure 7.6: Numerical results for various values of α for $\mu = 1$, with $x(0) = 2$, $\dot{x}(0) = 0$.

Physical application
One interpretation to the fractionally damped system can be given through the perspective of viscous materials having a memory effect when applying damping. Successful experimental evidence suggests modeling through fractional order damping can achieve good accuracy for real world problems when materials show viscoelastic properties such as material fatigue [22, 14, 27].

From the point of view of electrical circuits such as outlined for for the integer-order system in Section 7.1.1, the fractionally damped system can be seen as an oscillator in which the damping effect is *memory-dependent*: this can be seen as either the resistance R or capacitator C depending on the previous state of $\dot{x}(s)$ for $0 \leq s \leq t$ and not merely the current state $\dot{x}(t)$. This can be modeled through a *fractance* instead of a capacitance, where a fractance is an electrical component with properties of both a resistor and a capacitor (see [27], Chapter 10). This is applied to the Van der Pol oscillator in [1]. Another well-known thorough result studying this time-dependent memory effect for capacitators is given by [40].

7.2. Existing literature on properties of the fractional system

In this section, existing research on fractional-order Van der Pol oscillators will be discussed, concluding with remarks motivating the modeling choices in this thesis for the subsequent sections.

Systems with fractional damping
Chen and Chen [5] apply the method of Diethelm, Ford, and Freed [6] to study the chaotic behavior of solutions using the system formulation:

$$\ddot{x}(t) + \mu \left(x(t)^2 - 1\right) {}_0^{\mathrm{C}}\mathrm{D}_t^{\alpha} x(t) + x(t) = a \sin(\omega t).$$

Strange attractors and responses to parameter values are examined, yielding sensitive changes in behavior of the system. Limit cycle results using a homotopy type memory-free method are provided by Liu, Liu, and Chen [19], showing good accordance with methods such as Diethelm's predictor-corrector method [6].

Using a more detailed system notation, Shen, Yang, and Sui [33] provide numerous details for the behavior of the amplitude and frequency properties of the limit cycle of the fractional order oscillator as given by

$$\ddot{x} + \omega_0^2 x + \varepsilon_1 \left(x^2 - 1\right) D^{p_1}[x(t)] + \varepsilon_2 \left(x^2 - 1\right) D^{p_2}[x(t)] = 0, \quad 0 < p_1 < 1, \quad 1 < p_2 < 2,$$

using an averaging-based method.

Other system adaptations
Stability properties of the fractional order van der pol oscillator with

$$ {}_0^{\mathrm{C}}\mathrm{D}_t^{1+\alpha} x(t) + \mu(x^2 - 1) {}_0^{\mathrm{C}}\mathrm{D}_t^{\alpha} x(t) = 0, \quad \mu > 0, \quad \alpha \in (0, 1), \tag{7.15}$$

are given in [35]. A main result is provided in Equation (50) as shown in Figure 6, which describes the exact region where choices of α_1 and μ provide an oscillatory or non-oscillatory system.

A similar, more general study is provided in [1] using an equation of the form of (7.15), providing mostly general dynamical properties of the system and a few detailed visual representations of the response of the limit cycle to fractional order choices.

Finally, a thorough paper of [20] gives a modification of Diethelm's predictor-corrector method [6], compared with a homotopy analysis method as provided in [18] applied to the system formulated as in (7.15). Here, results at the boundary of oscillatory and non-oscillatory behavior according to the results of [35] are examined. Furthermore, a proof of existence of the limit cycle is provided, following the method of the Poincare–Bendixson theorem with Lyapunov's technique as outlined in [36].

Chaos is studied for another adaptation in [12], exploring a system with periodic forcing as given by

$$\begin{cases} {}_0\mathrm{D}_t^{\alpha} x_1 = x_2, \\ {}_0\mathrm{D}_t^{\beta} x_2 = -x_1 - \varepsilon\left(1 - x_1^2\right)\left(c - a x_1^2\right) x_2 + b\sin(\omega x_3), \\ {}_0\mathrm{D}_t^{\gamma} x_3 = 1. \end{cases}$$

The system is analyzed using a Laplace-frequency domain method. Parameters are found for which chaotic behavior is apparent, as shown by providing bifurcation diagrams and Poincaré maps.

Remarks and motivation for new results

Existing research on the fractional-order Van der Pol oscillator can be roughly divided into two approaches for the system choice of the highest order derivative $\frac{\mathrm{d}t^{\alpha}}{\mathrm{d}t^{\alpha}}x(t)$: systems where $\alpha = 2$ and systems with $\alpha \neq 2$. In both cases, chaos and various oscillatory behavior is found. In this thesis however, we will choose an approach of $\alpha = 2$, leading to the integer-order derivative $\ddot{x}$. This is motivated by the derivation of Section 7.1.1, where the $\ddot{x}$ term is seen to originate from Newton's second law of motion (7.4). We are of the opinion one has to be much more careful in interpretation when changing this fundamental conservation law as opposed to changing the dynamics of the damping to depend on a fractional-order derivative. Furthermore, we conjecture that the approach of $\alpha \neq 2$ leads to more fundamental changes in dynamics which do not necessarily have an interpretation or derivation in real-world physics, such as the decreasing limit cycles found by Barbosa et al. [1] and Tavazoei et al. [35].

Another point of interest is the sensitivity of limit cycle behavior to initial conditions, as noted by Tavazoei et al. [35]. We conjecture this sensitivity also holds for the system with fractional damping using $\ddot{x}$ and is in general more pronounced for lower orders of fractional derivatives.

Finally, in terms of the differential operators, all above papers consider either the Caputo or Riemann-Liouville operator. In the case of the Riemann-Liouville operator, initial conditions are taken to be $\mathbf{0}$, for which the operator coincides with the Caputo derivative. Using the developed methods in this thesis, one can look at the effect of choosing nonzero initial conditions for the $\beta \in (0, 1)$ Hilfer and Riemann-Liouville ($\beta = 0$) derivatives for the Van der Pol oscillator.

7.3. Results on the fractionally damped Van der Pol oscillator using Bernstein splines

To implement the Van der Pol oscillator with fractional damping, equation (7.2) can be rewritten in system notation as:

$$\begin{cases} {}_0^{\mathrm{C}}\mathrm{D}_t^{\alpha} x(t) & = z(t), \\ {}_0^{\mathrm{C}}\mathrm{D}_t^{1-\alpha/2} y(t) & = \mu(1 - x(t)^2) z(t) - x(t), \\ {}_0^{\mathrm{C}}\mathrm{D}_t^{1-\alpha/2} z(t) & = y(t), \end{cases} \tag{7.16}$$

This ensures that all integration orders satisfy $0 \leq \alpha \leq 1$. However, for computational efficiency, (7.2) can be simplified further to two dimensions, where the choice of $z(0) = 0$, $\dot{y}(0) = 0$ leads to:

$$\begin{cases} {}_0^{\mathrm{C}}\mathrm{D}_t^{\alpha} x(t) & = y(t), \\ {}_0^{\mathrm{C}}\mathrm{D}_t^{2-\alpha} y(t) & = \mu(1 - x(t)^2) y(t) - x(t). \end{cases} \tag{7.17}$$

This identity holds for $z(0) = 0$ by the Caputo-derivative equivalent integral equation (Theorem 3.1.1, $\beta = 1$) and the semigroup property of the fractional integral (Proposition 2.2.2). The same system implementation is chosen by Chen and Chen [5].

7.3.1. Approximate limit cycle

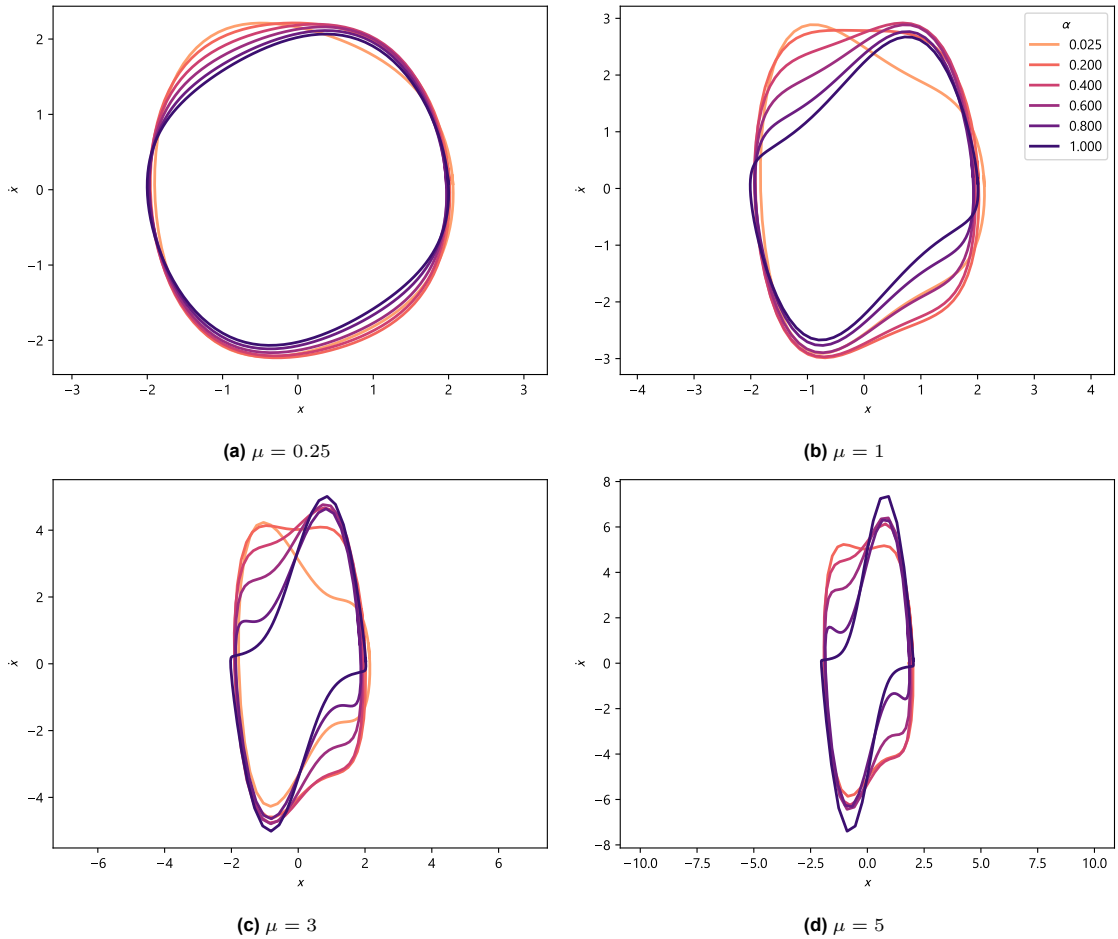

(a) $\mu = 0.25$ **(b)** $\mu = 1$

(c) $\mu = 3$ **(d)** $\mu = 5$

Figure 7.7: Approximate limit cycle of the unforced fractionally damped Van der Pol oscillator. All axes are taken equal in scale of x and $\dot{x}$ but do adjust according to the size of $\dot{x}$ for higher values of μ. Note that $(\mu = 5, \alpha = 0.025)$ is not included.

To show the effect of the fractional damping order α on the approximate limit cycle, a number of numerical simulations of system (7.17) is ran. We take $\mu \in [0, 5]$ with equidistant steps of $\Delta\mu = 0.25$ and $\alpha \in [0.025, 1]$ with $\Delta\alpha = 0.025$, resulting in a total of 840 parameter setups. Here, $\alpha = 1$ is used as notation for the integer-order system. The simulations are ran for $(x(0), y(0)) = (2, 0)$, $T = 300$, a linear Bernstein spline order $q = 1$ and a uniform knot size $h = 0.05$ with the local-splines approximation setup as outlined in Section 5.1.3. When required for visualization, $\dot{x}$ is approximated numerically by a finite first-order difference, taking $\dot{x}(t) \approx \frac{x(t_{k+1}) - x(k_i)}{h}$, where k represents the corresponding knot such that $t_k \leq t < t_{k+1}$. Results for selected values are shown in Figure 7.7. It appears that, as expected from Proposition 2.2.5, the limit cycle changes continuously with α. Furthermore, the same behavior for μ is obtained as in the integer-order system, with “sharper peaks” in the “build-up”, leading to higher values of $\dot{x}$. The amplitudes of x however appear to have roughly the same values for all parameter choices, ranging approximately in $[-2, 2]$. This contradicts the findings of Tavazoei et al. [35], most likely because of the different fractional system studied, with the choice of fractional derivative orders leading to different non-integer derivative conservation laws. Hence, the system (7.2) appears to be a more consistent extension of the classical integer-order derivative system compared to the choice of Tavazoei et al. [35]. Finally, note that no oscillatory limit cycle is obtained for $\mu = 5$, $\alpha = 0.025$.

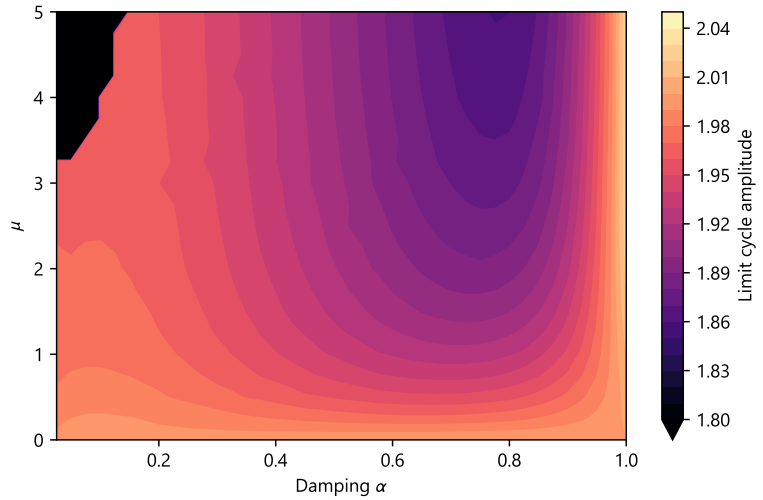

Figure 7.8: Amplitudes of the approximate limit cycle for μ and α. The black region in the top-left indicates an amplitude of near-0.

Limit cycle amplitude and stability

To further study the amplitude and this missing oscillatory limit cycle, we look at the full values of the approximate limit cycle amplitudes presented in Figure 7.8. Results on the approximate limit cycle amplitude are consistent with expectations, remaining in a range of 1.80- 2.05 for most parameter values, contrary to the results found by Tavazoei et al. [35]. This is most likely due to the different system formulation, as discussed in Section 7.2.

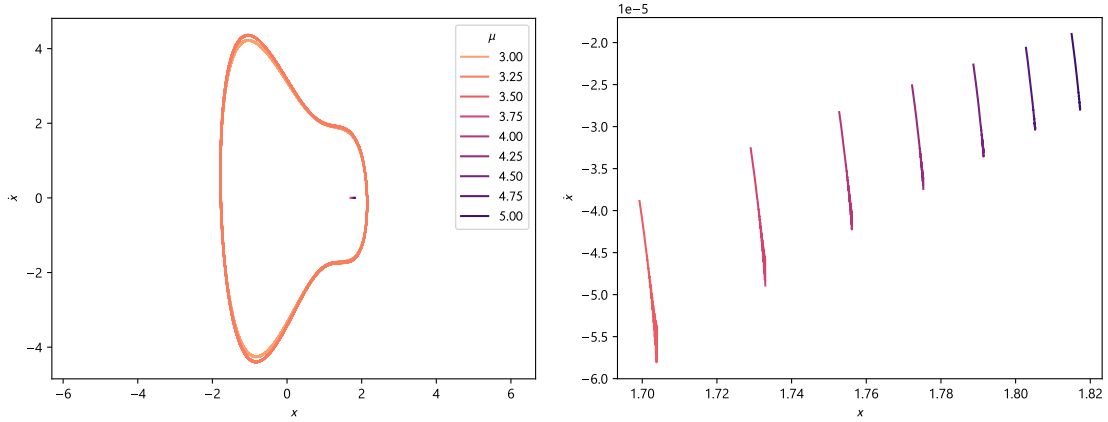

Figure 7.9: Results for $200 \leq t \leq T$ for $\alpha = 0.025$ in full (a) and detailed for the non-oscillatory regimes (b).

However, a region for low α and high μ appears to be attracted to another limit cycle or fixed point. To further study this behavior, results are shown for $\alpha = 0.025$ in Figure 7.9. A clear transition to what appears to be non-oscillatory critical points is observed.

Analytically, this may be seen as follows: as $\alpha \downarrow 0$, the Caputo fractional derivative become more "memory-full", with higher influence of solution values closer to $t = 0$ instead of the regular "memoryless" integer-order derivative of $\alpha = 1$, which is not influenced by past solution values. Looking at the definition of the Caputo-derivative in Definition 2.3.2, this can be seen as the kernel of ${}_0\mathrm{I}_t^{1-\alpha}$ adds more weight to values further in the past, hence closer to 0 in the integration interval $[0, t]$. This will require a longer time to reach the "memory-free" limit-cycle state regardless of initial conditions (see for instance [20]).

In the limiting case of $\alpha \downarrow 0$, this even results in a system where the initial conditions are present. To see this, note that as in Remark 2.3.4, we have $\lim_{\alpha \downarrow 0} {}_0^{\mathrm{C}}\mathrm{D}_t^{\alpha} x(t) = x(t) - x(0)$. Plugging this back in to

equation (7.17) and taking $\alpha \downarrow 0$ for all derivative orders, one obtains a resulting differential equation of:

$$\begin{cases} x(t) = y(t) + x(0), \\ \ddot{y}(t) = \mu(1 - x(t)^2)y(t) - x(t), \end{cases}$$

which expressed in $x(t)$ gives $\ddot{x}(t) = \mu(1 - x(t)^2)(x(t) - x(0)) - x(t)$. Since $x(0) = 2 \neq 0$ in the simulations, this results in a different system compared to the classic Van der Pol equation (7.1). Writing in system notation gives:

$$\begin{cases} \dot{x}(t) = y, \\ \dot{y}(t) = \mu(1 - x(t)^2)(x(t) - 2) - x(t). \end{cases} \tag{7.18}$$

The fixed points of system (7.18) are given by $y_c = 0$ and $\mu(1 - x_c^2)(x_c - 2) - x_c = 0$. This gives a bifurcation with one fixed point for $0 < \mu < \mu_b$ and three fixed points for $\mu > \mu_b$, where $\mu_b \approx 2.389$. Taking for instance $\mu = 5$ then gives $y_c = 0$, $x_c \approx -0.9669$, $x_c \approx 1.1201$ and $x_c \approx 1.8468$, of which the last value is closest to the limiting behavior as obtained in Figure 7.9. The corresponding phase portrait for $\mu = 5$ is shown in Figure 7.10. It appears however that for this integer order system, a Lyapunov-stable oscillating limit cycle is reached for the critical point, contrary to the fractional results showing an attracting non-oscillatory fixed point. This might be due to the fractional nature of the problem compared to the integer-order limiting case. However, more analysis is required.

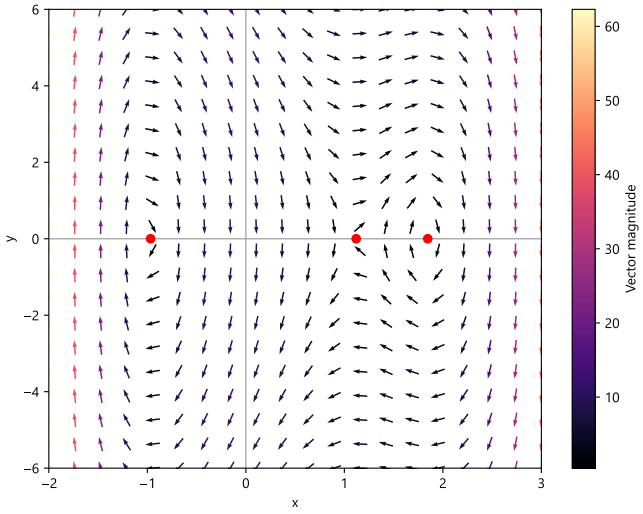

Figure 7.10: Phase portrait of system (7.18) for $\mu = 5$ with a solution starting at $x(0) = 2, y(0) = 0$.

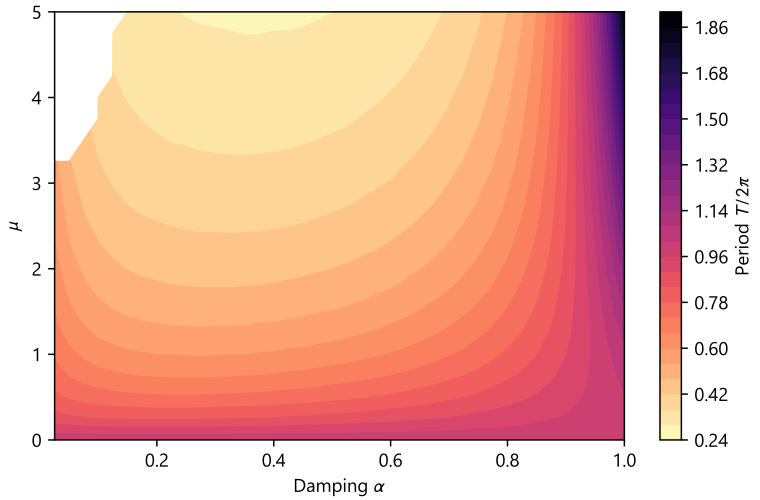

Figure 7.11: Normalized period of oscillatory limit cycles.

Limit cycle period

The period T of the approximate limit cycle is shown in Figure 7.11. Interestingly, on the contrary to the integer-order system, the limit cycle period can also decrease with μ for certain values of α. This decreasing effect can be seen for values approximately lower than $\alpha = 0.9$. Similar to the amplitude, a continuous effect of α can be seen for values of the limit cycle period T.

Comparison to analytical literature results

Results on the limit cycle correspond to the results found by Liu, Liu, and Chen [19], using an analytical method based on the memory-free principle. The same setup for Figure 8 of [19] is used to create a detail of Figure 7.8 and 7.11 for $\mu = 0.5$ as used in their results. A clear correspondence with the analytical behavior is found for $\alpha >> 0$, with discrepancies corresponding to values of α closer to 0. This is most likely due to the memory effect in initial conditions, and would be mitigated by either choosing a larger value of T or smaller values for $\tilde{\mathbf{x}}_0$.

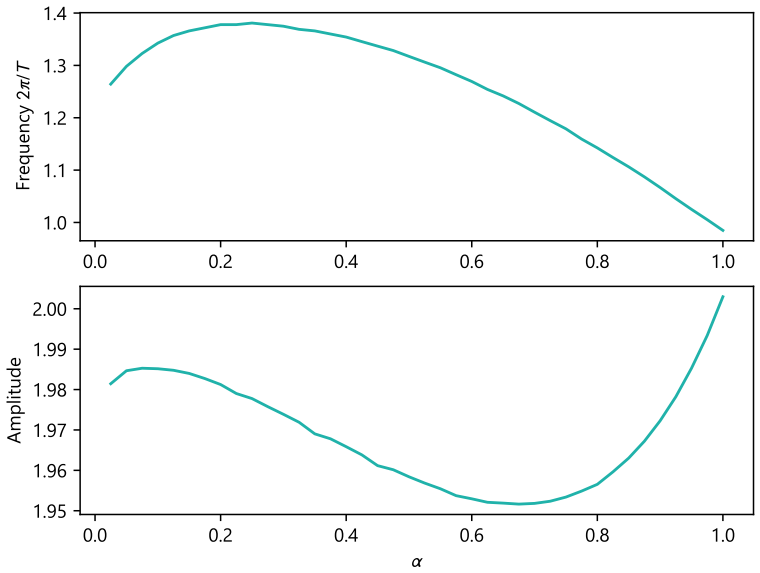

Figure 7.12: Approximate limit cycle amplitude and frequency for $\mu = 0.5$, showing correspondence to the analytical results of Liu, Liu, and Chen [19], Fig. 8 for $\alpha >> 0$.

7.3.2. Hilfer-fractional derivative damping

To study the behavior of the Hilfer derivative type β, an adaptation of system (7.16) is made, taking the Hilfer derivative (Definition 2.3.3) instead of the Caputo fractional derivative operator. This results in the following system:

$$\begin{cases} {}_0\mathrm{D}_t^{\alpha,\beta} x(t) & = z(t), \\ {}_0\mathrm{D}_t^{1-\alpha/2,\beta} y(t) & = \mu(1-x(t)^2)z(t) - x(t), \\ {}_0\mathrm{D}_t^{1-\alpha/2,\beta} z(t) & = y(t). \end{cases}$$

Using the splines methods of Section 5.2, approximations to this system are made for a choice of $\mu = 1$, $\alpha = 0.8$ and various choices of β. For implementation purposes, linear splines ($q = 0$) are chosen with knot size $h = 0.025$ in general and $h = 0.00025$ for the first 100 knots. The integration time-shift parameter is taken as $\varepsilon = 10^{-10}$.

Fixed-point convergence can be satisfied numerically for all cases, showing a successful practical implementation of the method for nonlinear Hilfer-derivative problems. Phase-portrait results are presented in Figure 7.13, showing a quick convergence to the limit cycle regardless of type β. This quick convergence is most likely due to the relatively high value of α. However, we conjecture long-term behavior to be the same regardless of β for all α, albeit at different convergence speeds.

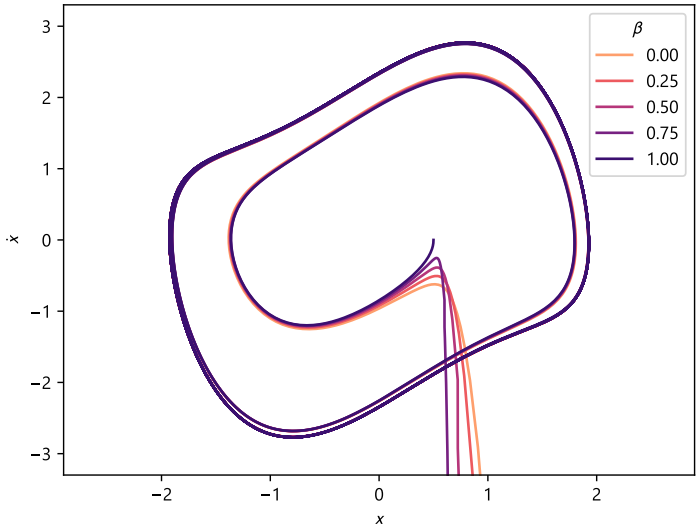

Figure 7.13: Phase portrait of the Hilfer-fractionally damped Van der Pol oscillator for different Hilfer derivative types β for $\alpha = 0.8$, $\mu = 1$ and $\tilde{\mathbf{x}}_0 = (0.5, 0, 0)$ for $T = 50$.

7.3.3. Periodic forcing

Finally, considering again the Caputo derivative, forcing can be applied, resulting in the differential equation (7.3). This system is implemented as (7.19).

$$\begin{cases} {}_0^{\mathrm{C}}\mathrm{D}_t^{\alpha} x(t) & = y(t), \\ {}_0^{\mathrm{C}}\mathrm{D}_t^{2-\alpha} y(t) & = \mu(1-x(t)^2)y(t) - x(t) + A\sin(\omega t). \end{cases} \tag{7.19}$$

For the integer order system of $\alpha = 1$, limit cycle behavior and parameter responses can be obtained by analytical methods such as the multiple time scale perturbation method as applied for instance in a recent analysis by Monwanou et al. [23]. Since fractional derivation of sine functions affects the amplitude and not the oscillation frequency as shown in Appendix C, it can be expected similar type of forcing behavior can be found as in the integer-order case, albeit it possibly for different parameter regimes. However, the memory effect of fractional derivation could play a role, possibly causing different behavior of solutions by their past dependence memory effect. To assess an example of the behavior of forced solutions, simulations are ran for $\alpha = 0.5$, $\mu = 2$, $A = 3$ for varying forcing frequencies ω. Results are presented in Figure 7.14 and 7.15.

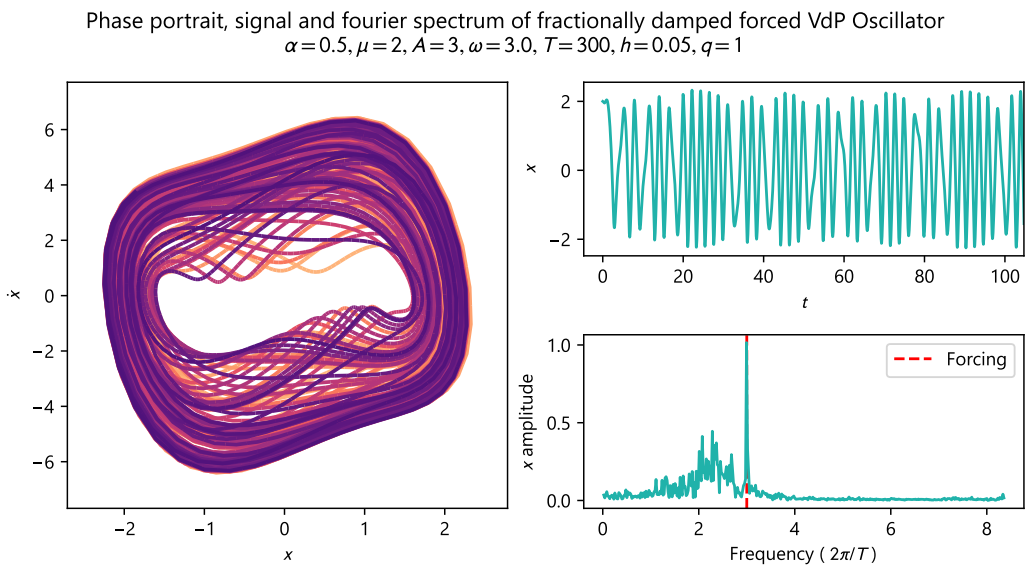

(a) Chaotic behavior for forcing frequency $\omega = 3$.

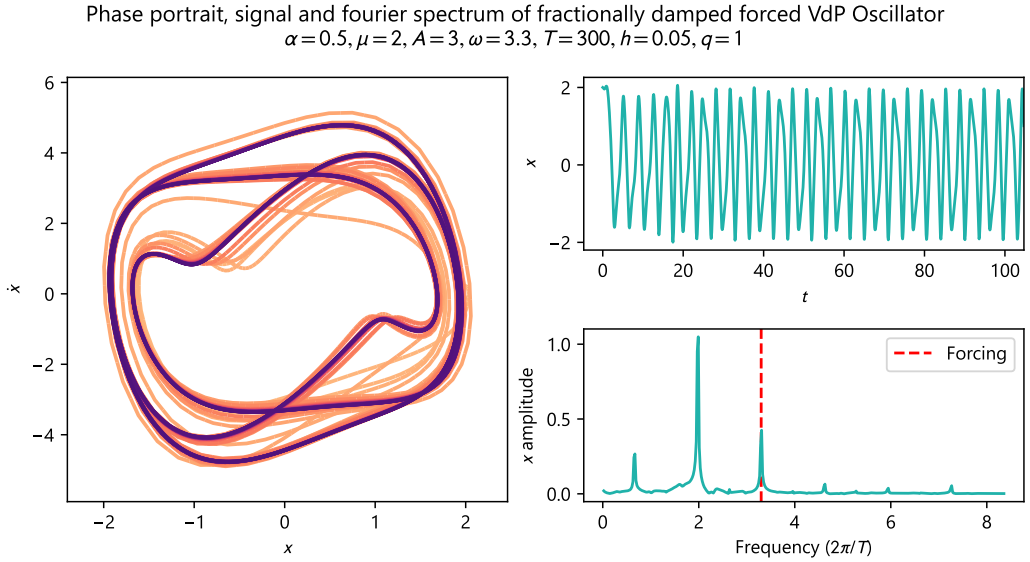

(b) Multi- or quasiperiodic behavior for $\omega = 3.3$.

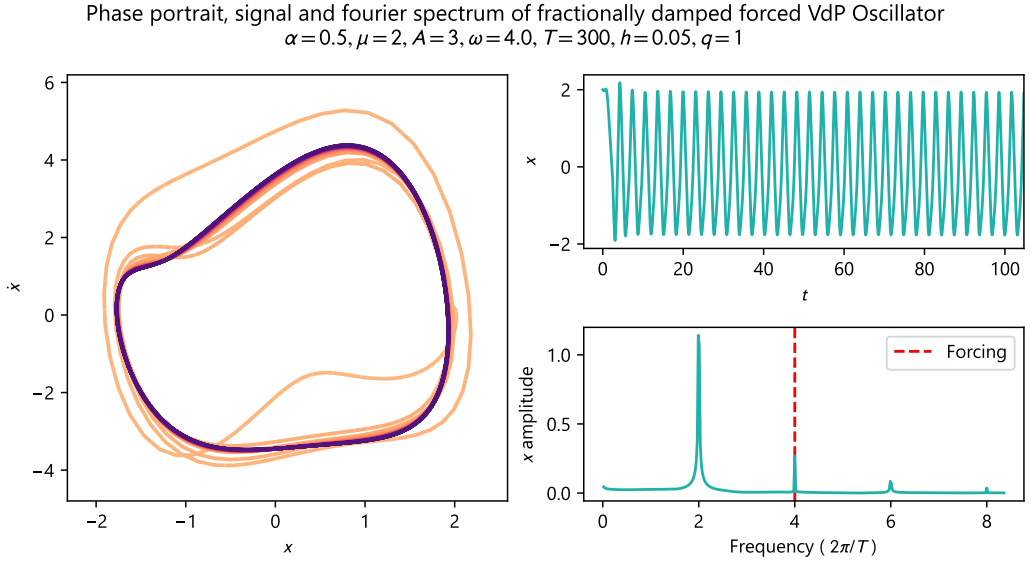

(c) Stable periodic limit cycle for $\omega = 4$.

Figure 7.14: Behavior of solutions of the forced fractionally damped Van der Pol oscillator.

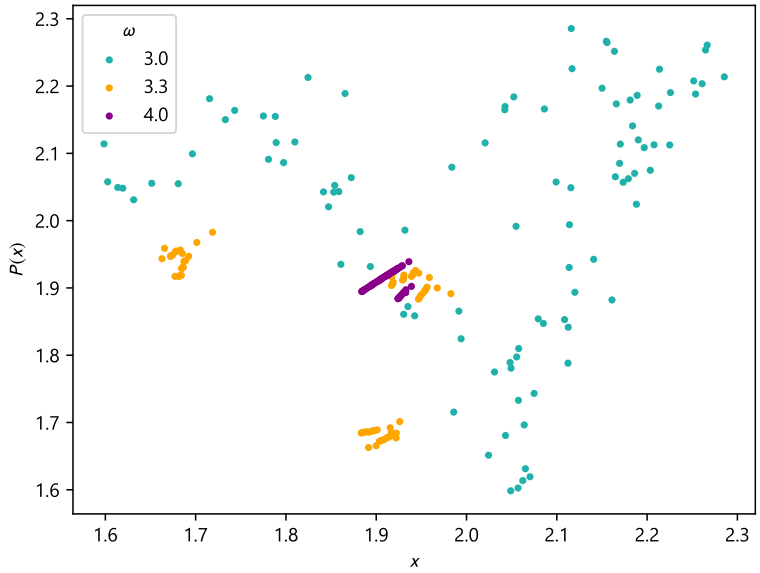

Figure 7.15: Poincaré map of results of the forced fractionally damped Van der Pol oscillator for $\alpha = 0.5$, $\mu = 2$ and $A = 3$, taking intersections in the plane $(\dot{x} = 0, x > 0)$. The first 10 intersections are discarded to reduce the influence of the initial condition choices.

A number of different solution behaviors can be observed for different forcing values: stable quasi-or multiperiodic, stable periodic and chaotic behavior. This aligns with the existing literature, showing a wide range of possible behavior in the fractional order Van der Pol oscillator. It can thus safely be concluded this also applies to the fractionally damped system.

Furthermore, a behavior of “period-locking” can be observed similar to the findings of Barbosa et al. [1]. The unforced system $A = 0$ corresponding to the parameter choices can be numerically shown to have a frequency of $\omega_0 = 2.06$. From the Fourier spectrum in Figure 7.14, a clear effect can be seen of interaction with the forcing frequency and the natural, unforced frequency, creating stable oscillations when an exact multiple is reached **(c)**, stable subharmonics **(b)** or chaotic, non-harmonic behavior **(a)**.

The Poincaré map of Figure 7.15 shows similar behavior, with most likely one attractor region for the stable case of $\omega = 4.0$, three regions for the multiperiodic case of $\omega = 3.3$ and a possibly scattered strange attractor behavior for $\omega = 3.0$. We note that the variance in points for the case of $\omega = 4.0, 3.3$ is most likely due to numerical inaccuracy. Furthermore, more points should be obtained for a more accurate Poincaré-map depiction, though this would yield high memory requirements for simulation.

References

[1] Ramiro S. Barbosa et al. “Analysis of the Van der Pol oscillator containing derivatives of fractional order”. In: *JVC/Journal of Vibration and Control* 13.9-10 (2007), pp. 1291–1301. DOI: 10.1177/1077546307077463.

[2] Alexandru Mihai Bica. “On the order of convergence of the iterative Bernstein splines method for fractional order initial value problems”. In: *Journal of Computational and Applied Mathematics* 432 (2023), p. 115274. DOI: 10.1016/j.cam.2023.115274.

[3] A. J. Calderón, B. M. Vinagre, and V. Feliu. “Fractional order control strategies for power electronic buck converters”. In: *Signal Processing* 86.10 (2006), pp. 2803–2819. ISSN: 01651684. DOI: 10.1016/j.sigpro.2006.02.022.

[4] A. Charef et al. “Fractal system as represented by singularity function”. In: *IEEE Transactions on Automatic Control* 37.9 (1992), pp. 1465–1470. DOI: 10.1109/9.159595.

[5] Juhn Horng Chen and Wei Ching Chen. “Chaotic dynamics of the fractionally damped van der Pol equation”. In: *Chaos, Solitons and Fractals* 35.1 (2008), pp. 188–198. DOI: 10.1016/j.chaos.2006.05.010.

[6] Kai Diethelm, Neville J Ford, and Alan D Freed. “A Predictor-Corrector Approach for the Numerical Solution of Fractional Differential Equations”. In: *Nonlinear Dynamics* 29.1 (2002), pp. 3–22. DOI: 10.1023/A:1016592219341.

[7] Kai Diethelm, Neville J Ford, and Alan D Freed. “Detailed error analysis for a fractional Adams method”. In: *Numerical algorithms* 36 (2004), pp. 31–52. DOI: 10.1023/B:NUMA.0000027736.85078.be.

[8] Michal Fečkan and Kateryna Marynets. “Approximation approach to periodic BVP for fractional differential systems”. In: *European Physical Journal: Special Topics* 226.16-18 (2017), pp. 3681–3692. DOI: 10.1140/epjst/e2018-00017-9.

[9] Michal Fečkan and Kateryna Marynets. “Approximation approach to periodic BVP for mixed fractional differential systems”. In: *Journal of Computational and Applied Mathematics* 339 (2018), pp. 208–217. DOI: 10.1016/j.cam.2017.10.028.

[10] Michal Fečkan and Kateryna Marynets. “Non-Local Fractional Boundary Value Problems With Applications To Predator-Prey Models”. In: *Electronic Journal of Differential Equations* 2023 (2023). ISSN: 10726691. DOI: 10.58997/ejde.2023.58.

[11] K. M. Furati, M. D. Kassim, and N. E. Tatar. “Existence and uniqueness for a problem involving Hilfer fractional derivative”. In: *Computers and Mathematics with Applications* 64.6 (2012), pp. 1616–1626. ISSN: 08981221. DOI: 10.1016/j.camwa.2012.01.009.

[12] Zheng Ming Ge and Mao Yuan Hsu. “Chaos in a generalized van der Pol system and in its fractional order system”. In: *Chaos, Solitons and Fractals* 33.5 (2007), pp. 1711–1745. DOI: 10.1016/j.chaos.2006.03.028.

[13] J. Can Marc Ginoux. “From nonlinear oscillations to chaos theory”. In: *CHAOS 2015 - 8th Chaotic Modeling and Simulation International Conference, Proceedings*. 2015, pp. 273–298.

[14] R. Hilfer. “Experimental evidence for fractional time evolution in glass forming materials”. In: *Chemical Physics* 284.1-2 (2002), pp. 399–408. ISSN: 03010104. DOI: 10.1016/S0301-0104(02)00670-5.

[15] Rudolf Hilfer. *Applications of Fractional Calculus in Physics*. World Scientific Publishing Co. Pte. Ltd., 2000. DOI: 10.1142/9789812817747_0002.

[16] A.A. Kilbas, H. M. Srivastava, and J.J. Trujillo. *Theory and Applications of Fractional Differential Equations*. Elsevier North-Holland, 2006.

[17] Gottfried Wilhelm Leibniz. *Leibnizens mathematische schriften*. Vol. 4. Schmidt, 1859.

[18] Shi Jun Liao. “An analytic approximate technique for free oscillations of positively damped systems with algebraically decaying amplitude”. In: *International Journal of Non-Linear Mechanics* 38.8 (2003), pp. 1173–1183. DOI: 10.1016/S0020-7462(02)00062-8.

[19] Q. X. Liu, J. K. Liu, and Y. M. Chen. “Asymptotic limit cycle of fractional van der Pol oscillator by homotopy analysis method and memory-free principle”. In: *Applied Mathematical Modelling* 40.4 (2016), pp. 3211–3220. DOI: 10.1016/j.apm.2015.10.005.

[20] Q. X. Liu, J. K. Liu, and Y. M. Chen. “Initial conditions-independent limit cycles of a fractional-order van der Pol oscillator”. In: *JVC/Journal of Vibration and Control* 22.8 (2016), pp. 2135–2146. DOI: 10.1177/1077546315588031.

[21] George G. Lorentz. *Bernstein Polynomials*. 1986th ed. Chelsea Publishing Company, 1953. DOI: 10.1007/978-3-662-02888-9_10.

[22] Nicos Makris and MC Constantinou. “Fractional-derivative Maxwell model for viscous dampers”. In: *Journal of Structural Engineering* 117.9 (1991), pp. 2708–2724. DOI: 10.1061/(ASCE)0733-9445(1991)117:9(2708).

[23] A.V. Monwanou et al. “Nonlinear dynamics of system oscillations modeled by a forced Van der Pol generalized oscillator”. In: *International Journal of Engineering and Applied Sciences* 4.8 (2017), p. 257398.

[24] Jan van Neerven. *Functional Analysis*. Cambridge University Press, June 2022. ISBN: 9781009232470. DOI: 10.1017/9781009232487.

[25] David Osborn and Richard Madey. “The incomplete beta function and its ratio to the complete beta function”. In: *Mathematics of Computation* 22.101 (1968), pp. 159–162.

[26] Alain Oustaloup, Jocelyn Sabatier, and Xavier Moreau. “From fractal robustness to the CRONE approach”. In: *ESAIM: Proceedings* 5 (1998), pp. 177–192. DOI: 10.1051/proc:1998006.

[27] Igor Podlubny. *Fractional Differential Equations*. Academic Press, 1999. ISBN: 0-12 558840-2.

[28] Igor Podlubny. “Fractional-order systems and $PI^{\lambda}D^{\mu}$- controllers”. In: *IEEE Transactions on automatic control* 44.1 (1999), pp. 208–214. DOI: 10.1109/9.739144.

[29] S.G. Samko, A.A. Kilbas, and O.I. Marichev. *Fractional Integrals and Derivatives*. Gordon and Breach Science Publishers, 1987. ISBN: 2881248640. DOI: 10.1007/978-981-99-6080-4_6.

[30] Zoltan Satmari. “Iterative Bernstein splines technique applied to fractional order differential equations.” In: *Mathematical Foundations of Computing* 6.1 (2023). DOI: 10.3934/mfc.2021039.

[31] L.L. Schumaker. *Spline Functions: Basic Theory*. Cambridge, 2007. ISBN: 9780521705127. DOI: 10.1017/CBO9780511618994.

[32] Rüdiger Seydel. *Practical bifurcation and stability analysis*. Vol. 5. Springer Science & Business Media, 2009.

[33] Yongjun Shen, Shaopu Yang, and Chuanyi Sui. “Analysis on limit cycle of fractional-order van der Pol oscillator”. In: *Chaos, Solitons and Fractals* 67 (2014), pp. 94–102. DOI: 10.1016/j.chaos.2014.07.001.

[34] H. Strogatz. *Nonlinear dynamics and chaos*. Taylor and Francis, 2016, pp. 93–117. ISBN: 978-0738204536. DOI: 10.1201/9780429492563.

[35] Mohammad S. Tavazoei et al. “More details on analysis of fractional-order Van der Pol oscillator”. In: *JVC/Journal of Vibration and Control* 15.6 (2009), pp. 803–819. DOI: 10.1177/1077546308096101.

[36] J.C. Trigeassou et al. “A Lyapunov approach to the stability of fractional differential equations”. In: *Signal Processing* 91.3 (2011), pp. 437–445. DOI: 10.1016/j.sigpro.2010.04.024.

[37] Balth van der Pol. “LXXXVIII. On “relaxation-oscillations””. In: *The London, Edinburgh, and Dublin Philosophical Magazine and Journal of Science* 2.11 (1926), pp. 978–992. DOI: 10.1080/14786442608564127.

[38] Balth van der Pol and J. van der Mark. *Frequency demultiplication*. 1927. DOI: 10.1038/120363a0.

[39] F. Verhulst. *Nonlinear Differential Equations and Dynamical Systems*. Universitext. Springer Berlin Heidelberg, 2006. ISBN: 9783540609346.

[40] Svante Westerlund. “Dead matter has memory”. In: *Physica Scripta* 43.2 (1991), pp. 174–179. ISSN: 14024896. DOI: 10.1088/0031-8949/43/2/011.

[41] Haiping Ye, Jianming Gao, and Yongsheng Ding. “A generalized Gronwall inequality and its application to a fractional differential equation”. In: *Journal of Mathematical Analysis and Applications* 328.2 (2007), pp. 1075–1081. ISSN: 0022-247X. DOI: https://doi.org/10.1016/j.jmaa.2006.05.061.

A

Calculations of an explicit bound for the Hilfer-BVP operator

First, as an analogue to Lemma 3.2.1, one has:

Lemma A.0.1. *Let* $\mathbf{f}(t) \in C_{1-\gamma}[0,T]$. *Then for all* $t \in [0,T]$, *we have*

$$\left| \frac{t^{1-\gamma}}{\Gamma(\alpha)} \left[\int_0^t (t-s)^{\alpha-1} \mathbf{f}(s)\,\mathrm{d}s - \left(\frac{1-\gamma}{\alpha} + 1 \right) T^{\gamma-1} \left(\frac{t}{T} \right)^{\alpha} \int_0^T (T-s)^{\alpha-\gamma} \mathbf{f}(s)\,\mathrm{d}s \right] \right| \leq \xi_1(t) ||\mathbf{f}||_{1-\gamma},$$

where

$$\begin{aligned} \xi_1(t) = \frac{t^{\alpha}\Gamma(\gamma)}{\Gamma(\alpha+\gamma)} - \frac{T^{\alpha}\left(\frac{t}{T}\right)^{\alpha+1}}{\gamma\Gamma(\alpha)} + \frac{T^{\gamma-1}\left(\frac{t}{T}\right)^{\alpha}(T-t)^{\alpha-\gamma+1}}{(\alpha-\gamma+1)\Gamma(\alpha)} \\ + \frac{T^{\alpha}\left(\frac{t}{T}\right)^{\alpha-\gamma+1}(1-\gamma)\Gamma(\alpha-\gamma+1)\Gamma(\gamma)}{\Gamma(\alpha+1)^2}. \end{aligned} \tag{A.1}$$

Here, the inequalities on both $|\,.\,|$ *and* $||\,.\,||_{1-\gamma}$ *can be seen component wise.*

Proof. Writing out the integral expression gives:

$$\begin{aligned} &\left| \frac{t^{1-\gamma}}{\Gamma(\alpha)} \left[\int_0^t (t-s)^{\alpha-1} \mathbf{f}(s)\,\mathrm{d}s - \left(\frac{1-\gamma}{\alpha} + 1 \right) T^{\gamma-1} \left(\frac{t}{T} \right)^{\alpha} \int_0^T (T-s)^{\alpha-\gamma} \mathbf{f}(s)\,\mathrm{d}s \right] \right|, \\ &= \left| \frac{t^{1-\gamma}}{\Gamma(\alpha)} \left[\int_0^t \frac{(t-s)^{\alpha-1}}{s^{1-\gamma}} s^{1-\gamma}\mathbf{f}(s)\,\mathrm{d}s - \left(\frac{1-\gamma}{\alpha} + 1 \right) T^{\gamma-1} \left(\frac{t}{T} \right)^{\alpha} \int_0^T \frac{(T-s)^{\alpha-\gamma}}{s^{1-\gamma}} s^{1-\gamma}\mathbf{f}(s)\,\mathrm{d}s \right] \right|, \\ &= \left| \frac{t^{1-\gamma}}{\Gamma(\alpha)} \left[\int_0^t \frac{(t-s)^{\alpha-1} - T^{\gamma-1}\left(\frac{t}{T}\right)^{\alpha}(T-s)^{\alpha-\gamma}}{s^{1-\gamma}} s^{1-\gamma}\mathbf{f}(s)\,\mathrm{d}s - T^{\gamma-1}\left(\frac{t}{T}\right)^{\alpha} \int_t^T \frac{(T-s)^{\alpha-\gamma}}{s^{1-\gamma}} s^{1-\gamma}\mathbf{f}(s)\,\mathrm{d}s \right. \right. \\ &\quad \left. \left. - \left(\frac{1-\gamma}{\alpha} \right) T^{\gamma-1} \left(\frac{t}{T} \right)^{\alpha} \int_0^T \frac{(T-s)^{\alpha-\gamma}}{s^{1-\gamma}} s^{1-\gamma}\mathbf{f}(s)\,\mathrm{d}s \right] \right|, \\ &\leq \frac{t^{1-\gamma}}{\Gamma(\alpha)} \left[\int_0^t \frac{(t-s)^{\alpha-1} - T^{\gamma-1}\left(\frac{t}{T}\right)^{\alpha}(T-s)^{\alpha-\gamma}}{s^{1-\gamma}} \left| s^{1-\gamma}\mathbf{f}(s) \right| \mathrm{d}s + T^{\gamma-1}\left(\frac{t}{T}\right)^{\alpha} \int_t^T \frac{(T-s)^{\alpha-\gamma}}{s^{1-\gamma}} \left| s^{1-\gamma}\mathbf{f}(s) \right| \mathrm{d}s \right. \\ &\quad \left. + \left(\frac{1-\gamma}{\alpha} \right) T^{\gamma-1} \left(\frac{t}{T} \right)^{\alpha} \int_0^T \frac{(T-s)^{\alpha-\gamma}}{s^{1-\gamma}} \left| s^{1-\gamma}\mathbf{f}(s) \right| \mathrm{d}s \right]. \end{aligned} \tag{A.2}$$

Here, (A.2) follows from the triangle inequality and Young's inequality for integrals, since

$$\begin{aligned}(t-s)^{\alpha-1} - T^{\gamma-1}\left(\frac{t}{T}\right)^{\alpha}(T-s)^{\alpha-\gamma} &= (t-s)^{\alpha-1} - T^{\gamma-1}\left(\frac{t}{T}\right)^{\alpha}(T-s)^{\alpha-1+1-\gamma},\\ &= (t-s)^{\alpha-1} - \left(\frac{T-s}{T}\right)^{1-\gamma}\left(\frac{t}{T}\right)^{\alpha}(T-s)^{\alpha-1},\\ &\geq (t-s)^{\alpha-1} - \left(\frac{t}{T}\right)^{\alpha}(T-s)^{\alpha-1},\\ &\geq (t-s)^{\alpha-1}\frac{T-t}{T} \geq 0, \end{aligned} \tag{A.3}$$

for $s \in [0,t]$, $\alpha \in (0,1)$, $\gamma \in [0,1]$, where the final line follows from [8]. The same holds for the second and third integral, since

$$\frac{(T-s)^{\alpha-\gamma}}{s^{1-\gamma}} \geq 0 \quad \text{for } s \in [t,T],\, \alpha \in (0,1),\, \gamma \in [0,1].$$

Then, continuing from (A.2), one has

$$\begin{aligned}&\left|\frac{t^{1-\gamma}}{\Gamma(\alpha)}\left[\int_0^t (t-s)^{\alpha-1}\mathbf{f}(s)\,\mathrm{d}s - \left(\frac{1-\gamma}{\alpha}+1\right)T^{\gamma-1}\left(\frac{t}{T}\right)^{\alpha}\int_0^T (T-s)^{\alpha-\gamma}\mathbf{f}(s)\,\mathrm{d}s\right]\right|,\\ &\leq \frac{t^{1-\gamma}}{\Gamma(\alpha)}\left[\int_0^t \frac{(t-s)^{\alpha-1} - T^{\gamma-1}\left(\frac{t}{T}\right)^{\alpha}T^{\alpha-\gamma}}{s^{1-\gamma}}\left|s^{1-\gamma}\mathbf{f}(s)\right|\,\mathrm{d}s + T^{\gamma-1}\left(\frac{t}{T}\right)^{\alpha}\int_t^T \frac{(T-s)^{\alpha-\gamma}}{t^{1-\gamma}}\left|s^{1-\gamma}\mathbf{f}(s)\right|\,\mathrm{d}s\right.\\ &\qquad \left. + \left(\frac{1-\gamma}{\alpha}\right)T^{\gamma-1}\left(\frac{t}{T}\right)^{\alpha}\int_0^T \frac{(T-s)^{\alpha-\gamma}}{s^{1-\gamma}}\left|s^{1-\gamma}\mathbf{f}(s)\right|\,\mathrm{d}s\right], \end{aligned} \tag{A.4}$$

Inequality (A.4) holds since

$$(T-s)^{\alpha-\gamma} = (T-s)^{\beta(\alpha-1)} \geq T^{\beta(\alpha-1)} = T^{\alpha-\gamma}, \quad \text{for } s \in [0,t],\, \alpha \in (0,1),\, \beta \in [0,1],$$

as $\beta(\alpha-1) \leq 0$, and $s^{\gamma-1} \leq t^{\gamma-1}$, for $s \in [t,T]$, $\gamma \in (0,1)$. Then, finally we arrive at the expression:

$$\begin{aligned}&\left|\frac{t^{1-\gamma}}{\Gamma(\alpha)}\left[\int_0^t (t-s)^{\alpha-1}\mathbf{f}(s)\,\mathrm{d}s - \left(\frac{1-\gamma}{\alpha}+1\right)T^{\gamma-1}\left(\frac{t}{T}\right)^{\alpha}\int_0^T (T-s)^{\alpha-\gamma}\mathbf{f}(s)\,\mathrm{d}s\right]\right|,\\ &\leq \frac{t^{1-\gamma}}{\Gamma(\alpha)}\left[\int_0^t \frac{(t-s)^{\alpha-1} - T^{\gamma-1}\left(\frac{t}{T}\right)^{\alpha}T^{\alpha-\gamma}}{s^{1-\gamma}}\,\mathrm{d}s\,||\mathbf{f}||_{1-\gamma}\right.\\ &\qquad + T^{\gamma-1}\left(\frac{t}{T}\right)^{\alpha}\int_t^T \frac{(T-s)^{\alpha-\gamma}}{t^{1-\gamma}}\,\mathrm{d}s\,||\mathbf{f}||_{1-\gamma}\\ &\qquad \left. + \left(\frac{1-\gamma}{\alpha}\right)T^{\gamma-1}\left(\frac{t}{T}\right)^{\alpha}\int_0^T \frac{(T-s)^{\alpha-\gamma}}{s^{1-\gamma}}\,\mathrm{d}s||\mathbf{f}||_{1-\gamma}\right], \end{aligned} \tag{A.5}$$

$$\begin{aligned}&= \frac{t^{1-\gamma}}{\Gamma(\alpha)}\left[\int_0^t \frac{(t-s)^{\alpha-1}}{s^{1-\gamma}}\,\mathrm{d}s - \left(\frac{t}{T}\right)^{\alpha}T^{\alpha-1}\int_0^t s^{\gamma-1}\,\mathrm{d}s + (tT)^{\gamma-1}\left(\frac{t}{T}\right)^{\alpha}\int_t^T (T-s)^{\alpha-\gamma}\,\mathrm{d}s\right.\\ &\qquad \left. + \left(\frac{1-\gamma}{\alpha}\right)T^{\gamma-1}\left(\frac{t}{T}\right)^{\alpha}\int_0^T \frac{(T-s)^{\alpha-\gamma}}{s^{1-\gamma}}\,\mathrm{d}s\right]||\mathbf{f}||_{1-\gamma},\\ &= \left(\frac{t^{\alpha}\Gamma(\gamma)}{\Gamma(\alpha+\gamma)} - \frac{T^{\alpha}\left(\frac{t}{T}\right)^{\alpha+1}}{\gamma\Gamma(\alpha)} + \frac{T^{\gamma-1}\left(\frac{t}{T}\right)^{\alpha}(T-t)^{\alpha-\gamma+1}}{(\alpha-\gamma+1)\Gamma(\alpha)}\right.\\ &\qquad \left. + \frac{T^{\alpha}\left(\frac{t}{T}\right)^{\alpha-\gamma+1}(1-\gamma)\Gamma(\alpha-\gamma+1)\Gamma(\gamma)}{\Gamma(\alpha+1)^2}\right)||\mathbf{f}||_{1-\gamma},\\ &=: \xi_1(t)||\mathbf{f}||_{1-\gamma}. \end{aligned}$$

Here, (A.5) follows from Hölder's inequality to L^1 and L^∞. Note that the three expressions for $\xi_1(t)$ as stated in the final formulation correspond with the integrals respectively, which will be of use in the proof of the following lemma. □

Now, for the analogue of Lemma 3.2.2, using the result of Lemma A.0.1 gives

Lemma A.0.2. *Let* $\{\xi_m(t)\}_{m\in\{\mathbb{N}\cup\{0\}\}}$ *be a sequence of functions in* $C_{1-\gamma}[0,T]$ *as given by*

$$\xi_m(t) := \frac{t^{1-\gamma}}{\Gamma(\alpha)}\Bigg[\int_0^t \frac{(t-s)^{\alpha-1} - T^{\gamma-1}\left(\frac{t}{T}\right)^{\alpha} T^{\alpha-\gamma}}{s^{1-\gamma}}\xi_{m-1}(s)\,\mathrm{d}s + (tT)^{\gamma-1}\left(\frac{t}{T}\right)^{\alpha}\int_t^T (T-s)^{\alpha-\gamma}\xi_{m-1}(s)\,\mathrm{d}s + \left(\frac{1-\gamma}{\alpha}\right)T^{\gamma-1}\left(\frac{t}{T}\right)^{\alpha}\int_0^T \frac{(T-s)^{\alpha-\gamma}}{s^{1-\gamma}}\xi_{m-1}(s)\,\mathrm{d}s\Bigg], \tag{A.6}$$

with $\xi_0(t) := 1$ *and* $\xi_1(t)$ *is given by formula* (A.1)*. Then, for all* $m \in \mathbb{N}$*, the following estimate holds:*

$$\xi_{m+1}(t) \le \Xi^m \xi_1(t) \le \Xi^{m+1}, \tag{A.7}$$

where

$$\Xi = T^{\alpha}\left[\frac{\left(\frac{\alpha}{2\alpha-\gamma+1}\right)^{\alpha}\left(1-\frac{\alpha}{2\alpha-\gamma+1}\right)^{\alpha-\gamma+1}}{(\alpha-\gamma+1)\,\Gamma(\alpha)} + \frac{\left(\frac{\Gamma(\alpha+1)\Gamma(\gamma+1)}{(\alpha+1)\Gamma(\alpha+\gamma)}\right)^{\alpha}\Gamma(\gamma)}{(\alpha+1)\,\Gamma(\alpha+\gamma)}\right].$$

Proof. The proof follows an induction argument. First, for $m = 0$, we have by (A.1) that

$$\xi_1(t) = \frac{t^{\alpha}\Gamma(\gamma)}{\Gamma(\alpha+\gamma)} - \frac{T^{\alpha}\left(\frac{t}{T}\right)^{\alpha+1}}{\gamma\Gamma(\alpha)} + \frac{T^{\gamma-1}\left(\frac{t}{T}\right)^{\alpha}(T-t)^{\alpha-\gamma+1}}{(\alpha-\gamma+1)\Gamma(\alpha)} + \frac{T^{\alpha}\left(\frac{t}{T}\right)^{\alpha-\gamma+1}(1-\gamma)\Gamma(\alpha-\gamma+1)\Gamma(\gamma)}{\Gamma(\alpha+1)^2}.$$

Now, to find an upper bound, we split $\xi_1(t)$ in two parts. First, note that by (A.3) in the proof of Lemma 1, we know that

$$\frac{t^{\alpha}\Gamma(\gamma)}{\Gamma(\alpha+\gamma)} - \frac{T^{\alpha}\left(\frac{t}{T}\right)^{\alpha+1}}{\gamma\Gamma(\alpha)} \ge 0,$$

holds, since it is the result of an integral of a nonnegative expression multiplied by $\frac{t^{1-\gamma}}{\Gamma(\alpha)} \ge 0$. Since also $\frac{T^{\gamma-1}\left(\frac{t}{T}\right)^{\alpha}(T-t)^{\alpha-\gamma+1}}{(\alpha-\gamma+1)\Gamma(\alpha)} \ge 0$, we know,

$$\sup_{t\in[0,T]}\xi_1(t) = \sup_{t\in[0,T]}\left[\frac{t^{\alpha}\Gamma(\gamma)}{\Gamma(\alpha+\gamma)} - \frac{T^{\alpha}\left(\frac{t}{T}\right)^{\alpha+1}}{\gamma\Gamma(\alpha)} + \frac{T^{\gamma-1}\left(\frac{t}{T}\right)^{\alpha}(T-t)^{\alpha-\gamma+1}}{(\alpha-\gamma+1)\Gamma(\alpha)} + \frac{T^{\alpha}\left(\frac{t}{T}\right)^{\alpha-\gamma+1}(1-\gamma)\Gamma(\alpha-\gamma+1)\Gamma(\gamma)}{\Gamma(\alpha+1)^2}\right],$$

$$\le \sup_{t\in[0,T]}\left[\frac{t^{\alpha}\Gamma(\gamma)}{\Gamma(\alpha+\gamma)} - \frac{T^{\alpha}\left(\frac{t}{T}\right)^{\alpha+1}}{\gamma\Gamma(\alpha)}\right] + \sup_{t\in[0,T]}\left[\frac{T^{\gamma-1}\left(\frac{t}{T}\right)^{\alpha}(T-t)^{\alpha-\gamma+1}}{(\alpha-\gamma+1)\Gamma(\alpha)}\right] + \sup_{t\in[0,T]}\left[\frac{T^{\alpha}\left(\frac{t}{T}\right)^{\alpha-\gamma+1}(1-\gamma)\Gamma(\alpha-\gamma+1)\Gamma(\gamma)}{\Gamma(\alpha+1)^2}\right].$$

Analytically computing the supremum of both expressions w.r.t. $t \in [0,T]$ gives a supremememum attained at $t_1 = \frac{T\Gamma(\alpha+1)\Gamma(\gamma+1)}{(\alpha+1)\Gamma(\alpha+\gamma)}$ for the first expression and $t_2 = \frac{T\alpha}{2\alpha-\gamma+1}$ for the second expression. The third expression does not attain a derivative of zero, but reaches its maxiumum at $t_3 = T$ since the derivative yields

$$\frac{T^{\alpha+\gamma-1}t^{-\gamma}\left(\frac{t}{T}\right)^{\alpha}(1-\gamma)\,\Gamma(\gamma)\,\Gamma(\alpha-\gamma+2)}{\Gamma^2(\alpha+1)} \ge 0, \quad \text{for } \gamma \in (0,1).$$

Thus the function is nondecreasing and hence must attain its maximum at $t = T$. This yields, after simplification:

$$\begin{aligned}
\xi_1(t) &\le \sup_{t\in[0,T]}\xi_1(t),\\
&\le \sup_{t\in[0,T]}\left[\frac{t^{\alpha}\Gamma(\gamma)}{\Gamma(\alpha+\gamma)} - \frac{T^{\alpha}\left(\frac{t}{T}\right)^{\alpha+1}}{\gamma\Gamma(\alpha)}\right] + \sup_{t\in[0,T]}\left[\frac{T^{\gamma-1}\left(\frac{t}{T}\right)^{\alpha}(T-t)^{\alpha-\gamma+1}}{(\alpha-\gamma+1)\Gamma(\alpha)}\right]\\
&\quad + \sup_{t\in[0,T]}\left[\frac{T^{\alpha}\left(\frac{t}{T}\right)^{\alpha-\gamma+1}(1-\gamma)\Gamma(\alpha-\gamma+1)\Gamma(\gamma)}{\Gamma(\alpha+1)^2}\right],\\
&= T^{\alpha}\Bigg[\frac{\left(\frac{\alpha}{2\alpha-\gamma+1}\right)^{\alpha}\left(1-\frac{\alpha}{2\alpha-\gamma+1}\right)^{\alpha-\gamma+1}}{(\alpha-\gamma+1)\,\Gamma(\alpha)} + \frac{\left(\frac{\alpha\gamma}{\alpha+1}\mathrm{B}(\alpha,\gamma)\right)^{\alpha}\Gamma(\gamma)}{(\alpha+1)\,\Gamma(\alpha+\gamma)}\\
&\quad + \frac{(1-\gamma)\,\mathrm{B}(\alpha-\gamma+1,\gamma)}{\Gamma(\alpha+1)}\Bigg].
\end{aligned}$$

Here, B represents the beta-function, with the property $\mathrm{B}(a,b) = \frac{\Gamma(a)\Gamma(b)}{\Gamma(a+b)}$. Now that we have an upper bound, assume (A.7) holds for some $k-1$, hence

$$\xi_k(t) \leq \Xi^{k-1}\xi_1(t) \leq \Xi^k. \tag{A.8}$$

Then, for k, we have

$$\begin{aligned}
\xi_{k+1}(t) &= \frac{t^{1-\gamma}}{\Gamma(\alpha)}\Bigg[\int_0^t \frac{(t-s)^{\alpha-1} - \left(\frac{t}{T}\right)^{\alpha} T^{\alpha-1}}{s^{1-\gamma}}\,\xi_k(s)\,\mathrm{d}s + \left(\frac{t}{T}\right)^{\alpha}\int_t^T \frac{T^{\alpha-1}}{s^{1-\gamma}}\,\xi_k(s)\,\mathrm{d}s \\
&\qquad + \left(\frac{1-\gamma}{\alpha}\right) T^{\gamma-1}\left(\frac{t}{T}\right)^{\alpha}\int_0^T \frac{(T-s)^{\alpha-\gamma}}{s^{1-\gamma}}\xi_k(s)\,\mathrm{d}s\Bigg], \\
&\leq \frac{t^{1-\gamma}}{\Gamma(\alpha)}\Bigg[\int_0^t \frac{(t-s)^{\alpha-1} - \left(\frac{t}{T}\right)^{\alpha} T^{\alpha-1}}{s^{1-\gamma}}\,\Xi^k\,\mathrm{d}s + \left(\frac{t}{T}\right)^{\alpha}\int_t^T \frac{T^{\alpha-1}}{s^{1-\gamma}}\,\Xi^k\,\mathrm{d}s \\
&\qquad + \left(\frac{1-\gamma}{\alpha}\right) T^{\gamma-1}\left(\frac{t}{T}\right)^{\alpha}\int_0^T \frac{(T-s)^{\alpha-\gamma}}{s^{1-\gamma}}\Xi^k\,\mathrm{d}s\Bigg], \qquad \text{(A.9)} \\
&= \frac{\Xi^k t^{1-\gamma}}{\Gamma(\alpha)}\Bigg[\int_0^t \frac{(t-s)^{\alpha-1} - \left(\frac{t}{T}\right)^{\alpha} T^{\alpha-1}}{s^{1-\gamma}}\,\mathrm{d}s + \left(\frac{t}{T}\right)^{\alpha}\int_t^T \frac{T^{\alpha-1}}{s^{1-\gamma}}\,\mathrm{d}s \\
&\qquad + \left(\frac{1-\gamma}{\alpha}\right) T^{\gamma-1}\left(\frac{t}{T}\right)^{\alpha}\int_0^T \frac{(T-s)^{\alpha-\gamma}}{s^{1-\gamma}}\,\mathrm{d}s\Bigg], \\
&= \Xi^k\xi_1(t), \qquad \text{(A.10)} \\
&\leq \Xi^{k+1}.
\end{aligned}$$

Here, line (A.9) follows from the induction hypothesis (A.8), line (A.10) follows from the definition (A.6) using the fact that $\xi_0(t) = 1$ and the final result follows from the induction hypothesis again. Hence, the result holds for $k+1$, and thus we have proven the inequality holds for any $m \in \{\mathbb{N} \cup \{0\}\}$. □

B

Existence and uniqueness for a Caputo-derivative initial value problem with general initial solution

Numerous sources exist on the existence and uniqueness of fractional order Caputo derivative initial value problems, such as provided in [11, 27]. In this appendix chapter, an overview of the proof will be provided when using a general choice of $\mathbf{x}_0 \neq \tilde{\mathbf{x}}_0$ with "global" iterations on the interval $[0, T]$, to establish intermediate results as will be used splines applications.

Take the general Caputo initial value problem of order $\alpha \in (0, 1)$:

$$\begin{cases} {}_0^{\mathrm{C}}\mathrm{D}_t^{\alpha}\mathbf{x}(t) = \mathbf{f}(t, \mathbf{x}), \\ \mathbf{x}(0) = \tilde{\mathbf{x}}_0, \end{cases} \tag{B.1}$$

for $t \in [0, T]$, $\mathbf{f} : [0, T] \times D_{\mathbf{f}} \to \mathbb{R}^d$ continuous with $D_{\mathbf{f}} \subset \mathbb{R}^d$ closed and bounded and $\tilde{\mathbf{x}}_0 \in \mathbb{R}^d$.

Now, for a choice of $\mathbf{x}_0(t) : [0, T] \to \mathbb{R}^d$, define an iterative sequence $\mathbf{x}_m : [0, T] \to \mathbb{R}^d$ as:

$$\mathbf{x}_{m+1}(t) = \tilde{\mathbf{x}}_0 + {}_0\mathrm{I}_t^{\alpha}\mathbf{f}(t, \mathbf{x}_m(t)). \tag{B.2}$$

Theorem B.0.1 (Existence and uniqueness of solutions to the Caputo-IVP)**.** *Assume:*

(i) $\mathbf{f}$ *is bounded by* $\mathbf{m}$*. Hence*

$$|\mathbf{f}(t, \mathbf{u})| < \mathbf{m} \in \mathbb{R}^d_{\geq 0}, \quad \textit{for all } t \in [0, T], \mathbf{u} \in D_{\mathbf{f}}.$$

(ii) $\mathbf{f}$ *is Lipschitz. Hence, there exists a matrix* $\mathbf{K} \in \mathcal{M}_{d\times d}(\mathbb{R}_{\geq 0})$ *such that:*

$$|\mathbf{f}(t, \mathbf{u}) - \mathbf{f}(t, \mathbf{v})| \leq \mathbf{K}|\mathbf{u} - \mathbf{v}|, \quad \textit{for all } t \in [0, T],\ \mathbf{u}, \mathbf{v} \in D_{\mathbf{f}}.$$

(iii) $\mathbf{x}_0 : [0, T] \to \mathbb{R}^d$ *is chosen such that the set*

$$D_{\mathbf{b}} = \{\{\mathbf{u} \in D_{\mathbf{f}} : ||\mathbf{u} - \mathbf{x}_0||_{\infty} \leq \mathbf{b}\} \subset D_{\mathbf{f}}\}$$

is non-empty, where $\mathbf{b} := \frac{T^{\alpha}\mathbf{m}}{\Gamma(\alpha+1)} + ||\tilde{\mathbf{x}}_0 - \mathbf{x}_0||_{\infty}$.

(iv) The matrix defined by

$$\mathbf{Q} := \frac{T^{\alpha}\mathbf{K}}{\Gamma(\alpha + 1)},$$

satisfies $||\mathbf{Q}|| < 1$.

Then, the sequence $\mathbf{x}_m$ *as provided in* (B.2) *converges uniformly to the unique continuous solution* $\mathbf{x} : [0, T] \to \mathbb{R}^d$ *of initial value problem* (B.1)*. Furthermore, the following error estimate holds:*

$$||\mathbf{x}_\infty - \mathbf{x}_m||_\infty \leq \mathbf{Q}^m(\mathbf{I} - \mathbf{Q})^{-1}\mathbf{b}. \tag{B.3}$$

Proof. First, it goes to prove $\mathbf{x}_m \in D_\mathbf{f}$ for all $m = \mathbb{N} \cup \{0\}$. Using Proposition 2.2.3, we know that for $u : [0, T] \to \mathbb{R}$ continuous,

$$||{}_0\mathrm{I}_t^\alpha u(t)||_\infty \leq \frac{t^\alpha}{\Gamma(\alpha+1)}||u||_\infty \leq \frac{T^\alpha}{\Gamma(\alpha+1)}||u||_\infty$$

Then, for $m = 0$, using the definition of the sequence (B.2) we have:

$$\begin{aligned} ||\mathbf{x}_1 - \mathbf{x}_0||_\infty &= ||\tilde{\mathbf{x}}_0 + {}_0\mathrm{I}_t^\alpha \mathbf{f}(t, \mathbf{x}_0(t)) - \mathbf{x}_0||_\infty, \\ &\leq ||{}_0\mathrm{I}_t^\alpha \mathbf{f}(t, \mathbf{x}_0(t))||_\infty + ||\tilde{\mathbf{x}}_0 - \mathbf{x}_0||_\infty, \\ &\leq \underbrace{\frac{T^\alpha \mathbf{m}}{\Gamma(\alpha+1)} + ||\tilde{\mathbf{x}}_0 - \mathbf{x}_0||_\infty}_{:=\mathbf{b}}. \end{aligned} \tag{B.4}$$

Hence, $\mathbf{x}_1 \in D_\mathbf{f}$. Furthermore, by induction, we have that for $m \geq 1$,

$$\begin{aligned} ||\mathbf{x}_m - \mathbf{x}_0||_\infty &\leq ||{}_0\mathrm{I}_t^\alpha \mathbf{f}(t, \mathbf{x}_{m-1}(t))||_\infty + ||\tilde{\mathbf{x}}_0 - \mathbf{x}_0||_\infty, \\ &\leq \underbrace{\frac{T^\alpha \mathbf{m}}{\Gamma(\alpha+1)} + ||\tilde{\mathbf{x}}_0 - \mathbf{x}_0||_\infty}_{=\mathbf{b}}, \end{aligned} \tag{B.5}$$

Thus, $\mathbf{x}_m \in D_\mathbf{f}$ for all $m \in \mathbb{N} \cup \{0\}$.

Now, for the convergence of the sequence, taking the increments, we have for $m \in \mathbb{N}$,

$$\begin{aligned} ||\mathbf{x}_{m+1} - \mathbf{x}_m||_\infty &= ||{}_0\mathrm{I}_t^\alpha[\mathbf{f}(t, \mathbf{x}_m(t)) - \mathbf{f}(t, \mathbf{x}_{m-1}(t))]||_\infty, \\ &\leq \frac{T^\alpha}{\Gamma(\alpha+1)}||\mathbf{f}(t, \mathbf{x}_m(t)) - \mathbf{f}(t, \mathbf{x}_{m-1}(t))||_\infty, \\ &\leq \underbrace{\frac{T^\alpha \mathbf{K}}{\Gamma(\alpha+1)}}_{:=\mathbf{Q}} ||\mathbf{x}_m - \mathbf{x}_{m-1}||_\infty. \end{aligned}$$

Now, iterating and using the result of (B.4) gives

$$||\mathbf{x}_{m+1} - \mathbf{x}_m||_\infty \leq \mathbf{Q}^m \mathbf{b}.$$

Since $||\mathbf{Q}|| < 1$, this thus gives

$$\lim_{m\to\infty} ||\mathbf{x}_{m+1} - \mathbf{x}_m||_\infty = \mathbf{0}.$$

Then, by the completeness of the space of continuous functions $D_\mathbf{f} \in \mathbb{R}^d$ by compactness of $D_\mathbf{f}$, we have convergence of $\mathbf{x}_m$, hence for some $\mathbf{x}_\infty \in D_\mathbf{f}$,

$$\lim_{m\to\infty} ||\mathbf{x}_m - \mathbf{x}_\infty||_\infty = \mathbf{0}.$$

Furthermore, $\mathbf{x}_\infty$ is continuous as well as it is the uniform limit of continuous functions. Now, passing the limit in the iterative equation (B.2) gives that $\mathbf{x}_\infty$ satisfies

$$\mathbf{x}_\infty(t) = \tilde{\mathbf{x}}_0 + {}_0\mathrm{I}_t^\alpha \mathbf{f}(t, \mathbf{x}_\infty(t)),$$

which is equivalent to the initial value problem (B.1) as proven in e.g. [11], Theorem 23. Thus, we haev proven existence of a solution to the initial value problem.

For uniqueness, assume $\mathbf{x}^a$ and $\mathbf{x}^b$ are both limits of the sequence $\mathbf{x}_m$. Then,

$$\begin{aligned}||\mathbf{x}^a - \mathbf{x}^b||_\infty &= \left|\left|{}_0\mathrm{I}_t^\alpha \left[\mathbf{f}(t, \mathbf{x}^a(t)) - \mathbf{f}(t, \mathbf{x}^b(t))\right]\right|\right|_\infty, \\ &\leq \frac{T^\alpha \mathbf{K}}{\Gamma(\alpha+1)}||\mathbf{x}^a - \mathbf{x}^b||_\infty, \\ &= \mathbf{Q}||\mathbf{x}^a - \mathbf{x}^b||_\infty.\end{aligned}$$

Since $||\mathbf{Q}|| < 1$, this equation can only be satisfied for $||\mathbf{x}^a - \mathbf{x}^b||_\infty = \mathbf{0}$, hence $\mathbf{x}^a(t) = \mathbf{x}^b(t)$ for all $t \in [0, T]$.

Finally, to prove the estimate of (B.3), let us write

$$\begin{aligned}||\mathbf{x}_{m+j} - \mathbf{x}_m||_\infty &\leq \sum_{k=1}^{j} ||\mathbf{x}_{m+k} - \mathbf{x}_{m+k-1}||_\infty, \\ &\leq \sum_{k=1}^{j} \mathbf{Q}^{m+k-1}\mathbf{b}, \\ &= \mathbf{Q}^m \sum_{k=0}^{j-1} \mathbf{Q}^k \mathbf{b}, \\ &\leq \mathbf{Q}^m (\mathbf{I} - \mathbf{Q})^{-1}\mathbf{b}.\end{aligned}$$

And hence,

$$||\mathbf{x}_\infty - \mathbf{x}_m||_\infty \leq \mathbf{Q}^m (\mathbf{I} - \mathbf{Q})^{-1}\mathbf{b}.$$

□

C

Fractional derivation of the sine function

Since the analytical expression for ${}_0^{\mathrm{C}}\mathrm{D}_t^{\alpha} \sin(\omega t)$ does not admit an easily interpretable closed-form solution[1], this section presents a numerical approach to assess the behavior of the fractionally differentiated sine. In Figure C.1, an overview of the fractionally differentiated sine is given for selected values, showing a rapid amplitude stabilization and a seemingly unaffected oscillation frequency. This is further supported when assessing a larger parameter range, as shown in Figure C.2. Hence, it appears the oscillation frequency is not affected by fractional differentiation.

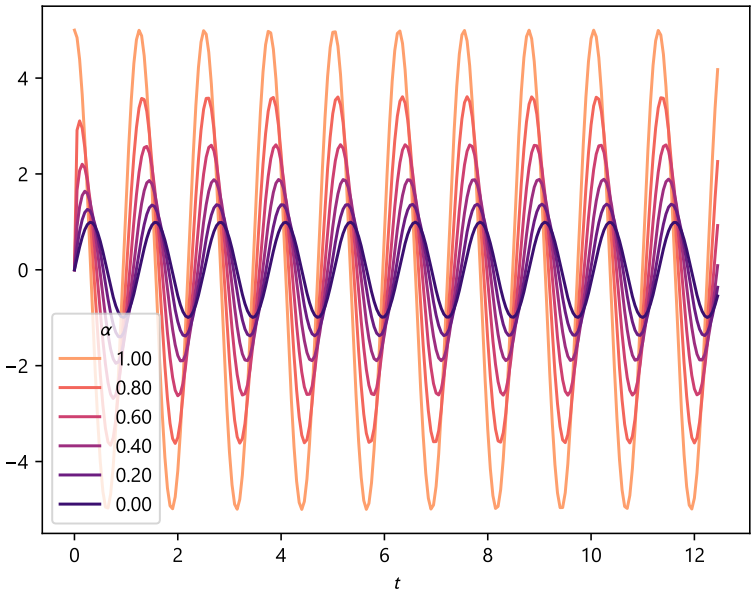

Figure C.1: ${}_0^{\mathrm{C}}\mathrm{D}_t^{\alpha} \sin(\omega t)$ for $\omega = 5$ and varying order α.

[1] Using the Laplace transform, a formulation can be made for ${}_0\mathrm{I}_t^{\alpha} \sin(\omega t)$, involving multiple hypergeometric functions. In the splines solution approaches with forcing, this expression is implemented using the Python library `mpmath`. Differentiating this expression can then be used for an approximation of ${}_0^{\mathrm{C}}\mathrm{D}_t^{\alpha} \sin(\omega t) = {}_0\mathrm{D}_t^{\alpha} \sin(\omega t)$.

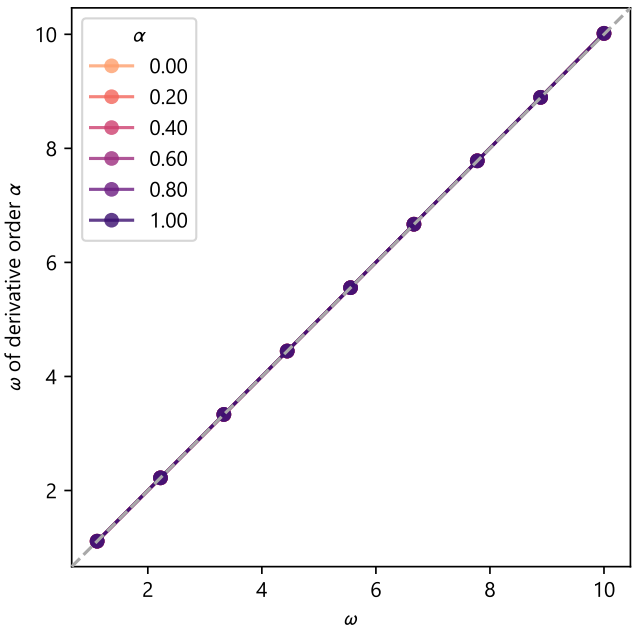

Figure C.2: Initial ω vs. the numerically obtained frequency of ${}_0^{\mathrm{C}}\mathrm{D}_t^{\alpha} \sin(\omega t)$, with the line $x = y$ in grey, dashed. Results are in the same range for all values of α.